

DEVELOPMENT OF AN NE-213 FAST-NEUTRON TAC SPECTROMETER SYSTEM
UTILIZING OFF-LINE GAMMA-RAY DISCRIMINATION

by *Richard Seck*

RICHARD EARL SECK
B.S., Kansas State University, 1970

A MASTER'S THESIS

submitted in partial fulfillment of the
requirements for the degree

MASTER OF SCIENCE

Department of Nuclear Engineering

KANSAS STATE UNIVERSITY
Manhattan, Kansas

1971

Approved by

Walt Meyer
Major Professor

L D
2668

T4

1971

538

612

TABLE OF CONTENTS

1.0 INTRODUCTION	1
2.0 NE-213 FAST-NEUTRON SPECTROMETER SYSTEM	3
2.1 Basic Characteristics of the NE-213 Scintillator	3
2.2 Assembly of the NE-213 Detector, Photomultiplier Tube, and Static Shield	4
2.3 Photomultiplier Tube Base Assembly	4
2.4 Operating Principles of the TAC Spectrometer	6
3.0 FAST NEUTRON PULSE HEIGHT MEASUREMENTS	13
3.1 Neutron Spectra Measured	13
3.2 Calibration of the Ne-213 TAC Spectrometer System	13
3.3 Packaged PuBe Source Pulse Height Measurement	15
3.4 $T(d,n)^4\text{He}$ Reaction Spectrum	15
3.5 Fast-Neutron Pulse Height Measurements at the KSU TRIGA Mark II Reactor Fast Beam Port	16
4.0 ANALYSIS OF DATA	17
4.1 Gamma-Ray Discrimination in the Raw Data	17
4.2 Analysis of Neutron Pulse Height Spectra	17
5.0 RESULTS AND CONCLUSIONS	21
5.1 14 MeV $T(d,n)^4\text{He}$ Neutron Energy Spectrum	21
5.2 TRIGA Mark II Fast Beam Port Neutron Spectra	21
5.3 TRIGA Mark II Fast Beam Port Spectra after Transmission Through a Thick Oxygen Absorber	24
5.4 PuBe Neutron Energy Spectrum	24
5.5 Conclusions	29
6.0 SUGGESTIONS FOR FURTHER STUDY	32
7.0 ACKNOWLEDGEMENTS	35
8.0 REFERENCES	36

ILLEGIBLE DOCUMENT

**THE FOLLOWING
DOCUMENT(S) IS OF
POOR LEGIBILITY IN
THE ORIGINAL**

**THIS IS THE BEST
COPY AVAILABLE**

**THIS BOOK
CONTAINS
NUMEROUS PAGES
WITH DIAGRAMS
THAT ARE CROOKED
COMPARED TO THE
REST OF THE
INFORMATION ON
THE PAGE.**

**THIS IS AS
RECEIVED FROM
CUSTOMER.**

9.0 APPENDICES	37
APPENDIX A: Derivation of Weighted Least Squares Curve Fitting Equations	38
APPENDIX B: Computer Codes	42
B-1.0 Gamma-Ray Discrimination Code, DISCRIM	42
B-1.1 DISCRIM Input Data Format	44
B-1.2 DISCRIM Code Listing	46
B-1.3 Sample Data Set and Results	60
B-2.0 Data Binning Code, DATABIN	69
B-2.1 DATABIN Input Data Format	70
B-2.2 DATABIN Code Listing	72
APPENDIX C: Raw Pulse Height Spectra	79
APPENDIX D: Sample FERDOR Input Data and Results	84
APPENDIX E: Detailed Block Diagram of NE-213 Fast- Neutron TAC Spectrometer System	88

1.0 INTRODUCTION

A number of organic scintillators yield light pulses whose shape varies with the rate of energy loss of an exciting particle. This property makes them useful for fast-neutron spectroscopy work using a fission reactor because the difference in pulse shape between a neutron induced light pulse and a gamma-ray induced light pulse provides a means of separating neutron pulses from gamma pulses. In light of this fact, many electronic pulse shape discrimination (PSD) systems have been developed which perform on-line pulse shape discrimination in fast-neutron spectrometer systems. On-line pulse shape discrimination systems generally work well for neutron energies above 1.5 MeV; however, below that energy, little pulse shape difference exists between neutron induced and gamma induced light pulses, and gamma discrimination becomes less and less exact. Uncertainty in gamma discrimination effectively puts a lower limit on the useful energy range of fast neutron spectrometers using organic scintillators which is well above their neutron threshold level of around 0.7 MeV.

In this study, an attempt is made to optimize the gamma discrimination process by off-line computer analysis of the data from a TAC spectrometer system somewhat similar to that reported by Haas.¹ In the system developed in this work, the linear signal from an NE-213 detector is integrated and double differentiated to produce a bipolar pulse whose cross over point is a function of the original pulse shape. A time to amplitude converter (TAC) converts the zero cross-over time of the bipolar pulse to a pulse height. The TAC signal and the NE-213 linear signal are fed to a 4096 channel multi-parameter analyzer operated in a two parameter mode. The analyzer produces a 64 X 64 array of data in which neutrons and gammas lie in two "ridges". The 64 X 64 array of data is analyzed by a specifically constructed computer

code and the neutron and gamma information are separated. In the low energy region, an attempt is made to optimize the gamma discrimination by an iterative weighted least squares gaussian fitting routine.

2.0 NE-213 FAST NEUTRON TAC SPECTROMETER SYSTEM

2.1 Basic Characteristics of The NE-213 Scintillator

NE-213 is an organic scintillator which responds to incident radiation indirectly through recoil protons, recoil electrons, and carbon nuclei interactions which result in recoil alpha particles. Neutrons incident on the solution interact to produce recoil protons and carbon scattering events while the only evident gamma ray interaction in the solution is by Compton scattering.² Owen¹² has shown that the pulse shape of the light pulse from a scintillation producing event is a function of the rate of energy loss of the exciting particle and that the light pulse can be expressed as the sum of two exponentials with different decay constants. It is obvious then that neutrons and gamma rays will produce light pulses of different pulse shape since they react through mechanisms which are known to have different specific ionizations. In fact, it has been shown that the slow exponential decay component of a neutron induced light pulse has a greater relative magnitude than that of a gamma induced light pulse.

Roush¹¹ has shown that if a pulse is integrated, then double differentiated a bipolar pulse is produced whose zero cross-over point is, ideally, invariant with amplitude and a function only of pulse shape. Ideally then, neutron and gamma pulses from the detector treated in this manner should yield bipolar pulses with definite and different zero cross-over points. With nonideal electronic components however, it is not possible to produce a bipolar pulse with a zero cross-over point which is entirely invariant with pulse height. This problem has plagued TAC spectrometer systems similar to that reported by Haas¹ which use this principle, especially in the energy range below about 2 MeV. The non-ideality of the zero cross-over

method posed no problem in this study however, since subsequent computer analysis of the raw data required only that the zero cross-over points for neutrons and gamma pulses be different at any given pulse height. It is not necessary that the zero cross-over points also be invariant for all pulse heights as is necessary for the operation of spectrometers using the TAC procedure for on-line gamma discrimination.

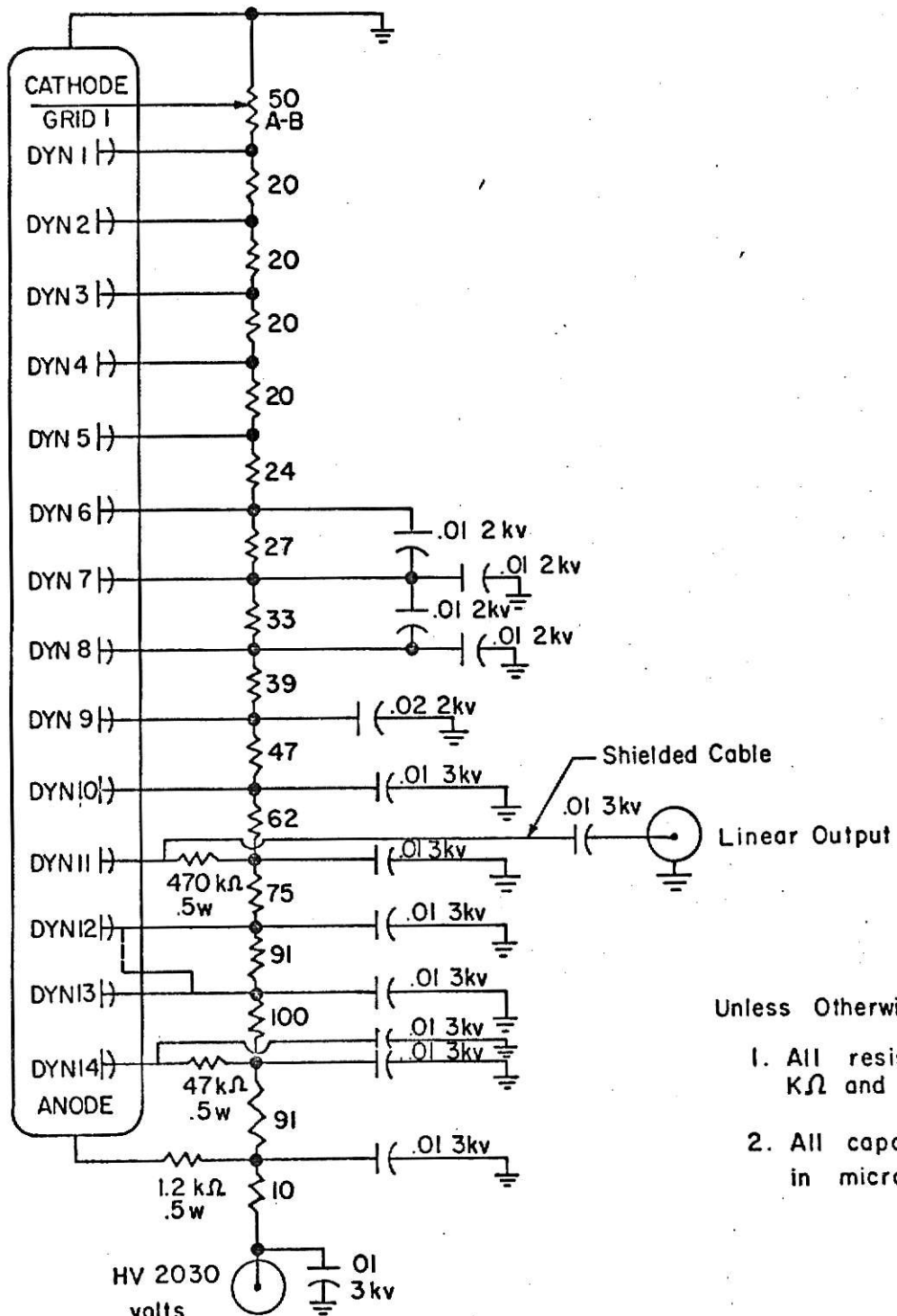
2.2 Assembly of the NE-213 Detector, Photomultiplier Tube, and Static Shield

The NE-213 detector, photomultiplier tube, and static shield are of the same configuration as that reported by Simons.² The NE-213 Scintillation solution, a purified solution of Xylene and napthalene activators with POPOP added to shift the emission spectrum to match the photomultiplier tube response, was encapsulated at the factory in a glass cell 2.00 inches high and 2.03 inches in diameter with a scintillator volume of approximately 103 cc. The glass cell was optically coupled to an RCA 6810-A photomultiplier tube using Dow Corning 10⁶ centistokes compound. The glass cell was carefully wrapped with light weight aluminum foil to act as a light reflector, and finally the entire glass cell and photomultiplier tube assembly was wrapped with black plastic electrician's tape to ensure a mechanically sound, light tight unit. Two concentric 6-3/4 inch long static shields separated by 3/16 inch of polyethylene were placed around the photomultiplier tube to shield it from stray magnetic fields which would alter its operating characteristics since it was the electrostatically focused type.

2.3 Photomultiplier Tube Base Assembly

The photomultiplier tube base, shown in figure 1, contains the electronic network necessary to properly bias the tube. In addition to the

RCA 5810-A Photomultiplier Tube



Unless Otherwise Noted :

1. All resistors are in KΩ and are 1 watt.
2. All capacities expressed in microfarads.

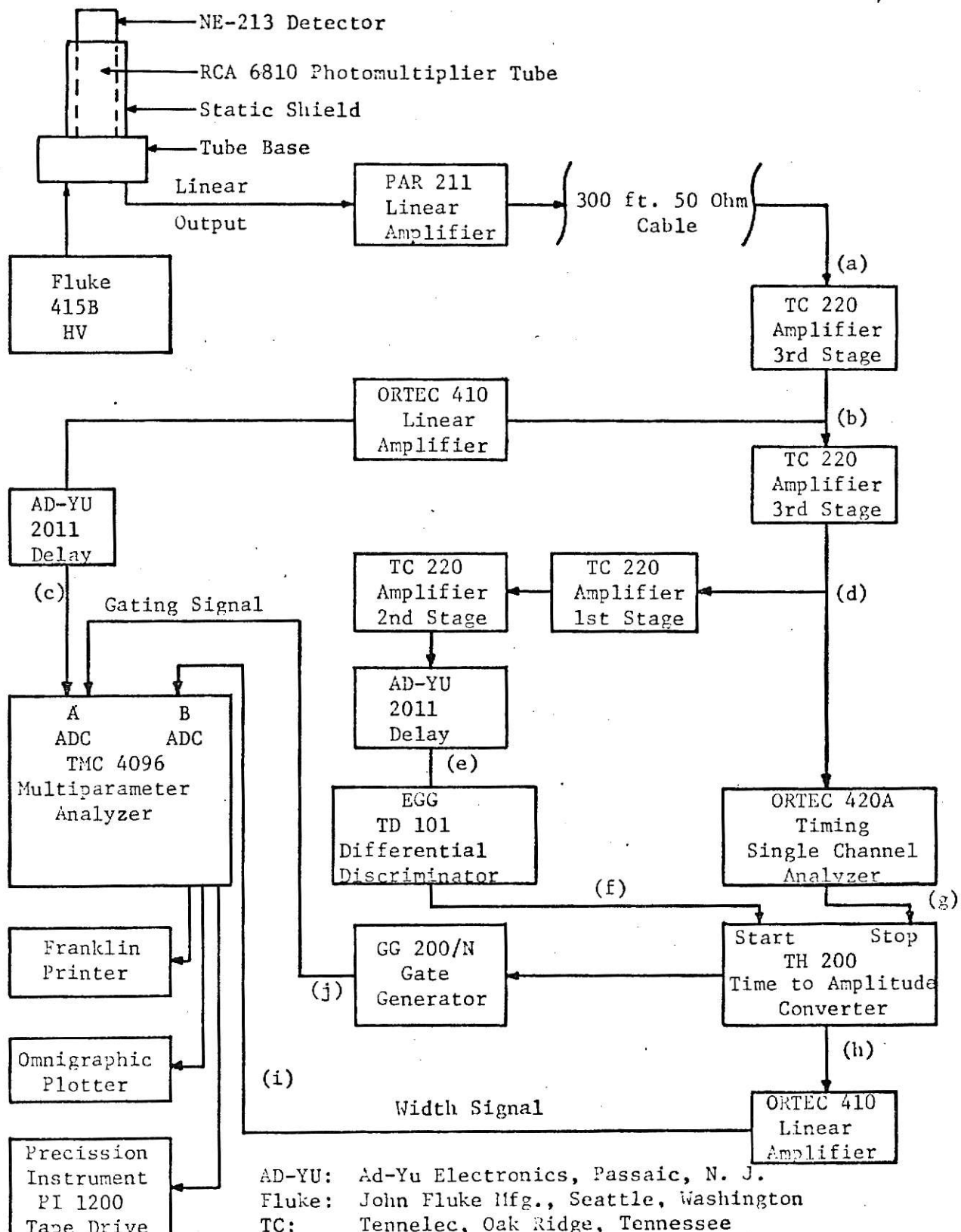
Figure 1. Schematic Diagram of NE-213 Photomultiplier Tube Base Assembly

biasing circuitry in the tube base, the linear signal is taken from the eleventh dynode and passed through a capacitor to remove its dc component before being transmitted to the rest of the circuitry.

2.4 Operating Principles of the TAC Spectrometer

A block diagram of the NE-211 fast-neutron TAC spectrometer system and sketches of the signals at various points in the system showing their relative shapes and timing are presented in figures 2 and 3 respectively. The electronic circuitry of the spectrometer system consists primarily of solid state AEC standard, NIM, modules selected for maximum stability, flexibility, minimum linear signal distortion, precise pulse shaping, and low level timing.

The linear signal from the eleventh dynode of the photomultiplier tube is passed through an eight foot cable to a Princeton Applied Research PAR-211 amplifier. This low noise, high gain amplifier was found suitable for transmitting the linear signal with minimal distortion from the Reactor Bay (location of the KSU TRIGA Mark II Reactor where all measurements were made) through 300 feet of 50 ohm cable to room 117 Ward Hall where the remainder of the TAC spectrometer system was located. After transmission from the Reactor Bay the signal passes through the third stage of a Tennelec TC-220 amplifier where it is integrated and differentiated to shorten and smooth the signal. After leaving the TC-220 amplifier, figure 2 position b, the signal is split. Part of the signal is led to an ORTEC model 410 amplifier where it is shaped to match the input requirements of a Technical Measurements Corporation, TMC, model 217 A analog to digital converter³ (ADC) (Achieving proper input pulse shape for the TMC ADC units is crucial if pulse height distortion is to be avoided.). The linear signal is led from the ORTEC 410 amplifier to an AD-YU 2011 continuously variable delay to put the linear



AD-YU: Ad-Yu Electronics, Passaic, N. J.

Fluke: John Fluke Mfg., Seattle, Washington

TC: Tennelec, Oak Ridge, Tennessee

Omnigraphic: Houston Omnigraphic Corp., Bellaire, Tx.

TMC: Technical Measurements, Corp., North Haven, Ct.

EGG: EG & G Inc., Salem, Massachusetts

ORTEC: ORTEC Incorporated, Oak Ridge, Tennessee

PI: Precision Instruments Co., Palo Alto, Calif.

Figure 2. Block Diagram of NE-213 Fast-Neutron TAC Spectrometer

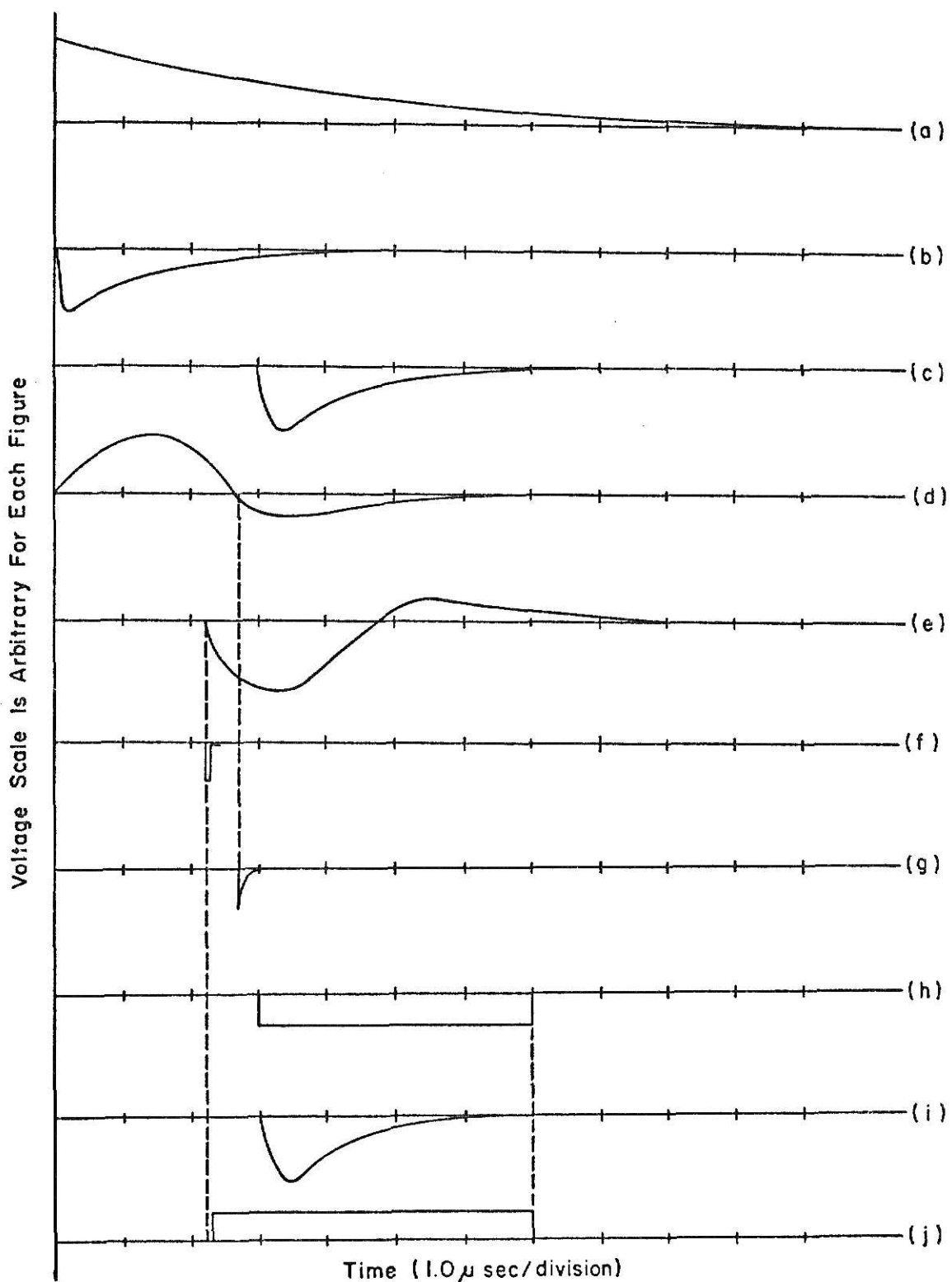


Figure 3. Relative Timing of Signals at the Labeled Locations in Figure 2.

signal in the proper time sequence with the output of the TAC unit, figure 3c and 3h, which will be described later, and then to the 217 A ADC unit at the A input of a TMC 4096 multiparameter analyzer.

The other branch of the linear signal, figure 2 position b, is passed to the third stage of a TC-220 amplifier. At this point, the signal is integrated and differentiated to produce a bipolar pulse as shown in figures 4 and 5. The cross over point of this bipolar pulse is a function of its pulse shape as described in section 2.1 and is different for a neutron pulse and a gamma-ray pulse of the same pulse height as illustrated in figure 5. In addition to this, it should be noted from figure 5 that the time to the zero cross-over point of the bipolar signal (This signal will be referred to as the "pulse shape signal") for a very low level pulse is shorter than for a high level pulse but does not go to zero. Choice of the best pulse shape signal form to be used was made by varying the parameters of the pulse shape signal and choosing that pulse shape which gave the best separation between neutron and gamma information (See section 4.1.) without raising the low energy cutoff of the system. It should be mentioned that in the course of this study it was found that proper choice of the parameters of the pulse shape signal was crucial to obtain maximum separation of neutron and gamma information.

The pulse shape signal is used to initiate the START and STOP commands for a time to amplitude converter (TAC). To initiate the START command, the pulse shape signal (figure 2 position d) is passed through the first and second stages of TC-220 amplifier where it is inverted and greatly amplified to eliminate any low energy cut-off problems in subsequent triggering circuitry. The pulse shape signal is then delayed a length of time about 0.2μ sec less than the time to cross-over of a pulse shape signal corresponding

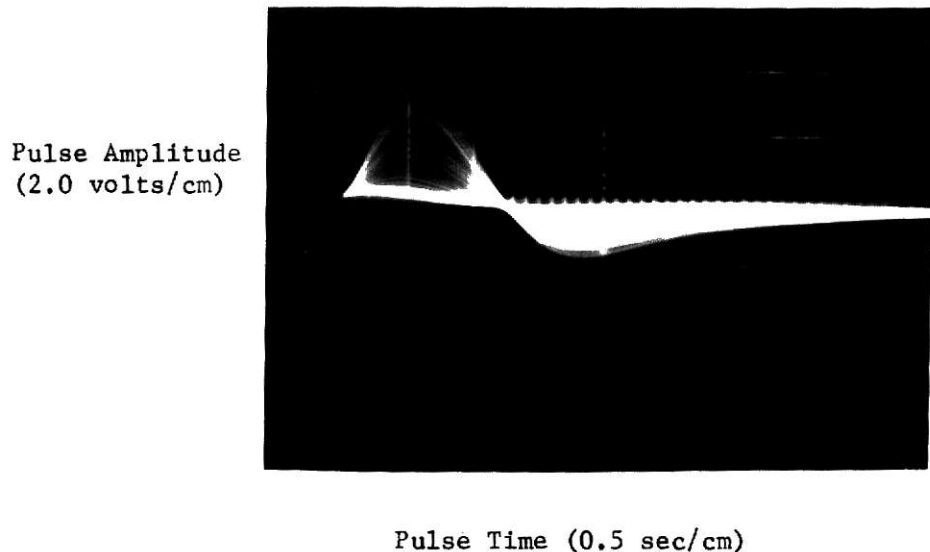


Figure 4. Photograph of PuBe Gamma-Ray and Neutron Induced "Pulse Shape Signals"

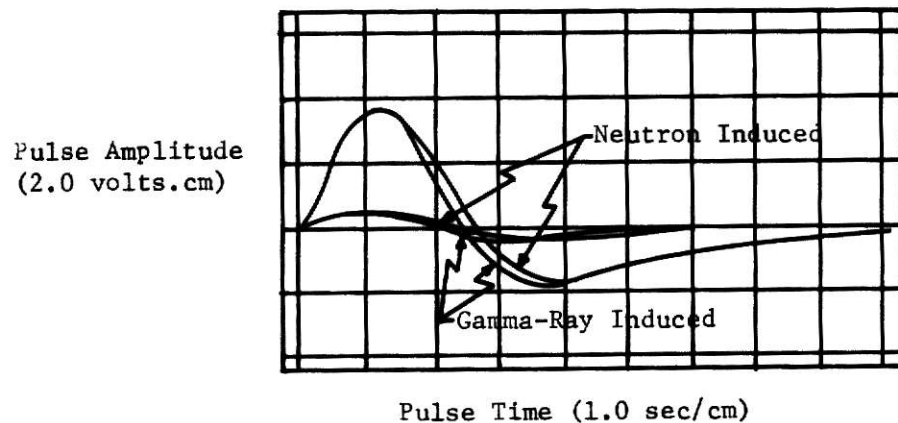


Figure 5. Skematic Diagram of PuBe Gamma-Ray and Neutron Induced "Pulse Shape Signals"

to the smallest linear signal to which the multiparameter analyzer will respond. The 0.2μ sec time cushion was used to ensure that the low energy end of the spectrum was being treated. The pulse shape signal from the AD-YU 2011 delay, figure 2 position e, is led to an EGG TD 101 differential discriminator operated in the integral mode. When the input signal rises above the threshold level of the discriminator, a fast timing output signal (figure 3F) is produced and led to the START input of an EGG TH 200 TAC module.

The STOP command for the TAC unit is generated by taking the pulse shape signal directly from the TC-220 third stage (figure 2 position d) and leading it to an ORTEC model 420 timing single channel analyzer operated in a cross-over pick-off mode. This unit provides a fast timing signal at the zero cross-over point of the pulse shape signal (figure 3g). The timing signal from the cross-over pick-off is led to the STOP input of the TAC unit.

The TAC unit provides a rectangular output signal of variable width (figure 3h) with a voltage proportional to the time between the START and STOP commands to the unit. The TAC output ("pulse width signal") is led to an ORTEC 410 amplifier where it is shaped to match the input signal requirements of a TMC 210 ADC unit (figure 3i). The pulse width signal is then led to a TMC 210 ADC unit at the B input of the multiparameter analyzer.

The VALID STOP output of the TAC unit is led to an EGG GG 200/N gate generator. The output of the gate generator (figure 3j) is led to the coincidence input of the TMC 217 ADC unit which accepts the linear detector signal. The gate signal effectively "slaves" the multiparameter analyzer to the TAC spectrometer by allowing the analyzer to accept only those detector signals which the TAC system treats.

A detailed block diagram of the TAC spectrometer system is presented in Appendix E.

2.5 Operational Mode of the TMC 4096 Multiparameter Analyzer

In this study, the TMC 4096 Multiparameter Analyzer is operated in a two parameter mode. In this mode, the memory of the analyzer is electronically arranged in a rectangular xy array with 4096 locations. Although several rectangular xy arrays can be obtained by appropriately wiring the patchboard of the format selector on the analyzer, a 64x64 array was used for this study because it provided the best combination of energy resolution and pulse shape separation.

When operating in this mode, the analyzer examines the input signals to the two ADC units simultaneously, determines the appropriate x and y address in the array, and adds one count to that array location. Each detector output signal which the TAC system analyzes is thus stored in the array at a location corresponding to the relative pulse height of the signal and the zero cross-over point of the corresponding pulse shape signal.

3.0 FAST NEUTRON PULSE HEIGHT MEASUREMENTS USING THE NE-213 TAC SPECTROMETER SYSTEM

3.1 Neutron Spectra Measured

The NE-213 TAC spectrometer was used to measure pulse height spectra of a packaged PuBe source, spectra of neutrons resulting from the $T(d,n)^4\text{He}$ reaction, and the spectra of KSU TRIGA Mark II reactor fast beam part neutron both before and after penetration through a thick sample of liquid oxygen. Included in this chapter are descriptions of the neutron sources, associated mechanical equipment, and procedure required for each experiment.

3.2 Calibration of the NE-213 TAC Spectrometer System

Prior to each measurement an energy calibration of the NE-213 TAC spectrometer was made using a "standard ^{60}Co pulse-height spectra." The multiparameter analyzer is operated in a single parameter 1024 channel mode during the calibration to facilitate the process. Calibration was accomplished by setting the gain of the linear signal to locate the extrapolated tail of the standard ^{60}Co pulse height spectra in channel 200 of the 1024 channel range (figure 6). After calibration, the patchboard of the format selector on the multiparameter analyzer was rewired to alter the operation of the analyzer from the single parameter mode to the two parameter mode.

Since only 64 channels of pulse height information are available when the analyzer is operated in the two parameter mode to produce a 64×64 array of data, it was necessary to take both a high gain and a low gain set of data for each spectral measurement. The energy calibration is used to calibrate only the low gain data. Once the low gain energy calibration had been established, the high gain energy calibration was known since the high gain was always set 2.5 times greater than the low gain. This was done by

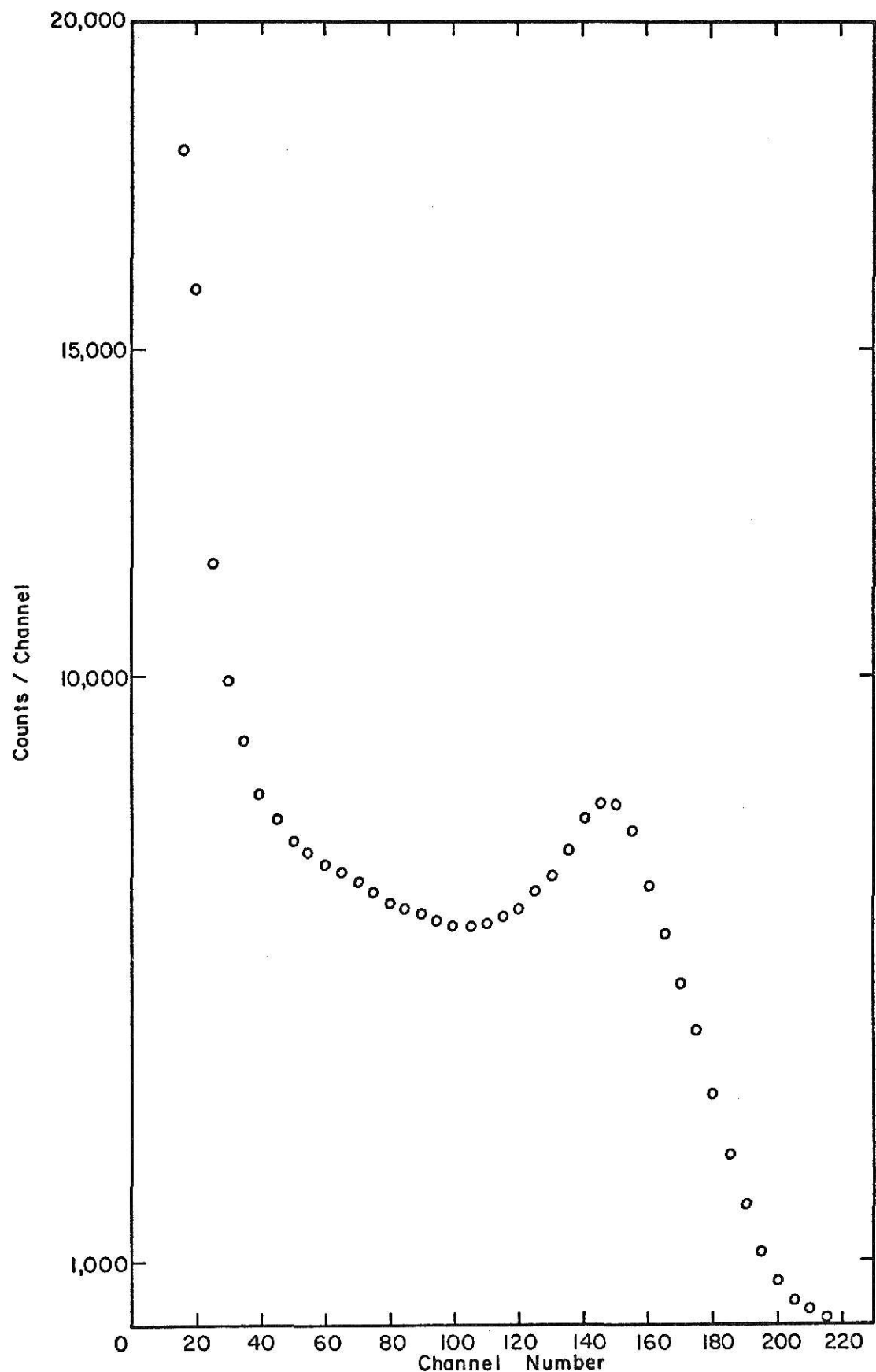


Figure 6. Standard ^{60}Co Pulse Height Spectrum

moving the input attenuator switch on the ORTEC 410 amplifier between two of its five positions, and it is used because it provides a quick, accurate, and easy means of determining the energy calibration of the high gain data.

Calibration of the TAC output signal at the "B" input of the multi-parameter analyzer is not done because it is only necessary that the gain be such that all neutron and gamma information lie in the 64x64 array.

3.3 Packaged PuBe Source Pulse Height Measurement

A 60 minute measurement was made of the spectrum from a PuBe source encapsulated in a cylindrical stainless steel container more than 3/16 in. thick. The center of the PuBe source was positioned 16 in. from the center of the detector and on the same horizontal plane as the detector. A background spectrum was taken by placing a plexyglass shield 12 in. long by 2 in. square between the detector and the PuBe source. The use of the shadow shield was necessary to correct foreground spectra for neutrons which reach the detector after scattering off the floor and walls of the Reactor Bay.

3.4 $T(d,n)^4\text{He}$ Reaction Spectrum

A Texas Nuclear Cockroft-Walton accelerator was used to produce 14 MeV neutrons from the $T(d,n)^4\text{He}$ reaction. The detector was placed in line with the beam and about 26 inches away from the tritium target. Because of the high efficiency of the detector and the difficulty of operating the accelerator at extremely low beam currents a plexyglass collimator approximately twenty-four inches long and four inches square in cross section with a 0.1 in.² aperture was placed between the detector and the accelerator target. The collimator was constructed so the aperture could be filled with water and thus provide an effective shadow shield to use during background measurements.

It should be noted that in order to measure neutrons of this energy it was necessary to reduce the gain of the linear signal so that ^{60}Co calibration tail fell in channel 140 instead of channel 200. This increased the energy range of the spectrometer from about 0-11 MeV to about 0-16 MeV. Normalization of foreground, background, high gain, and low gain measurements was done by aluminum foil activation.⁸

3.5 Fast-neutron Pulse Height Measurement at the KSU TRIGA Mark II Reactor Fast Beam Port

The KSU TRIGA Mark II fast radial beam port is aligned with a cylindrical void in the graphite core reflector and allows a fast neutron beam from the reactor core to pass through it. Direct beam measurements were made with the NE-213 detector positioned about 140 inches from the reactor wall along the center line of the fast beam port with the reactor operating at a nominal power of 30 watts.

The NE-213 detector is sensitive to gamma rays. If neutron spectra are measured in a strong gamma field using the TAC spectrometer system, difficulty may be encountered in effectively separating the neutron peak from the gamma peak in the composite neutron-gamma-ray grid of data. In direct beam measurements a strong gamma field was present. The problem was minimized by making the direct beam measurement after the reactor had been shut down for four days to allow residual gamma activity in the core to decay to some extent and by placing a 2 inch long bismuth metal plug in the collimator of the beam port to attenuate the gamma intensity.

The transmitted spectra through a 36 inch thick liquid oxygen sample was measured in the same manner as that reported by Miller.⁴

Normalization of foreground, background, high gain, and low gain measurements was completed using nickle foil activation in the reactor core.⁷

4.0 ANALYSIS OF DATA

4.1 Gamma-Ray Discrimination in the Raw Data

Figures 7 and 8 illustrate the form of the raw data obtained using the TAC system. In figure 7 the apparent height above the grid plane of each grid location is proportional to the number of counts in that grid location. Thus, it can easily be seen that neutron information and gamma-ray information tend to lie in two "ridges" in the data grid. Also, since neutrons have a greater pulse width to pulse height ratio than gamma-ray pulses, the upper "ridge" can be identified as the "neutron ridge."

Investigation of the distribution of information in the two "ridges" at various pulse height channels in the high gain data sets (figure 9) indicates that, above channel 10, the two "ridges" are nearly gaussian in cross section. Below channel 10 in the high gain pulse height spectrum the cross section of the two "ridges" becomes skewed, but are still somewhat gaussian in shape. In view of these facts a computer code, DISCRIM, was developed to effect an "optimal" separation of the neutron and gamma-ray information in the 64x64 channel data grid. The "optimal" separation is accomplished by fitting the neutron and gamma peaks at a given pulse height channel with a gaussian curve in a weighted least squares manner. The number of neutrons and gammas at that pulse height channel are then taken as the area under the gaussian fitted curve (See Appendix A and B-1).

4.2 Analysis of Neutron Pulse Height Spectra

The high and low gain neutron pulse height spectra calculated by the DISCRIM code were analyzed by a code, DATABIN, written during the course of this study (APPENDIX B-2). This code combines the low gain and high gain neutron pulse height spectra into a single set of data with one gain and

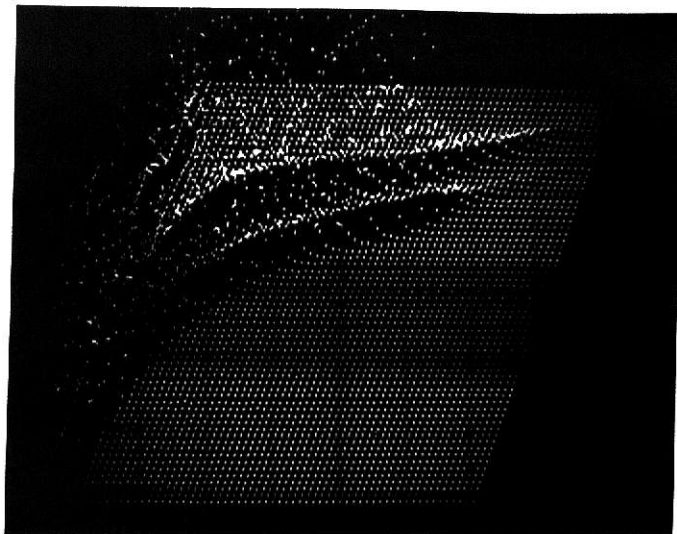


Figure 7. Photograph of Raw Data Grid from TAC Spectrometer System

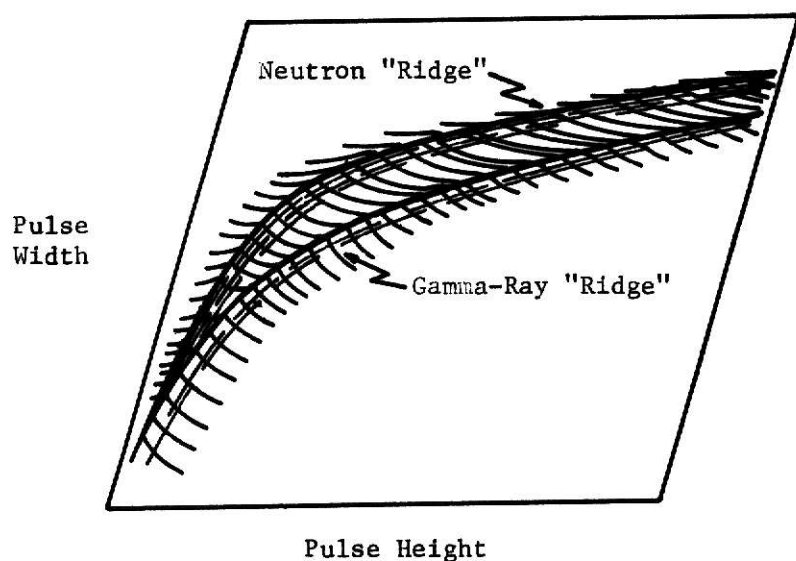


Figure 8. Diagram of Raw Data Grid from TAC Spectrometer System

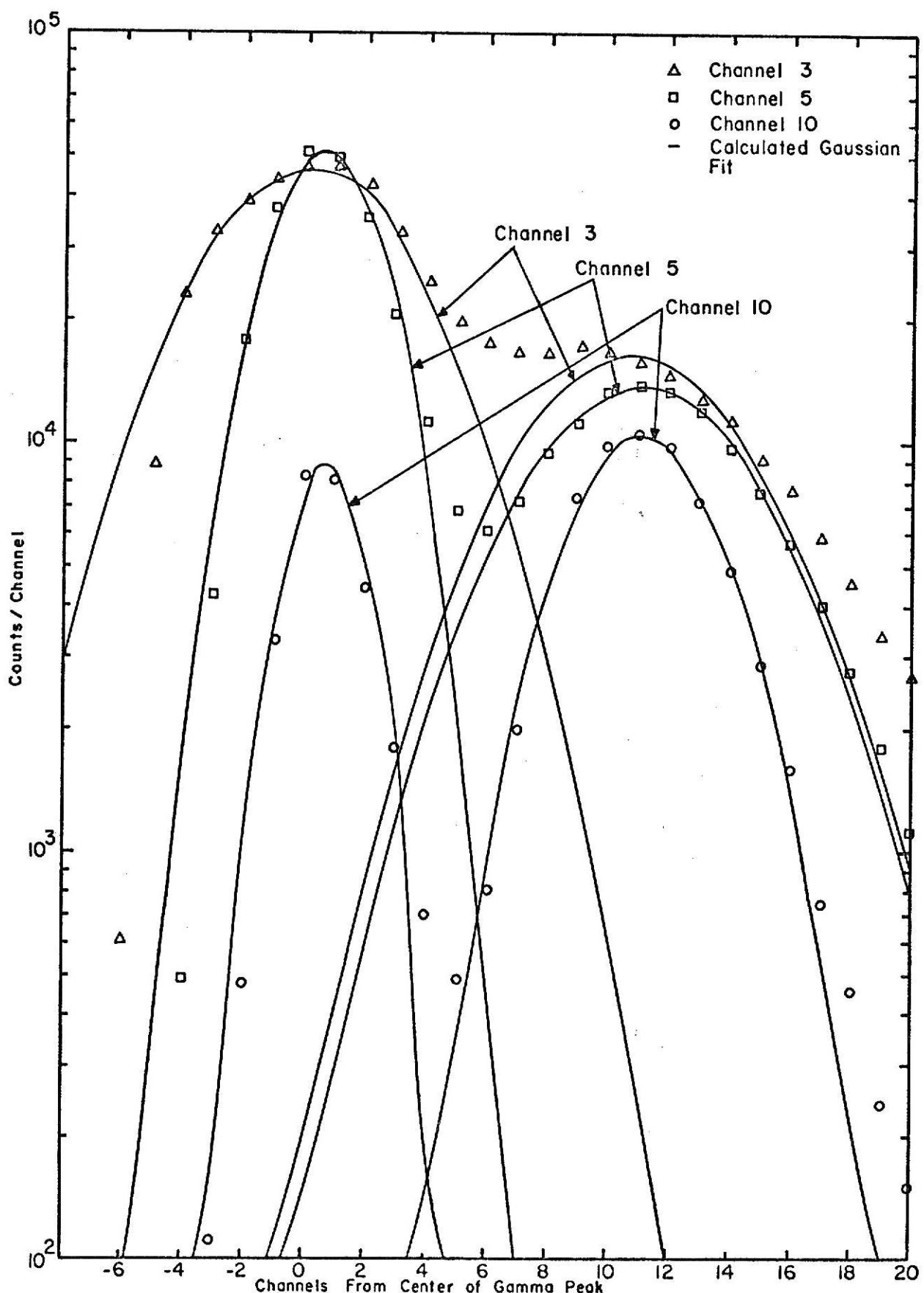


Figure 9. Distribution of Raw Data in Pulse Height-Pulse Width Data Grid at Various Pulse Height Channels

then arranges the data in a format of the form obtained using the KSU NE-213 neutron spectrometer system described by Meyer et al., and thus the data can be subsequently analyzed using existing computer codes.^{3,5,13}

With the neutron pulse height spectra in the proper format, it is then shifted to a "standard gain" using the standard ⁶⁰Co pulse height spectrum calibration data and the computer code, NUDASBIN I.¹³ The NUDASBIN I results are then unfolded using the unfolding codes FERDOR developed at ORNL by Burrus⁵ and DUFOLD developed at KSU by Coolbaugh.¹⁰

5.0 RESULTS AND CONCLUSIONS

5.1 14 MeV T(d,n)⁴He Neutron Energy Spectrum

The FERDOR unfolded neutron energy spectra of the T(d,n)⁴He reaction is presented in figure 10. The values of the flux in the peak region were fitted to a gaussian curve, and from this curve it was determined that the peak had a true center at 13.87 MeV and a full width at half-max, FWHM, of $1.384 \pm .016$ MeV. The calculated center of the peak, 13.87 MeV, is 0.23 Mev below the true 14.1 MeV energy of the product neutrons from the reaction. Although it is possible that this discrepancy is due to an error in the energy calibration of the system, this author feels that the shift is more likely caused by the FERDOR unfolding code. This is examined further in section 5.4.

The FWHM of the peak, a measure of the resolution of the spectrometer system, is nearly 25 per cent less than that reported by Verbinski using an NE-213 spectrometer system at ORNL. Thus, the KSU TAC spectrometer has better resolution at this energy than the ORNL NE-213 spectrometer.

Also evident in figure 10 is a 2.45 MeV peak due to the D(d,n)³He reaction which occurs when deuterons become embedded in the tritium target of the accelerator. The FWHM of the peak is approximately 0.7 MeV. This is also nearly 25 per cent better than the resolution reported by Verbinski at this energy and is in good agreement with other measurements made using the TAC system (Section 5.3).

5.2 TRIGA Mark II Fast Beam Port Neutron Spectra

Figure 11 shows the neutron energy spectrum of the fast beam port measured with both the TAC system and the 2 inch KSU NE-213 spectrometer.³ The measurements made with the two spectrometer systems are in good

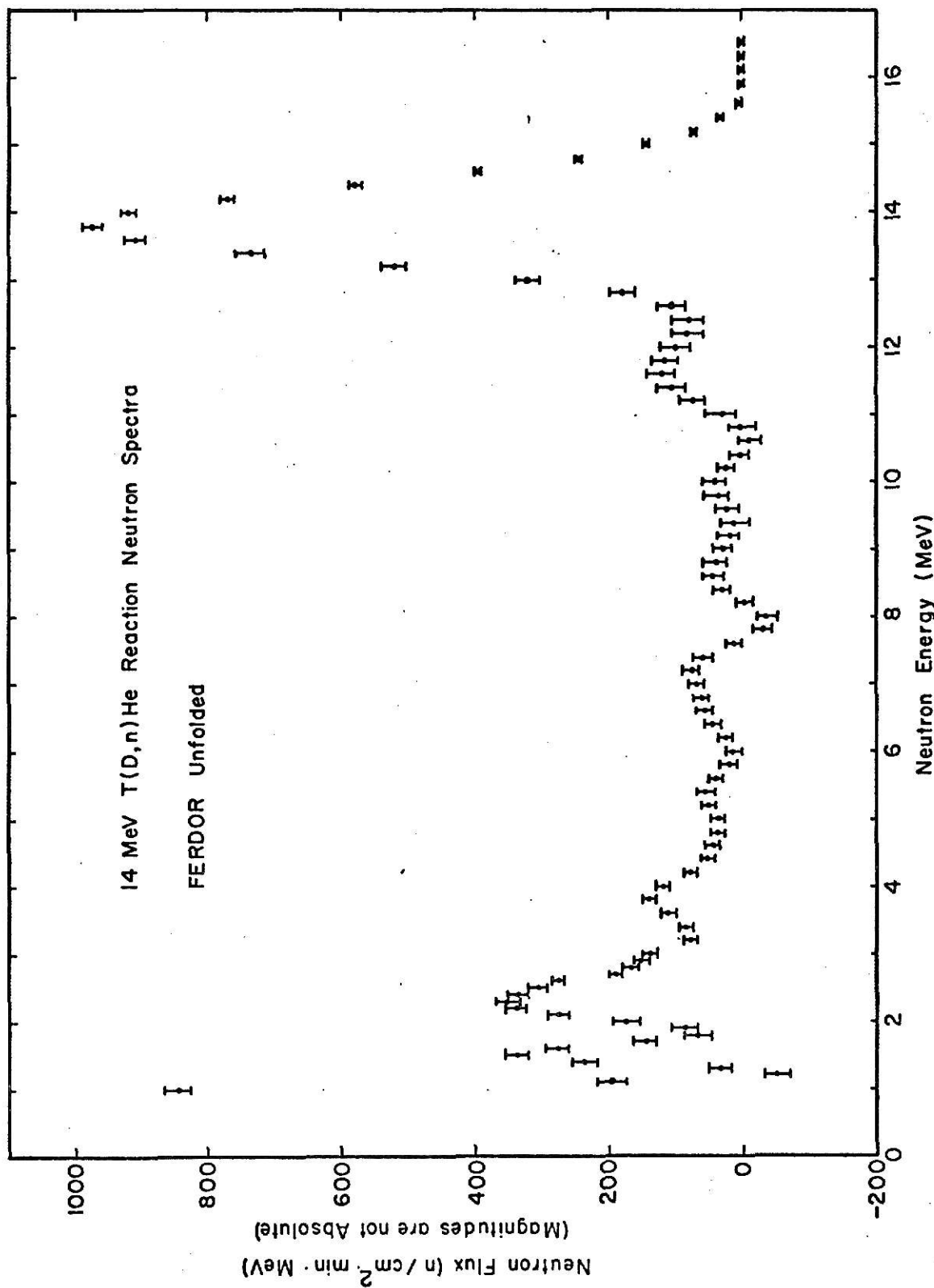


Figure 10. FERDOR Unfolded $T(d,n)^4\text{He}$ Reaction Neutron Spectra

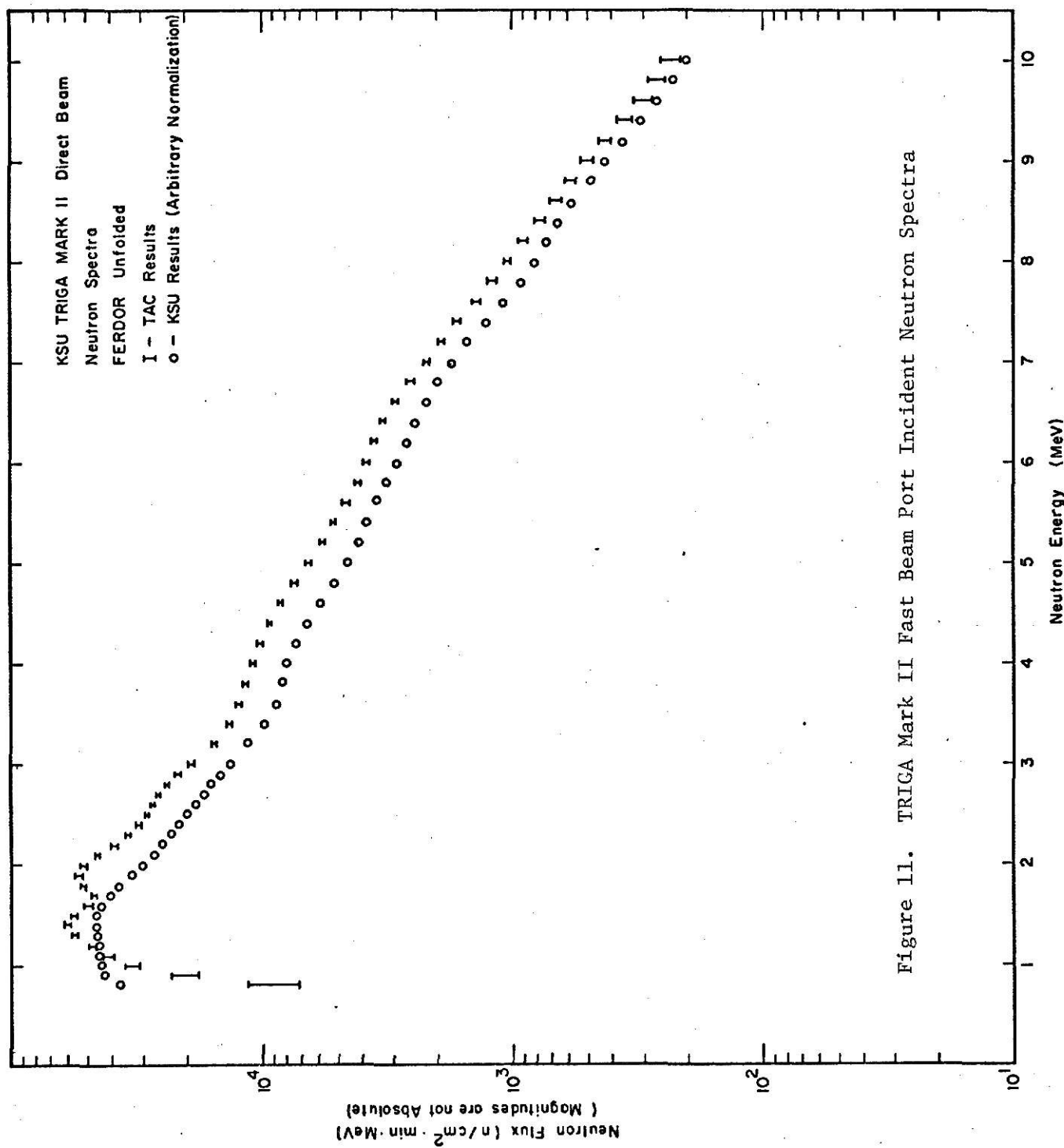


Figure 11. TRIGA Mark II Fast Beam Port Incident Neutron Spectra

agreement above about 1.7 MeV. Below 1.7 MeV the TAC measurement indicates a slight dip in the neutron flux which the measurement with the 2 inch KSU NE-213 spectrometer does not indicate. The dip in the flux indicated by the TAC measurement is probably in error because there is no physical reason to suspect such a depression at that energy. This phenomenon probably indicates that below about 1.7 Mev difficulty is encountered in separating neutrons from gammas in the raw data when a very strong gamma field is present while making the measurement as was the case in this instance.

5.3 TRIGA Mark II Fast Beam Port Neutron Spectra after Transmission

Through a Thick Oxygen Absorber

The neutron energy spectra after transmission through a thick oxygen absorber is shown in figure 12. The spectrum measured with the TAC spectrometer system is in good agreement with measurements made by Miller⁴ using the 2 inch KSU NE-213 spectrometer system. A gaussian fit of the peak indicates that the peak is centered at 2.34 ± 0.16 MeV with a FWHM of 0.599 ± 0.20 MeV. The center of the peak agrees well with the 2.35 MeV minimum in the oxygen cross section which causes the peak in the transmitted neutron spectrum.¹⁵ The FWHM of this peak is also about 25% less than that reported by Verbinski⁶ at ORNL for the same energy.

5.4 PuBe Neutron Energy Spectrum

Figure 13 shows the FERDOR unfolded PuBe neutron spectrum measured with the TAC system compared with that measured with the KSU spectrometer. Both spectra show minima at 1.7, 3.6, and 5.8 MeV, maxima at 1.3, 2.9, 4.2-4.4, and 6.4-7.0 MeV, and a shoulder at 9.4-9.6 MeV. The TAC results show a shoulder at 1.9-2.0 MeV, and the KSU results show a small peak at 1.8 MeV.

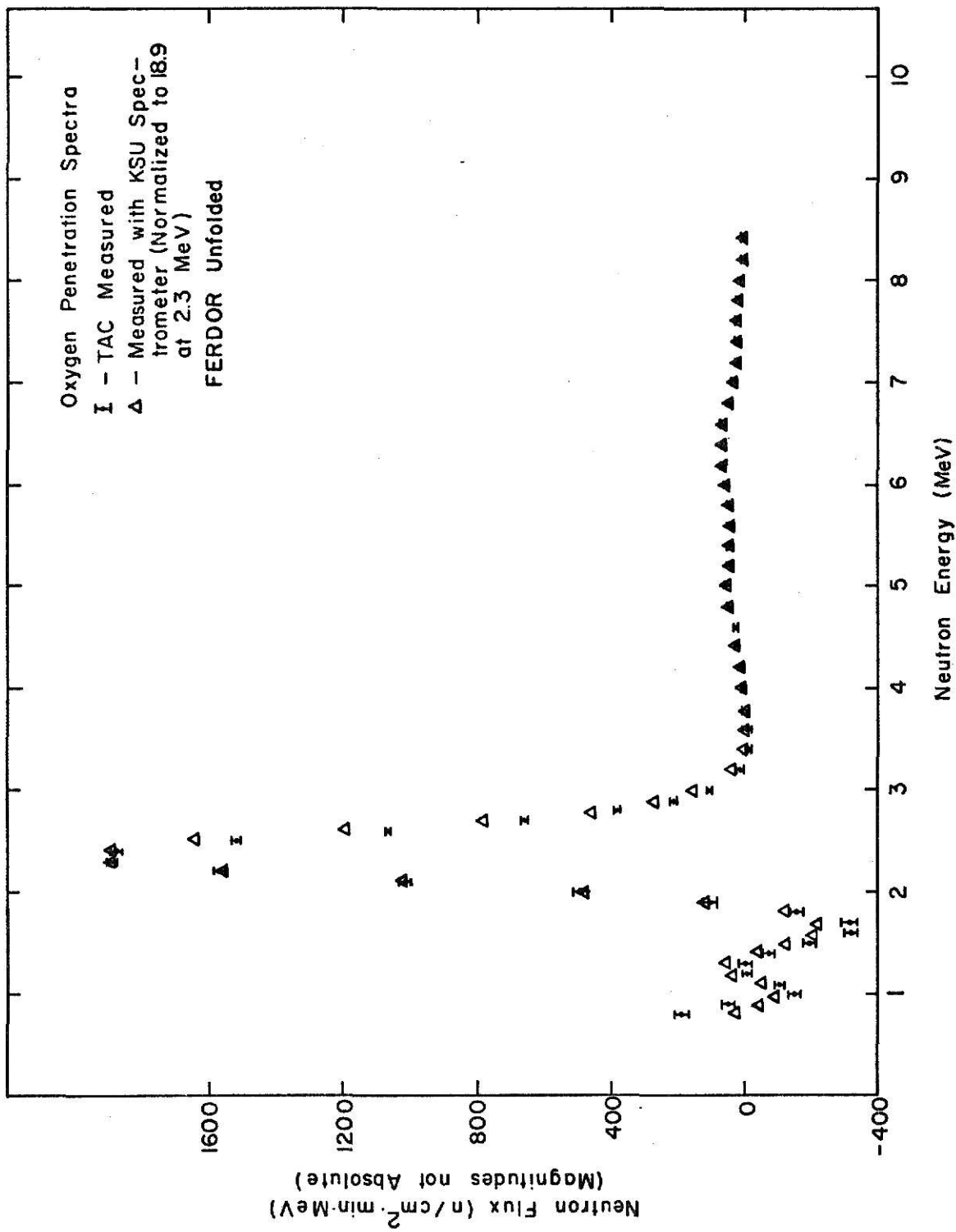


Figure 12. Oxygen Penetration Spectrum

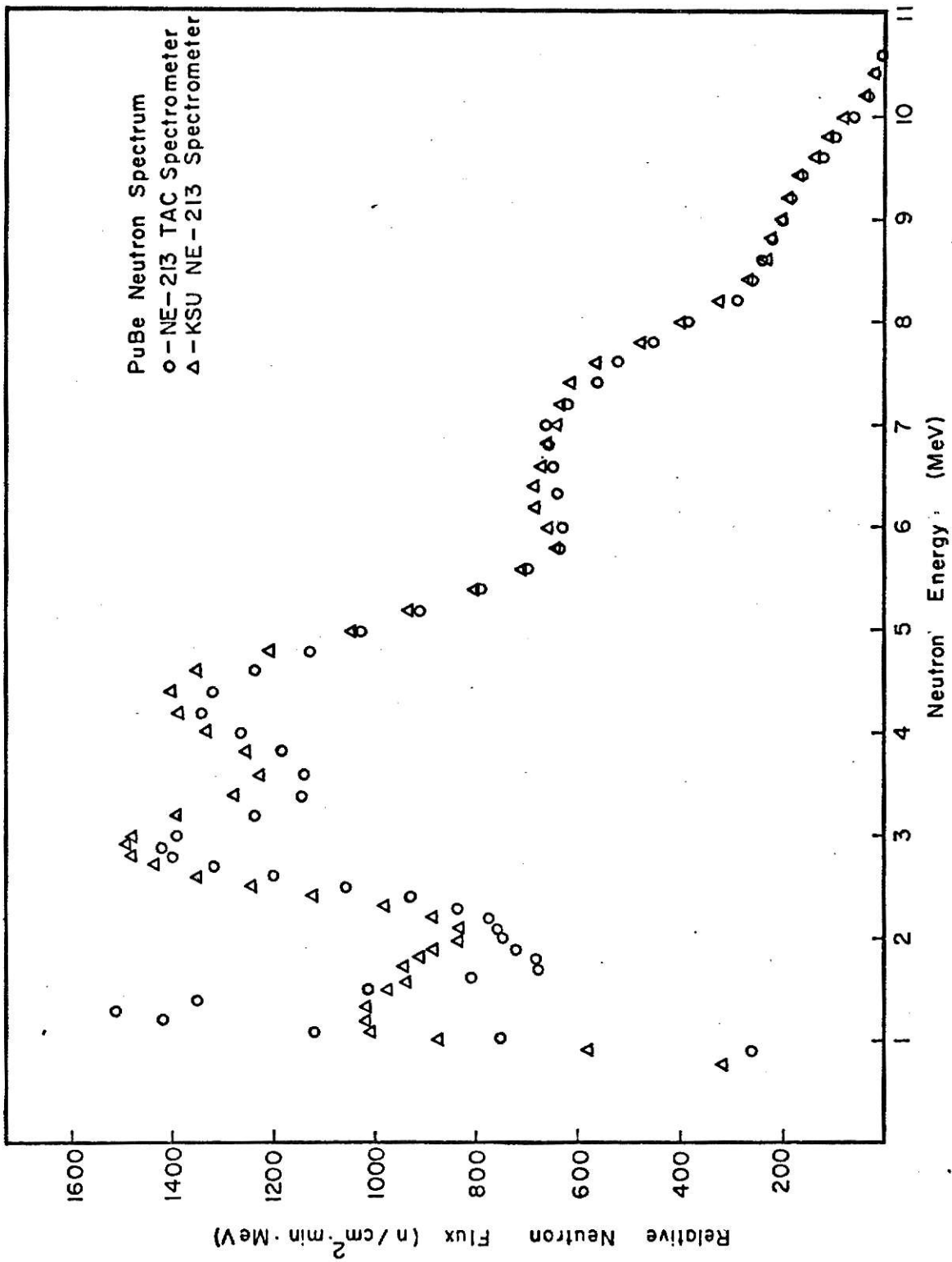


Figure 13. FERDOR Unfolded PuBe Neutron Spectrum

The TAC results are, in general, lower in magnitude than the KSU results. This is due to the fact that the TAC system has less overall efficiency than the KSU spectrometer (the TAC spectrometer is "dead" during the internal conversion time of the time to amplitude converter). Unfolding of the neutron pulse height spectra was completed using the known efficiency of the KSU spectrometer system because an absolute efficiency measurement of the TAC system has not been made. The unfolded TAC results thus lie below the unfolded KSU results because the TAC system is slightly less efficient than the 2 inch KSU spectrometer system.

Figure 14 shows the FERDOR unfolded PuBe spectrum compared with a normalized plot of the nuclear emulsion PuBe data of Lehman.⁹ The nuclear emulsion data are useful in describing the important features of the PuBe spectrum i.e., the minima at 1.6, 2.6, 3.8, 6.4, 7.1, and 9.0 MeV and maxima at 2.1, 3.5, 4.5, 6.6, 7.8, and 9.9 MeV.

In comparing the nuclear emulsion data and the FERDOR unfolded TAC results, it appears that a shift of about 0.2-0.3 MeV has occurred in the entire spectrum measured with the TAC system. It is difficult to say if this shift is a result of differences in the sources used or differences in measurement and unfolding techniques. This shift is in agreement however with the shift noticed in the measurement of the 14 MeV $T(d,n)^4\text{He}$ neutrons (section 5.1). This agreement tends to indicate that the shift may be caused by some anomaly in the unfolding technique used. Aside from the shift in the spectrum, the FERDOR unfolded TAC results agree well with the emulsion data although the TAC results exhibit poorer resolution as indicated by the shoulders at 2.0 and 9.4 MeV and the single broad peak from 6.0-7.5 MeV. In addition, the peak at 1.2 MeV in the TAC results is much larger than the rise in the spectrum shown in the emulsion data around 1.0 MeV.

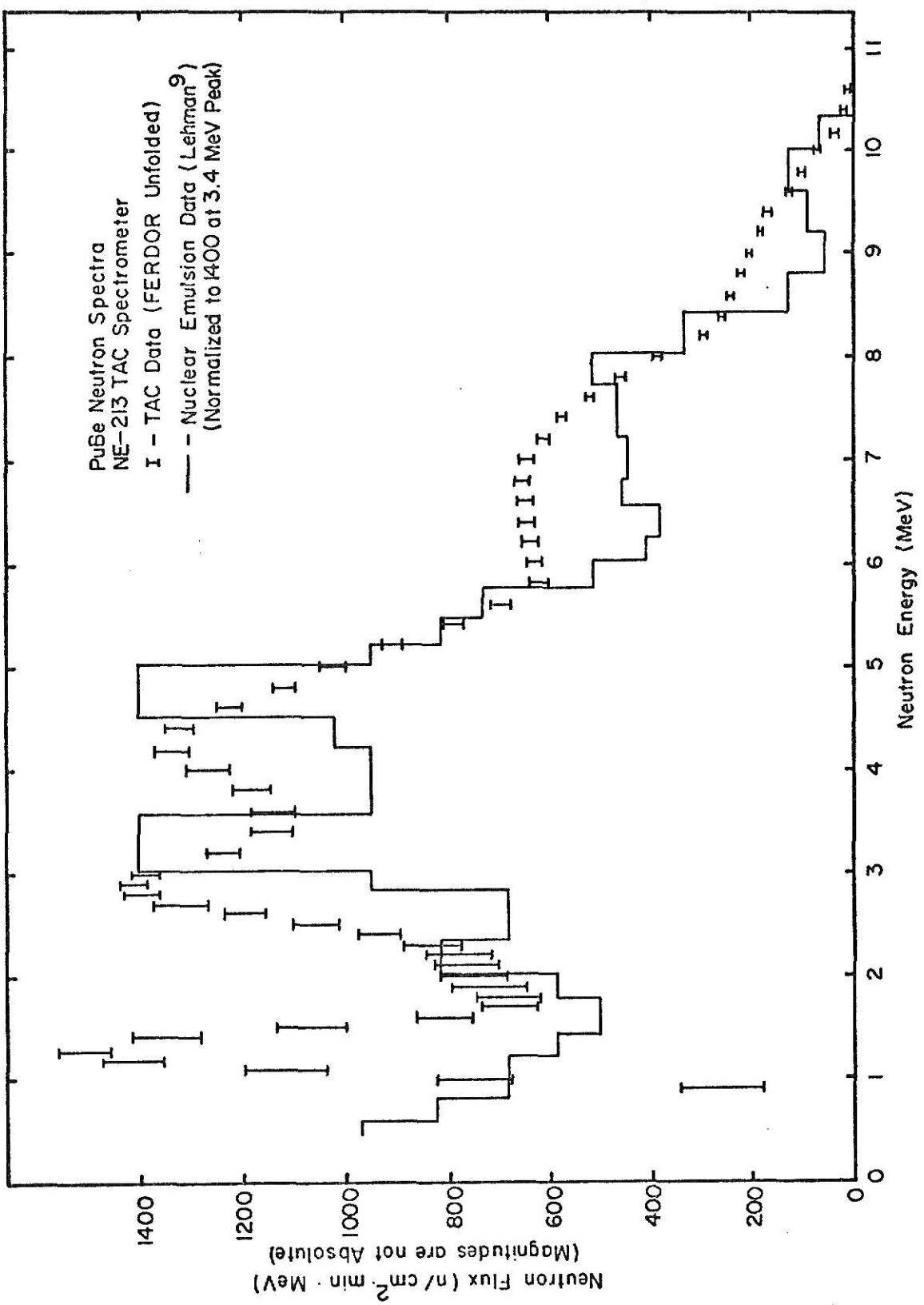


Figure 14. PuBe Neutron Spectrum

Though the results shown in figure 14 indicate that the TAC system has insufficient resolution to resolve the separate peaks in the emulsion data at 2.1, 6.6, 7.8, and 9.9 MeV, the results shown in figure 15 which were obtained by unfolding the same set of TAC data with the DUFOLD unfolding code¹⁰ show peaks at 2.0, 6.5, 7.5, and 9.9 MeV. The DUFOLD unfolded results indicate that the upper limit of the resolution of the PuBe spectrum shown in figure 14 is probably set by the FERDOR unfolding procedure and not by the raw data obtained with the TAC spectrometer.

5.5 Conclusions

In general, the results obtained by using the TAC spectrometer developed in this study agreed well at energies above 1.5 MeV with similar measurements using the KSU 2 inch spectrometer.^{3,4} Below 1.5 MeV considerable discrepancy was noted in the unfolded reactor fast beam port spectrum and the PuBe spectrum measured with the two systems. The unfolded PuBe spectra measured with the TAC spectrometer was also in disagreement with the nuclear emulsion data below about 1.5 MeV. The consistent disagreement of the TAC results with other measurements at energies below 1.5 MeV suggests that the TAC results are in error in this energy region. The error in this region is probably caused by the skewed gaussian distribution of the neutron and gamma-ray information in the raw data at low pulse heights as discussed in section 4.1. Attempting to fit a gaussian curve to a skewed distribution will obviously result in a large error, and that error in the low pulse height channels is probably the cause of the anomalous TAC results at energies below 1.5 MeV.

The oxygen penetration data and the $T(d,n)^4\text{He}$ data indicate that the resolution of the TAC spectrometer system is an improvement over the resolution reported by Verbinski⁶ for an NE-213 spectrometer at ORNL. In both

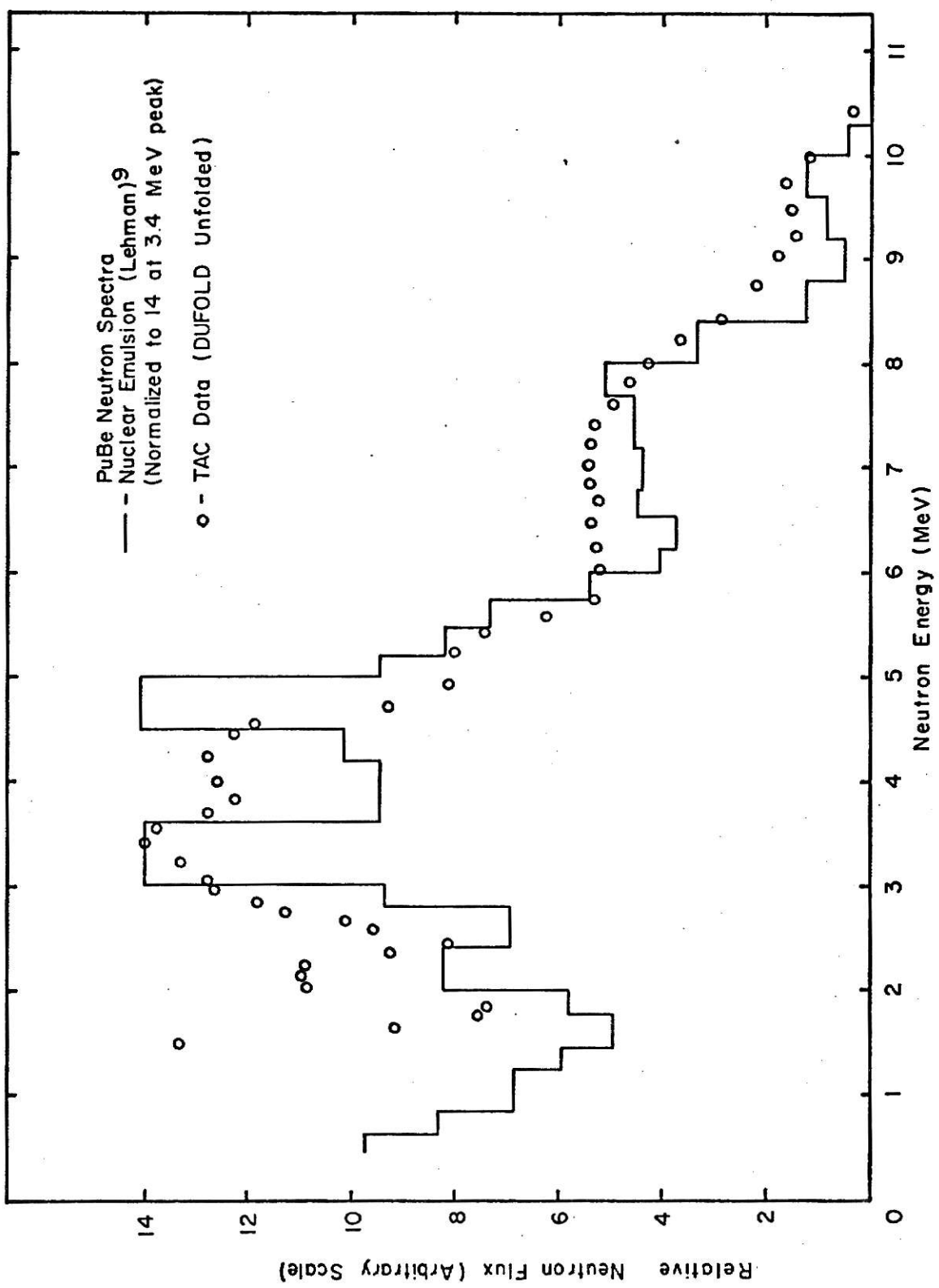


Figure 15. PuBe Neutron Spectrum

cases, the FWHM of the respective 2.34 and 13.87 MeV peaks was nearly 25% less than that reported by Verbinski at similar energies. These results indicate that the TAC spectrometer system is capable of providing results which are as good as those obtained using other NE-213 spectrometers even though the TAC spectrometer yields a total of just 128 channels of pulse height data.

This study has also demonstrated that optimal gamma-ray discrimination can be achieved by off-line computer analysis of the TAC data. This is certainly an advantage of this TAC system since the quality of the data obtained from a given measurement is not dependent upon some critical adjustment to determine the proper gamma-ray discrimination.

The TAC spectrometer system does have two disadvantages in comparison to other NE-213 spectrometers. First, since the data from the TAC system are collected in two large arrays, it is necessary to accumulate data for longer periods of time in order to obtain statistically meaningful data throughout the arrays. This necessitates tying up expensive auxiliary equipment such as a multiparameter analyzer, a reactor, or an accelerator for longer periods of time to make a specific measurement than is necessary with other NE-213 spectrometers. Secondly, an additional cost is incurred when doing the gamma-ray discrimination off-line by computer (The DISCRIM code costs about \$1.25 - \$1.50 per data set to run on an IBM 360/50 computer). This cost is not large however when compared with the cost of completing the remainder of the data analysis and unfolding procedure (\$65.00 - \$70.00 using the FERDOR unfolding routine).

In summary, the initial results presented in this study indicate that a TAC spectrometer system of the type described will produce results comparable to the results obtained by using other NE-213 spectrometer systems with little additional cost or effort.

6.0 SUGGESTIONS FOR FURTHER STUDY

Several aspects of the TAC spectrometer system developed in this study warrant further investigation. As noted in section 5.5, the erroneous TAC results below 1.5 MeV are probably caused by the attempt to fit a gaussian curve to the skewed distribution of neutron and gamma-ray information in the low pulse height channels during the off-line gamma-ray discrimination process in the DISCRIM code. This error can be corrected two ways. One way would be to investigate the present distribution of the neutron and gamma-ray information in the data grids and attempt to devise a procedure for fitting some type of skewed gaussian curve to the data where necessary. A second and probably more promising way to correct the error would be to search for a way of producing a "pulse shape signal" which has more nearly ideal characteristics. A more nearly ideal pulse shape signal would yield neutron and gamma-ray distributions in the data grids which are more nearly gaussian. The gaussian fitting procedure of the DISCRIM code would then better match the actual data and give correspondingly better results in the low energy region of the neutron spectra. Roush, Wilson, and Hornyak¹¹ have indicated that the use of delay-line pulse shaping to produce the bipolar "pulse shape signal" should provide better performance, particularly in the low energy region, than can be obtained by using the active amplifier in the present system.

Secondly, the efficiency of the TAC spectrometer system must be determined if the TAC spectrometer is to be used to make absolute flux measurements.

An investigation needs to be made of the optimum ratio of high gain to low gain for the two data sets that are taken for each spectrum measured.

The ratio of 2.5 used in this study is arbitrary and was chosen primarily for reasons of convenience. The high gain setting of the spectrometer system should be such that the resolution of the spectrometer in the low energy region, where the high gain data is applicable, is determined by the detector and photomultiplier tube rather than by the binning of the data in the multiparameter analyzer.

Fourth, additional monoenergetic responses need to be measured at energies other than those measured in this study. This information would provide enlarged knowledge of the variation in resolution with energy. It would also provide a much more meaningful comparison of the resolution of the TAC spectrometer developed in this study with the resolution of other spectrometers.

Fifth, a study should be made to determine if it is possible to propagate errors through the gamma-ray discrimination process in the DISCRIM code. This would provide a new and useful means of assessing the degree of confidence that can be placed in a particular set of data based on the degree of optimization that can be achieved in the gamma-ray discrimination procedure.

Finally, if at some future time additional equipment becomes available that is capable of producing a data grid larger than 64x64, many of the problems presently encountered with the TAC system can be eliminated. If the grid size could be increased by a factor of 2.5 to 64 X 160, a single set of data would contain all the information presently available in the two sets of data (high gain and low gain) taken for each measurement. A grid size larger than 64 X 160 would allow even greater energy resolution, particularly in the low energy region where the present TAC system gives anomalous results, or better neutron and gamma-ray separation in the data

grid, or both. Increasing the size of the data grid must be done with caution however because increasing the size of the data grid increases the length of time necessary to get statistically good results. This author feels that with the TAC system in its present configuration the "best" practical grid size would be 64 x 256. If improvement can be made in the neutron-gamma-ray distribution at low energies by the use of delay-line clipping to produce the pulse shape signal, then increasing the number of divisions in the pulse width parameter of the data grid may result in better neutron and gamma-ray separation. At present however, the problem of separating neutron and gamma-ray information in the low pulse height channels appears to be due primarily to the non-gaussian distribution of the data in those channels and not by the separation of the data in the data grid. Thus, unless the distribution of the data in the low pulse height channels can be made more gaussian very little improvement can probably be made in the gamma-ray discrimination process at low pulse height channels.

7.0 ACKNOWLEDGEMENTS

The author wishes to express his sincerest gratitude to Dr. W. Meyer under whose direction this study has been performed. A note of thanks is extended to Dr. M. S. Krick, B. Starr, and J. W. Thiesing of the Department of Nuclear Engineering at Kansas State University for their help and advice in this work. The Financial support provided by the Department of Nuclear Engineering, the Atomic Energy Commission, and the Department of Defense (Project THEMIS, Director Dr. H. J. Donnert) for this work is greatly appreciated. Also appreciated are the computer time and special services provided by the Kansas State University Computing Center. Finally, I wish to express my deepest love and appreciation to my wife, Elynor, for her continued help and encouragement throughout this study.

1. F. X. Haas, Jr., and J. T. McCarthy, "A Stilbene Fast-Neutron Spectrometer for the Study of the Neutron Spectrum of a PuBe Source," Nuc. Inst. and Meth., 50(1967) 340-342.
2. G. G. Simons, "Development, Calibration and Utilization of the KSU NE-213 Fast-Neutron Spectrometer," Ph.D. Dissertation, Nuclear Engineering, Kansas State University (1968).
3. W. Meyer, et al., "Fast Neutron Transmission Measurements for Reactor Core and Shielding Materials," Technical Progress Report to Division of Research US/AEC (AEC Contract No. AT(11-1) 2049), COO-2049-1 Nuclear Engineering, Kansas State University (February, 1970).
4. W. Miller "The Evaluation of Minima in Total Neutron Cross-Section by Transmission of Fission Spectra Through Thick Samples," Masters Thesis, Nuclear Engineering, Kansas State University (1971).
5. W. R. Burrus, "Utilization of a Priori Information in the Statistical Interpretation of Measured Distributions," (Dissertation) ORNL-3743 (1964).
6. V. V. Verbinski, et al., "Calibration of an Organic Scintillator for Neutron Spectrometry," Nucl. Inst. and Meth., 65, 8-25 (1968).
7. J. W. Thiesing, Personal Communication, Kansas State University.
8. C. E. Bliss, N. D. Eckhoff, and H. J. Donnert, "Fluence Measurements for 14.7 MeV Neutrons," Nuc. Inst. and Meth., 78 (1970) 86-92.
9. R. L. Lemman, "The Origin of Neutron Groups in Be(α ,n) Sources," Nuc. Inst. and Meth. 60, 253-260 (1968).
10. M. J. Coolbaugh, "Fast-Neutron Spectroscopy in Aqueous Media Using an NE-213 Proton Recoil Neutron Spectrometer System," Ph.D. Dissertation, Nuclear Engineering, Kansas State University (1971).
11. M. L. Roush, M. A. Wilson, and W. F. Hornyak, "Pulse Shape Discrimination," Nuc. Inst. and Meth., 31 (1964) 112.
12. R. B. Owen, "Pulse Shape Discrimination - A Survey of Current Techniques," I.E.E.E. Trans. Nuc. Sci., NS9, 3, 285.
13. W. Meyer, J. W. Thiesing, and C. M. Estes, "Intercalibration of the KSU NE-213 Fast-Neutron Spectrometer System," Technical Progress Report to Division of Research US/AEC (AEC Contract No. AT(11-1) 2049), COO-2049-3 Nuclear Engineering, Kansas State University (December, 1970).
14. N. D. Eckhoff, "Optimal Neutron Activation Analysis," Ph.D. Dissertation, Nuclear Engineering, Kansas State University (1968).
15. S. Cierjacks, P. Forti, D. Kopsch, L. Kropp, J. Nebe, and H. Unseld, "High Resolution Total Neutron Cross-Sections Between 0.5-30 MeV," KFK-1000, Institut fur Angewandte Kernphysik, Karlsruhe (June, 1968).

9.0 APPENDICES

APPENDIX A

Derivation of Weighted Least Squares Gaussian Curve Fitting Equations

The equations used in the DISCRIM code to effect the weighted least squares gaussian curve fitting to the neutron and gamma-ray "ridges" in the raw data from the TAC spectrometer are derived below.

The general equation for a gaussian curve can be written as

$$y = y_0 \cdot \text{EXP}(-(x - x_0)^2/b_0) \quad (1)$$

where y = value of gaussian at point x

y_0 = magnitude of gaussian at center

x_0 = center of gaussian

b_0 = decay constant.

Equation 1 can be discretized for any finite set of points by evaluating it at the desired set of points; i.e.,

$$y_i = y_0 \cdot \text{EXP}(-(x_i - x_0)^2/b_0) \quad . \quad (2)$$

This equation can be linearized by taking the natural logarithm of both sides.

This yields,

$$\ln(y_i) = \ln(y_0) - (x_i - x_0)^2/b_0 \quad (3)$$

After expanding the squared term and collecting like powers of x , equation 3 can be written as

$$z_i = x_i^2 s_1 + x_i s_2 + s_3 \quad (4)$$

where $z_i = \ln(y_i)$

$s_1 = -1/b_0$

$s_2 = 2x_0/b_0$

$s_3 = \ln(y_0) - x_0^2/b_0$

Equation 4 can be written in matrix form for n points as

$$\begin{bmatrix} x_1^2 & x_1 & 1 \\ x_2^2 & x_2 & 1 \\ \vdots & \vdots & \vdots \\ x_n^2 & x_n & 1 \end{bmatrix} \cdot \begin{bmatrix} s_1 \\ s_2 \\ s_3 \end{bmatrix} = \begin{bmatrix} z_1 \\ z_2 \\ \vdots \\ z_n \end{bmatrix} \quad (5)$$

This equation is of the form

$$X \cdot S = Z \quad (7)$$

If n is greater than 3, the weighted least squares solution of equation 7 for S is found by solving

$$X^T W X S = X^T W Z$$

The solution is

$$S = (X^T W X)^{-1} X^T W Z \quad (9)$$

W is a variance-covariance weighting matrix which weights each of the equations by the inverse variance and covariance of Z .¹⁴ In this work each of the Z_i is independent of the other Z_i . Thus, the covariance in the weighting matrix are zero.

The variance of Z_i is

$$Z_i^2 = (\partial Z_i / \partial y_i)^2 \sigma^2 y_i = (1/y_i)^2 \sigma^2 y_i \quad (10)$$

The weighting matrix can thus be written as

$$W = \begin{bmatrix} \frac{y_1^2}{\sigma^2 y_1} & 0 & 0 & \dots & 0 \\ 0 & \frac{y_2^2}{\sigma^2 y_2} & 0 & \dots & 0 \\ \vdots & & \ddots & & \vdots \\ 0 & \dots & & & \frac{y_n^2}{\sigma^2 y_n} \end{bmatrix} \quad (11)$$

After S has been solved for, the parameters of the gaussian fit are easily found from the relations

$$b_0 = -1/S_1 \quad (12)$$

$$x_0 = b_0 S_2 / 2 \quad (13)$$

$$y_0 = \text{EXP}(S_3 + x_0^2/b_0) \quad (14)$$

The full width at half-max (FWHM) of the gaussian is determined from

$$y_0/2 = y_0 \cdot \text{EXP}(-(\text{FWHM}/2)^2/b_0) \quad . \quad (15)$$

Solving for FWHM yields

$$\text{FWHM} = 2(b_0 \cdot \ln(2))^{\frac{1}{2}} \quad . \quad (16)$$

The area under the gaussian in the data grid is

$$\text{AREA} = \int_0^{64} y_0 \cdot \text{EXP}(-(x - x_0)^2/b_0) dx \quad . \quad (17)$$

or

$$\text{AREA} \approx y_0 \int_{-\infty}^{\infty} \text{EXP}(-(x - x_0)^2/b_0) dx \quad . \quad (18)$$

The exact closed form solution to 18 is

$$\text{AREA} = y_0 \sqrt{b_0 \pi} . \quad (19)$$

APPENDIX B

B-1.0 Gamma-Ray Discrimination Code, DISCRIM

This computer code separates the neutron and gamma-ray information in the data grids from the TAC spectrometer, prints both the neutron and gamma-ray pulse height spectra, plots a semilog plot of the neutron pulse height spectra, and, if desired, punches the neutron pulse height spectra for further analysis. In addition, background data can be subtracted from the foreground, if desired. This must be done with extreme caution however, because the subtraction is done point by point in the data grid. Thus, the pulse height and pulse width gain must be identical in both the foreground and background data grids if the background option is used. A provision is also made in the code to correct for overflows in the foreground data. No provision is made to correct for overflows in the background data.

The code divides the data grid into four pulse height regions. In the first region, the first two or three pulse height channels, there is little or no data because of the characteristics of the multiparameter analyzer. The code ignores this region and sets the number of neutron and gamma-ray counts in this region equal to zero.

In the next three regions, the program proceeds through the data one pulse height channel at a time. At each pulse height channel it looks at the corresponding 64 pulse width channels and separated the neutron induced and gamma-ray induced information.

In the second region the program fits a gaussian to the largest peak, subtracts the least squares fit from the data, then fits the peak that is left with a gaussian. The gaussian fit to the smaller peak is then subtracted from the original data to give a new estimate of the larger peak. This process

repeats itself until the change in the calculated area of the largest peak converges to a value smaller than a limit that is read in as input (The convergence limit was set at one per cent in this work.) or until a specified number of iterations is exceeded.

In the third region the two peaks in the data are only fit once with a gaussian curve. In this region the peaks are separated well enough that only a single iteration is necessary.

In the fourth and last region the data do not have sufficient statistics to enable an accurate gaussian fit of the peaks. The neutron and gamma-ray data in the grid are well separated however, and they are separated by simply summing the data on each side of the minima between the two peaks.

A print option is available in the computer code, but it should be used only if difficulty is encountered in analyzing a set of data. The print option, when used, will give a detailed listing of the raw data, every gaussian fit, and the raw data after each gaussian fit has been subtracted during the iteration process. This option is useful for locating errors in the data (usually unknown overflows) which cause erroneous results.

B-1.1 DISCRIM Input Data Format

Card	Format	Variable and Description
1	215	<p>1. J01MIN = Number of channels from center of largest peak toward smaller peak to be included in first gaussian fit of iterative routine</p> <p>2. J01MAX = Number of channels from center of largest peak away from smaller peak to be included in first gaussian fit of iterative routine</p>
2	15	1. NCHK = Maximum number of iterations allowed in iterative routine
3	2F5.0	<p>1. CONV = Convergence limit for iterative routine. Iteration is terminated when the relative change in area of the largest peak in n^{th} iteration becomes less than CONV</p> <p>2. YFRAC = Fraction of the peak to be excluded from gaussian fit. All data which are greater than YFRAC times the maximum value of the peak are included in the least squares fit.</p>
4	15,45H	<p>1. CHANE1 = First channel that discrimination is to be attempted</p> <p>2. LABEL = An arbitrary alphanumeric label to identify the data</p>
5	515	<p>1. IMAX1 = Last channel iterative routine is to be done</p> <p>2. IMAX2 = Last channel gaussian fit is to be done. Simple sum of peaks is done beyond IMAX2</p> <p>3. PNCH = 0 if punched output is not desired = 1 if punched output is desired</p> <p>4. PRNT = 0 if detailed printing is not desired = 1 if detailed printing is desired</p>

5. BKG = 0 if no background data is to be subtracted
= 1 if background data is to be subtracted

6(Deck) 6X,12F6.0 4096 Channel foreground data deck

7(Deck) 215 Specify all (I,J) locations of overflows in data grid. Use as many cards as necessary with just one (I,J) location per card.

8 ---- Blank card

9(Deck) ---- Background deck if any. (If "BKG" on card 5 is 1). Deck consists of cards 4, 6, and 8.

10(Decks) ---- Other sets of data (cards 4-9). Any number of data sets may be run at one time.

11 ---- Blank card. Put an extra blank card behind all the data to terminate the program.

- Notes:
1. The values specified on cards 1-3 are read only once and used for all data sets.
 2. If background is subtracted, the foreground and background data must both have identical pulse width and pulse height gains since the background subtraction is done point for point in the data grid.

B-1.2 DISCRIM Code Listing

```

C      PUT DATA IN THIS FORM.
C
C      CODE SPECIFICATIONS.....
C          0) SPECIFY THE TWO "J" CRITERIA FOR THE GAUSSIAN FITS.
C          1) MAX NO OF ITERATIONS ALLOWED IN STRIPPING ROUTINE (I5)
C          2) CONVERGENCE CRITERIA AND PEAK FRACTION VALUE FOR STRIPPING
C             ROUTINE. (2F5.0)

C      DATA PACK FORMAT.....
C          1) CHANNEL WHERE YOU WANT TO START DISCRIMINATING (I5).  SPECIFY
C             'CHANNEL' FOR EACH DATA SET.  LABELS MAY BE PUNCHED IN CH 10-45.
C          1A) SPECIFY IMAX1, IMAX2, PNCH, PRNT, AND BACKGROUND (5I5)
C              (MAKE "BACKGROUND" NONZERO IF BKG GRID IS TO BE SUBTRACTED)
C          2) 64 X 64 GRID OF DATA
C          3) GIVE (I,J) LOCATIONS OF ALL OVERFLOWS IN THE DATA GRID. (2I5)
C              ONLY ONE OVERFLOW LOCATION PER CARD.  USE AS MANY CARDS AS NECESSARY
C          3A) 64 X 64 GRID OF BKG DATA IF ANY.
C          4) PUT A BLANK CARD BEHIND EACH DATA SET.
C          5) PUT ANOTHER BLANK CARD BEHIND ALL THE DATA.  IE.. THERE SHOULD BE
C              TWO BLANK CARDS AT THE VERY END OF THE DATA.  THERE SHOULD BE ONE
C              BLANK CARD BETWEEN EACH SET OF DATA ( A 64 X 64 GRID).

C      "PRNT" IS A CODE TO CAUSE A DETAILED PRINTING OF THE PEAK FITS.
C      MAKE "PRNT" NONZERO TO CAUSE PRINTING
C      "NCHK" IS THE MAX NO OF ITERATIONS ALLOWED IN THE STRIPPING ROUTINE.
C      "CONV" IS THE CONVERGENCE CRITERIA FOR THE STRIPPING ROUTINE.
C      "CHANNEL" IS THE LOWEST ENERGY CHANNEL THAT CAN BE SEPARATED.
C      "PNCH" IS A CODE FOR PUNCHING NEUTRON SPECTRA.  MAKE NONZERO TO GET
C      PUNCHED CARDS.
C      IMAX1= THE LAST CHANNEL THAT THE STRIPPING IS TO BE DONE.
C      IMAX2= THE LAST CHANNEL THAT A GAUSSIAN FIT IS TO BE DONE. ( DONE FROM
C      IMAX1 TO IMAX2)
C      BEYOND IMAX2 JUST A SIMPLE SUM IS TAKEN 10 CHANNELS EITHER SIDE OF THE
C      MINIMUM BETWEEN THE PEAKS.

C      INTEGER CHANNEL,CHECK,PNCH,PRNT
C      DIMENSION Z(4096),XNEUT(64),GAMA(64),X(64),Y(64),V(64),BKG(4096)
C      DIMENSION C1(64),D2(64),PL(64),PS(64)
C      THE VARIABLES IN THIS READ STATEMENT ARE UPPER AND LOWER LIMIT CRITERIA
C      FOR THE GAUSSIAN FITTING SECTION.
C      READ 64,JO1MIN,JO1MAX
C      READ 64,NCHK
C      READ 65,CONV,YFRAC
100    READ 57,CHANNEL
        IF(CHANNEL.EQ.0) GO TO 101
        READ 51,IMAX1,IMAX2,PNCH,PRNT,NBKG
        READ 50,Z
        PRINT 56
        PRINT 57,CHANNEL
        PRINT 58
        PRINT 515
        PRINT 516
        PRINT 517
C      THIS SECTION CORRECTS FOR OVERFLOWS AT THE SPECIFIED (I,J) LOCATIONS
C      IN THE MAIN DATA.
1      READ 51,I,J
        IF(I.EQ.0) GO TO 603
        K=(J-1)*64 + I
        Z(K)=Z(K) + 1.0E5

```

```

GO TO 1
603 IF(NBKG.EQ.0) GO TO 2
READ 65,DUMMY
READ 50,BKG
READ 65,DUMMY
C      "DUMMY" IS A DUMMY VARIABLE TO MAKE THE BKG DATA PACKS THE SAME AS
C      THE OTHER DATA PACKS. IT IS NOT USED.
DO 602 I=1,4096
602 Z(I)=Z(I) - BKG(I)
2 E0=0.
KMIN=0
KG=0
KN=0
JLO=5
N=CHANNEL-1
DO 98 I=1,N
GAMA(I)=0.
XNEUT(I)=0.
98 PRINT 519,I,XNEUT(I),KN,GAMA(I),KG
KGCHK=1
KNCHK=1
C  THIS SECTION DOES THE DISCRIMINATION.
DO 1000 I=CHANNEL,64
DO 3 J=1,64
M=I + (J-1)*64
V(J)=Z(M)
Y(J)=Z(M)
3 X(J)=Z(M)
XN=0.
XG=0.
GAMA(I)=0.
XNEUT(I) = 0.
IF(KG.LT.KGCHK) KG=KGCHK
IF(KN.LT.KNCHK) KN=KNCHK
KNCHK=KN
KGCHK=KG
KMINCK=KMIN
LA=0
JLO=KG-6
KDIFF=KN-KG
KN=JLO
KG=JLO
IF(JLO.LT.5) JLO=5
C  **THIS SECTION STRIPS OUT THE PEAKS ONE AT A TIME
IF(I.GT.IMAX1) GO TO 70
IF(PRNT.EQ.0) GO TO 103
PRINT 512
PRINT 513,I
PRINT 505
PRINT 504,V
103 CHECK=0
X1CHK=1.0
X1=0.
M=0
C  THIS LOOP FINDS THE CENTER CHANNEL OF THE HIGHEST PEAK
DO 71 J=JLO,64
IF(X(J).LT.X1) GO TO 71
X1=X(J)
K1=J
71 CONTINUE

```

```

XK1=.5*V(K1)
JL=K1-6
JU=K1+6
CALL SSCHK(JL,JU)
RATIO=X(JU)/X(JL)
CALL DERIV(X,K1,RATIO,DMIN)
IF(1.-RATIO) 72,72,73
72 KUP1=K1 + JO1MIN
KLO1=K1 - JO1MAX
GO TO 74
73 KUP1= K1 + JO1MAX
KLO1= K1 - JO1MIN
74 CALL SSCHK(KLO1,KUP1)
IF(X(K1-1).LT.XK1) X(K1-1)=XK1
IF(X(K1+1).LT.XK1) X(K1+1)=XK1
NDP=KUP1 - KLO1 + 1
CALL PEAK(KLO1,NDP,Y,X)
CALL GAUSS(NDP,KLO1,Y,X1,E1,B1,Y1)
C THIS LOOP SUBTRACTS OFF THE FIRST PEAK
X2=0.
CALL CALPK(PL,Y1,E1,B1)
DO 76 J=5,64
X(J)= V(J) - PL(J)
IF(X(J).LT.1.) X(J)=1.
IF(X(J).LT.X2) GO TO 76
E=J
IF(ABS(E-E1).LT.DMIN) GO TO 76
X2=X(J)
K2=J
76 CONTINUE
XK2=.5*X(K2)
IF(X(K2-1).LT.XK2) X(K2-1)=XK2
IF(X(K2+1).LT.XK2) X(K2+1)=XK2
CALL DAMP(X,D2,CHECK)
IF(PRNT.EQ.0) GO TO 81
PRINT 506,CHECK
PRINT 504,PL
PRINT 508
PRINT 504,X
81 Y2X=YFRAC*T*X2
KLO2=1
KUP2 = 1
DO 600 J=2,5
JL=K2-J
JU=K2+J
CALL SSCHK(JL,JU)
IF(X(JL).GT.X(JL+1)) KLO2=JL+1
IF(X(JU).GT.X(JU-1)) KUP2=JU-1
IF(X(JL).LT.Y2X.AND.KLO2.EQ.1) KLO2=JL
IF(X(JU).LT.Y2X.AND.KUP2.EQ.1) KUP2=JU
600 CONTINUE
IF(KLO2.LT.JL) KLO2=JL
IF(KUP2.EQ.1) KUP2=JU
NDP=KUP2 - KLO2 + 1
CALL PEAK(KLO2,NDP,Y,X)
CALL GAUSS(NDP,KLO2,Y,X2,E2,B2,Y2)
K2=E2
CONVP=(X1-X1CHK)/X1CHK
C** THIS SECTION (TO 91) SUBTRACTS OFF THE SMALLER PEAK FROM THE ORIGINAL
C COMPLEX PEAK STRUCTURE THEN RETURNS TO STATEMENT 74 TO FIT A GAUSSIAN

```

```

C      TO THE LARGEST PEAK WHICH HAS BEEN CORRECTED BY AN ESTIMATE OF THE
C      CONTRIBUTION OF THE SECND PEAK.  THIS PROCESS WILL BE REPEATED UNTIL
C      THE NUMBER OF ITERATIONS SET IN THE FOLLOWING 'IF' STATEMENT HAS BEEN
C      MET OR THE ITERATION RESULTS IN LESS FRACTIONAL IMPROVEMENT THAN
C      SPECIFIED IN STATEMENT 900.
C      IF(CHECK.EQ.ACHK) GO TO 93
900 IF(ABS(ICONVP).LT.CONV) GO TO 93
      CHECK=CHECK+1
      X1CHK=X1
      CALL CALPK(PS,Y2,E2,B2)
C      THIS LOOP SUBTRACTS OFF THE SECOND PEAK
      DO 91 J=5,64
      X(J) = V(J) - PS(J)
      IF(X(J).LT.1.) X(J)=1.
91   CONTINUE
      L=CHECK-1
      CALL DAMP(X,O1,L)
      IF(PRNT.EQ.0) GO TO 82
      PRINT 507,CHECK
      PRINT 504,PS
      PRINT 508
      PRINT 504,X
      PRINT 514,X1,X2
82   Y1X=YFRACT*V(K1)
      KLO1=1
      KUP1=1
      DO 92 J=2,5
      JL=K1-J
      JU=K1+J
      CALL SSCHK(JL,JU)
      IF(X(JL).GT.X(JL+1)) KLO1=JL+1
      IF(X(JU).GT.X(JU-1)) KUP1=JU-1
      IF(X(JL).LT.Y1X.AND.KLO1.EQ.1) KLO1=JL
      IF(X(JU).LT.Y1X.AND.KUP1.EQ.1) KUP1=JU
92   CONTINUE
      IF(KLO1.EQ.1) KLO1=JL
      IF(KUP1.EQ.1) KUP1=JU
      GO TO 74
C      THIS STATEMENT DETERMINES WHICH PEAK IS THE NEUTRON PEAK
93   IF(E2-E1) 78,78,79
78   KN=K1
      EO=E1
      YO=Y1
      BO=B1
      BOG=B2
      EOG=E2
      XNEUT(I)=X1
      KG=K2
      GAMA(I)=X2
      KLO=KLO1
      GO TO 80
79   KN=K2
      EO=E2
      YO=Y2
      BO=B2
      BOG=B1
      EOG=E1
      XNEUT(I)=X2
      GAMA(I)=X1
      KG=K1

```

```

KLO=KLO2
80 KUP=KLO+10
IF(PRNT.GT.0) PRINT 512
IF(PRNT.EQ.0) GO TO 110
PRINT 515
PRINT 516
PRINT 517
110 IF(CHECK.EQ.NCHK) PRINT 66,NCHK
IF(CHECK.EQ.NCHK) PRINT 67,CONVP
FWHMN=2.*SQRT(B0*ALOG(2.))
FWHMG=2.*SCRT(B0G*ALOG(2.))
PRINT 518,I,XNEUT(I),E0,FWHMN,GAMA(I),E0G,FWHMG,CHECK
IF(PRNT.GT.0) PRINT 512
IF(I.LT.10) GO TO 1000
XP=V(KG)
CALL SSCHK(KG,KN)
DO 605 J=KG,KN
IF(V(J).LT.XP) XP=V(J)
605 CONTINUE
XPC=.5*YFRACT
IF(XP/V(KN).LT.XPC) IMAX=I
GO TO 1000
C THIS SECTION SEARCHES FOR THE TWO PEAKS.
70 DO 4 J=JLO,64
IF(X(J) - XN) 5,6,7
5 IF(X(J) - XG) 4,8,8
6 K=J-KN
IF(K.LT.2) GO TO 15
XG=XN
KG=KN
XN = X(J)
15 KN=J
GO TO 4
7 K=J-KN
IF(K.LT.2) GO TO 16
XG=XN
KG=KN
16 KN=J
XN = X(J)
GO TO 4
8 IF(X(J).LE.X(J-1)) GO TO 4
XG= XN
KG=KN
XN= X(J)
KN=J
4 CONTINUE
C THIS LOOP FINDS THE MIN. BETWEEN THE TWO PEAKS.
40 XMIN=1.E50
DO 12 J=KG,KN
IF(X(J) - XMIN) 10,12,12
10 XMIN=X(J)
KMIN=J
12 CONTINUE
IF(XN.LT.3..AND.XG.LT.3.) GO TO 108
IF(I.GT.1MAX2) GO TO 19
IF(KNCHK-KN.GT.5.OR.KG-KGCHK.GT.5) GO TO 102
IF(XN.LT.5..OR.XG.LT.5.) GO TO 102
IF(X(KMIN)/XN.GT..8) GO TO 103
KLO=KMIN+1
KUP=KN+1

```

```

XN=YFRAC*TZN
25 IF(X(KUP).LT.XN) GO TO 26
  KUP=KUP+1
  IF(KUP.GT.64) GO TO 19
  GO TO 25
26 NDP=KUP - KLO + 1
  M=0
  CALL PEAK(KLO,NDP,Y,X)
  CALL GAUSS(NDP,KLO,Y,XNEUT(I),E0,B0,Y0)
  EON=E0
  BON=B0
  IF(M.LT.1) GO TO 41
  PRINT 60,M
  PRINT 69
41 IF(PRNT.EQ.0) GO TO 111
  PRINT 505
  PRINT 504,V
  PRINT 509
  CALL CALPK(PS,Y0,E0,B0)
  PRINT 504,PL
C   THIS SECTION FITS A GAUSSIAN TO THE GAMMA PEAK.
111 KLO=KG-3
  KUP=KMIN
  CALL SSCHK(KLO,KUP)
  NDP=KUP - KLO + 1
  CALL PEAK(KLC,NDP,Y,X)
  CALL GAUSS(NDP,KLO,Y,GAMA(I),E0,B0,Y0)
  BOG=B0
  EOG=E0
  KG=EO
606 FWHMN=2.*SQRT(BON*ALCG(2.))
  FWHMG=2.*SCRT(BOG*ALCG(2.))
  IF(PRNT.EQ.0) GO TO 601
  PRINT 510
  CALL CALPK(PS,Y0,E0,B0)
  PRINT 504,PS
  PRINT 515
  PRINT 516
  PRINT 517
601 PRINT 518,I,XNEUT(I),EON,FWHMN,GAMA(I),EOG,FWHMG
  IF(PRNT.GT.0) PRINT 512
  GO TO 1000
C   THESE TWO LOOPS SUM THE NEUTRONS AND GAMMAS IN THE CHANNEL.
19 KL=KMIN
  KU=KL+10
  IF(KU.GT.64) KL=64
  DO 13 J=KL,KU
13 XNEUT(I) = XNEUT(I) + X(J)
  EO=0.0
20 KSTOP = KMIN - 1
  KL=KG - 10
  IF(KL.LT.1) KL=1
  DO 14 J=KL,KSTOP
14 GAMA(I) = GAMA(I) + X(J)
9 PRINT 519,I,XNEUT(I),KN,GAMA(I),KG
  GO TO 1000
C***** THIS SECTION (TO 108) HANDLES THE DATA IF ONLY ONE SIGNIFICANT PEAK
C      IS FOUND. A GAUSSIAN FIT IS MADE OF THE LARGER PEAK, THE LARGER PEAK
C      IS FOUND. A GAUSSIAN FIT IS MADE OF THE LARGER PEAK, THE CALCULATED
C      PEAK IS THEN SUBTRACTED FROM THE ORIGINAL DATA.

```

```

C      THE DATA REMAINING AFTER THE SUBTRACTION OF THE GAUSSIAN FIT IS THEN
C      SUMMED OVER THE CHANNELS WHERE THE OTHER PEAK SHOULD LIE. THE AREA
C      UNDER THE GAUSSIAN FIT AND THE SUM TAKEN OVER THE REMAINING DATA ARE
C      THEN TAKEN AS THE TOTAL COUNTS IN THE TWO PEAKS.
102 PRINT 503,I
PRINT 61,X
XN=0.
DO 105 J=JLO,64
IF(XN.GT.X(J)) GO TO 105
XN=X(J)
KN=J
105 CONTINUE
LA=1
IF(IABS(KNCHK-KN).LT.IABS(KGCHK - KN)) LA=-LA
KLO= KN - LA*5
KUP= KN + LA*2
CALL SSCHK(KLO,KUP)
NDP= KUP - KLO + 1
CALL PEAK(KLO,NDP,Y,X)
CALL GAUSS(NDP,KLO,Y,XNEUT(I),EON,BON,Y0)
KUP=KN + LA*15
KLO=KN
CALL SSCHK(KLC,KUP)
KG=KN - KDIFF
KMIN=KN-(KDIFF/2)
DO 106 J=KLO,KUP
EXPNT= -((EON-E)**2)/BON
IF(EXPNT.GT.1CC.) EXPNT=100.
IF(EXPNT.LT.-75.) EXPNT=-75.
X(J) = X(J) - Y0*EXP(EXPNT)
IF(X(J).LT.0.) X(J)=0.0
GAMA(I)=GAMA(I) + X(J)
106 X(J)=V(J)
IF(LA.LT.0) GO TO 606
KG=KN
KN=KG + KDIFF
KMIN=(KG + KN)/2
EOG=EON
BOG=BON
EON=0.0
BON=0.0
G=GAMA(I)
GAMA(I)= XNEUT(I)
XNEUT(I)=G
GO TO 601
C***** THIS STATEMENT PRINTS AN ERROR MESSAGE IF NO SIGNIFICANT PEAK IS FOUND.
108 PRINT 62,I
1000 CCNTINUE
C      THIS LOOP ESTABLISHES THE PARAMETERS FOR THE PLOTTING SUBROUTINE.
DO 84 J=1,64
PL(J)=J
X(J)=XNEUT(J)
IF(J.LT.CHANEL) X(J)=XNEUT(64)
IF(X(J).LT.0.0) X(J)=X(64)
IF(X(J).LT.1.) X(J)=1.
84 Y(J)= ALOG(X(J))
PRINT 511
PRINT 57,CHANEL
N=64
CALL PLAT2(PL,Y,N)

```

```

IF(PNCH.EQ.0) GO TO 100
PUNCH 58
PUNCH 61,(XNEUT(I), I=1,64)
GO TO 100
101 PRINT 501
STOP
50 FORMAT(6X,12F6.0,2X)
51 FORMAT(10I5)
56 FORMAT(1H1)
57 FORMAT(1X,I4,45H
58 FORMAT(1H )
60 FORMAT(1X,'**** WARNING.. DATA ERROR IN CHANNEL',I4,'. A DATA VAL
1UE .LE. 0 WAS ENCOUNTERED WHEN TRYING TO FIT A GAUSSIAN TO THE DAT
2A.')
61 FORMAT(1X,10F7.0)
62 FORMAT(1X,I2,'    NO SIGNIFICANT PEAK FOUND.')
64 FORMAT(10I5)
65 FORMAT(10F5.0)
66 FORMAT(1X,'****WARNING.. NO CONVERGENCE IN STRIPPING ROUTINE AFTE
1R ',I5,' ITERATIONS')
67 FORMAT(16X,'LAST ITERATION MADE FRACTIONAL CHANGE OF ',F10.6,' IN
1LARGEST PEAK')
69 FORMAT(16X,'STANDARD LINEAR FIXUP TAKEN')
501 FORMAT(1X,'      *****NORMAL END OF PROGRAM*****')
503 FORMAT(1X,' ONLY ONE DOMINANT PEAK FOUND IN CHANNEL',I3,'. ONE PEA
1K FIT ATTEMPTED')
504 FORMAT(1X,16F7.0)
505 FORMAT(/,1X,'64 CHANNELS OF RAW DATA')
506 FORMAT(/,1X,'CALCULATED VALUES IN LARGEST PEAK FOR ITERATION',I5)
507 FORMAT(/,1X,'CALCULATED VALUES IN SMALLEST PEAK FOR ITERATION',I5)
508 FORMAT(/,1X,'PEAK REMAINING AFTER SUBTRACTION OF LAST CALCULATED P
1EAK')
509 FORMAT(/,1X,'CALCULATED NEUTRON PEAK')
510 FORMAT(/,1X,'CALCULATED GAMMA PEAK')
511 FORMAT(1H1,1X,'SEMILOG PLOT OF CALCULATED NEUTRON PULSE HEIGHT SPE
1CTRA',//)
512 FORMAT(1X,'*****'
1*****')
513 FORMAT(40X,'*****CHANNEL',I4,' STATISTICS*****')
514 FORMAT(10X,'*****ITERATION STATISTICS ARE ---- (LARGEST PEAK AREA
1='F10.0,8X,'SMALLEST PEAK AREA=',F10.0,')*****')
515 FORMAT(' CHANNEL',10X,'NEUTRONS CENTER FWHM',10X,'GAMMAS
1 CENTER FWHM ITERATIONS')
516 FORMAT(29X,'CHANNEL',28X,'CHANNEL')
517 FORMAT(29X,'OF PEAK',28X,'OF PEAK')
518 FORMAT(I4,F20.0,C,F11.2,F9.2,F16.0,F11.2,F9.2,I16)
519 FORMAT(I4,F20.0,C,I9,F27.0,I9)
END
SUBROUTINE GAUSS(NDP,KLO,Y,AREA,E0,B0,Y0)

C THIS PROGRAM FITS A GAUSSIAN CURVE TO A SET OF POINTS IN A LEAST
C SQUARES MANNER.
C
C Y= Y0*EXP(-(E-E0)**2/B0) IS THE FORM OF THE FIT.
C Y = THE COUNTS IN CHANNEL E.
C E0= THE CENTER CHANNEL OF THE PEAK. (MAY BE A FRACTIONAL CHANNEL)
C Y0= THE COUNTS IN THE CENTER CHANNEL.
C NDP= THE NUMBER OF DATA PTS TO BE FIT.
C KLO= THE SUBSCRIPT CORRESPONDING TO THE FIRST Y
C

```

```

C
      DIMENSION Y(NDP),EN(25),A(3,3),B(3),VAR(25),BDUM(3,1)
      DO101 I=1,3
      B(I)=0.
      DO 101 J=1,3
101  A(I,J)=0.
      DO 102 I=1,NDP
      EN(I) = I
C****   THE NEXT STATEMENT CORRECTS FOR NEGATIVE VALUES WHICH MAY OCCUR
C       DURING THE ITERATION PROCESS.
      IF(Y(I).LE.0.) Y(I)=1.
      RATIO=Y(I)
      A(3,3)=A(3,3)+RATIO
      A(2,3)=A(2,3)+RATIO*EN(I)
      A(2,2)=A(2,2)+RATIO*EN(I)*EN(I)
      A(2,1)=A(2,1)+RATIO*(EN(I)**3)
      A(1,1)=A(1,1)+RATIO*(EN(I)**4)
      B(1) = B(1)+RATIO*ALOG(Y(I))*EN(I)*EN(I)
      B(2) = B(2)+RATIO*ALCG(Y(I))*EN(I)
102  B(3) = B(3)+RATIO*ALOG(Y(I))
      A(3,2)=A(2,3)
      A(3,1)=A(2,2)
      A(1,3)=A(2,2)
      A(1,2)=A(2,1)
      DO 176 I=1,3
176  BDUM(I,I)=B(I)
      N1 = 1
      N3 = 3
      CALL MATINV(A,N3,BDUM,N1,DETERM,N3)
      DO 177 I=1,3
177  B(I)=BDUM(I,I)
      B0=-1./B(1)
      E0=B0*B(2)/2.
      Y0 = EXP(B(3))+E0*E0/B0
      PI=3.1415927
      EO= E0 + KLO - 1
      IF(B0.LT.0.0) GO TO 201
      AREA = Y0*SQRT(B0*PI)
      RETURN
201 AREA = -999999.0
      RETURN
      END
      SUBROUTINE MATINV (A,N,B,M,DETERM,NMAX)
C
C      MATRIX INVERSION WITH ACCOMPANYING SOLUTION OF LINEAR EQUATIONS
C      A INPUT-COEFFICIENT MATRIX
C      RETURN-VERSE MATRIX
C      N NUMBER OF EQUATIONS
C      B INPUT-RIGHT HAND SIDE VECTOR(S)
C      RETURN-SOLUTION VECTOR(S)
C      M NUMBER OF RIGHT HAND SIDE VECTOR(S)
C      DETERM RETURN-DETERMINATE OF A
C      NMAX MAXIMUM NUMBER OF EQUATIONS AS DIMENSIONED IN MAIN PROGRAM
C
      REAL*4 PIVCT
      DIMENSION A(NMAX,NMAX),B(NMAX,1)
      COMMON /F402/ PIVOT(100), INDEX(100)
C
C      INITIALIZE DETERMINANT AND PIVOT ELEMENT ARRAY
      DETERM=1.0

```

```

DO 20 I=1,N
PIVOT(I)=0.0
20 CONTINUE
C
C     PERFORM SUCCESSIVE PIVOT OPERATIONS (GRAND LOOP)
C
DO 550 I=1,N
C
C     SEARCH FOR PIVOT ELEMENT AND EXTEND DETERMINANT PARTIAL PRODUCT
C
AMAX=0.0
DO 105 J=1,N
IF (PIVOT(J).NE.0.0) GO TO 105
DO 100 K=1,N
IF (PIVOT(K).NE.0.0) GO TO 100
TEMP= ABS(A(J,K))
IF (TEMP.LT.AMAX) GO TO 100
IROW=J
ICOLUMN=K
AMAX=TEMP
100 CONTINUE
105 CONTINUE
INDEX(I)=4C96*IROW+ICOLUMN
J=IROW
AMAX=A(J,ICOLUMN)
DETERM=AMAX*DETERM
C
C     RETURN IF MATRIX IS SINGULAR (ZERO PIVOT) AFTER COLUMN INTERCHANGE
C
IF (DETERM.EQ.0.0) GO TO 600
C
PIVOT(ICOLUMN)=AMAX
C
C     INTERCHANGE ROWS TO PUT PIVOT ELEMENT ON DIAGONAL
C
IF (IROW.EQ.ICOLUMN) GO TO 260
DETERM=-DETERM
DO 200 K=1,N
SWAP=A(J,K)
A(J,K)=A(ICOLUMN,K)
A(ICOLUMN,K)=SWAP
200 CCNTINUE
IF (M.LE.0) GO TO 260
DO 250 K=1,M
SWAP=B(J,K)
B(J,K)=B(ICOLUMN,K)
B(ICOLUMN,K)=SWAP
250 CONTINUE
C
C     DIVIDE PIVOT ROW BY PIVOT ELEMENT
C
260 K=ICOLUMN
A(ICOLUMN,K)=1.0
DO 350 K=1,N
A(ICOLUMN,K)=A(ICOLUMN,K)/AMAX
350 CONTINUE
IF (M.LE.0) GO TO 380
DO 370 K=1,M
B(ICOLUMN,K)=B(ICOLUMN,K)/AMAX
370 CONTINUE

```

```

C
C      REDUCE NON-PIVCT ROWS
C
380 DO 550 J=1,N
  IF (J.EQ.ICOLUMN) GO TO 550
  T=A( J,ICOLUMN)
  A( J,ICOLUMN)=0.0
  DO 450 K=1,N
    A( J,K)=A( J,K)-A( ICOLUMN,K)*T
450 CONTINUE
  IF (M.LE.0) GO TO 550
  DO 500 K=1,M
    B( J,K)=B( J,K)-B( ICOLUMN,K)*T
500 CONTINUE
550 CONTINUE
C
C      INTERCHANGE COLUMNS AFTER ALL PIVOT OPERATIONS HAVE BEEN PERFORMED
C
600 DO 710 I=1,N
  I1=N+1-I
  K=INDEX(I1)/4096
  ICOLUMN=INDEX(I1)-4096*K
  IF (K.EQ.ICOLUMN) GO TO 710
  DO 705 J=1,N
    SWAP=A(I,J,K)
    A(I,J,K)=A(I,ICOLUMN)
    A(I,ICOLUMN)=SWAP
705 CONTINUE
710 CONTINUE
C
      RETURN
      END
      SUBROUTINE PEAK(KLO,NDP,Y,X)
C**      THIS SUBROUTINE SHIFTS THE PEAK TO CHANNEL 1 FOR THE GAUSSIAN FIT.
      DIMENSION X(64),Y(NDP)
      KUP=KLO + NDP - 1
      DO 10 J=KLO,KUP
        K=J-KLO + 1
10      Y(K)=X(J)
      RETURN
      END
      SUBROUTINE SSCHK(KLO,KUP)
C**      THIS SUBROUTINE CHECKS THE SUBSCRIPTS TO SEE THAT THEY ARE INSIDE
C      THE GRID. (THE UPPER AND LOWER LIMITS ARE SET AT 2 AND 63 BECAUSE
C      SOME STATEMENTS IN THE MAIN PROGRAM REFER TO X(I +.OR- 1) SO "I"
C      MUST LIE BETWEEN 2 AND 63)
      IF(KUP.GT.KLO) GO TO 1
      K=KUP
      KUP=KLO
      KLO=K
1      IF(KLO.LT.2) KLO=2
      IF(KUP.GT.63) KUP=63
      RETURN
      END
      SUBROUTINE DAMP(X,D,N)
C**** THIS SUBROUTINE AVERAGES EACH NEW ESTIMATION OF THE PEAKS DURING THE
C      ITERATION PROCESS WITH THE LAST ESTIMATION OF THE PEAK. THIS IS DONE TO
C      DAMP OUT OSCILLATIONS WHICH SOMETIMES OCCUR DURING THE ITERATION
C      PROCESS.
      DIMENSION X(64),D(64)

```

```

IF(N.GT.0) GO TO 2
DO 1 I=1,64
1 D(I)=X(I)
RETURN
2 DO 3 I=1,64
   X(I) = (X(I) + D(I))/2.
3 D(I)= X(I)
RETURN
END
SUBROUTINE CALPKIX,Y,E0,B0)
C**** THIS SUBROUTINE CALCULATES HOW MANY COUNTS ARE IN A PARTICULAR CHANNEL
C BASED ON THE PARAMETERS DETERMINED IN THE LEAST SQUARES GAUSSIAN FIT.
C IT IS USED TO CALCULATE THE FITTED PEAKS FOR THE PRINT OPTION, AND TO
C CALCULATE THE PEAKS DURING THE ITERATION PROCESS SO THE CALCULATED PEAK
C CAN BE SUBTRACTED FROM THE ACTUAL PEAK.
DIMENSION X(64)
DO 1 J=1,64
E=J
EXPNT=-((E-E0)**2)/B0
IF(EXPNT.GT.120.) EXPNT=120.
IF(EXPNT.LT.-50.) EXPNT=-50.
1 X(J)=Y*EXP(EXPNT)
RETURN
END
SUBROUTINE DERIV(X,K1,R,DMIN)
C**** THIS SUBROUTINE LOOKS FOR A MINIMA IN THE DERIVATIVE OF THE DATA BETWEEN
C THE NEUTRON AND GAMMA PEAKS. THIS IS DONE SO THAT THE MAIN PROGRAM KNOWS
C WHERE TO SEARCH FOR THE SECOND PEAK DURING THE ITERATION PROCESS.
C THIS SUBROUTINE WAS ADDED BECAUSE THE RESIDUAL LEFT AFTER SUBTRACTING
C THE FIRST FIT TO THE GAMMA PEAK FROM THE ORIGINAL GAMMA PEAK WAS SOMETIMES
C LARGER THAN THE ACTUAL NEUTRON PEAK.(THIS IS A PROBLEM AT LOW PULSE HEIGHT
C CHANNELS WHERE THE GAMMA PEAK IS SKewed)
DIMENSION X(64),D(15)
DO 3 I=1,10
3 D(I)=0.0
I=1
IF(R.LT.1.) I=-I
N=10
IF(K1.GT.53) N=63-K1
IF(K1.LT.12) N=K1-2
DO 1 J=1,N
L=K1+I*J
1 D(J)=X(L-1)-X(L)
DMIN=0.0
DO 2 J=2,9
IF(DMIN.GT.0.) GO TO 2
IF(ABS(D(J)).GT.ABS(D(J-1))) GO TO 2
IF(ABS(D(J)).LT.ABS(D(J+1))) DMIN=J
2 CONTINUE
IF(DMIN.LT.3.) DMIN=3.
RETURN
END
SUBROUTINE PLAT2(Z,Y,N)
C**** THIS SUBROUTINE PLOTS THE CALCULATED PULSE HEIGHT SPECTRA. (THE DATA
C IN THE FIRST FEW CHANNELS THAT IS SET TO ZERO IN THE MAIN PROGRAM IS SET
C EQUAL TO THE DATA IN THE LAST CHANNEL DURING THE PLOT ROUTINE SO THAT THE
C PLOT WILL HAVE THE GREATEST DEFINITION POSSIBLE)
C
C PLOTTING SUBROUTINE PLAT2

```

```

C      Z=X AXIS DATA
C      Y=YAXIS DATA
C      N= NUMBER OF DATA POINTS.
C
C      INTEGER XX
DIMENSION XX(120),Z(N),Y(N),NN(2)
DATA NN/1H ,1H*/
YMAX = -1.E50
YMIN = 1.E50
DO 3 I=1,N
IF(Y(I) - YMAX) 5,5,4
4 YMAX=Y(I)
5 IF(YMIN - Y(I)) 3,3,6
6 YMIN = Y(I)
3 CCNTINUE
RANGE = YMAX - YMIN
DIV = RANGE/100.
PRINT 30, DIV
30 FORMAT(1H ,25X,' THE SCALE OF THIS GRAPH IS 1 DIVISION =',E12.5,'U
1NITS',//,29X,'1234567890123456789012345678901234567890123
2456789012345678901234567890123456789012345678901234567890123
DO 1 J=1,120
1 XX(J) = NN(1)
IX=1
DO 2 I=1,N
XX(IX)=NN(1)
X = 1.0 + (99./RANGE)*(Y(I)-YMIN)
IX = IFIX(X)
IF(IX.LT.1.OR. IX.GT.101) GO TO 2
XX(IX) = NN(2)
PRINT 20, Z(I),Y(I),(XX(J),J=1,101)
20 FORMAT(1H ,2E12.4,'----',10I1)
2 CONTINUE
RETURN
END

```

B-1.3 Sample Data Set and Results

DISCRIM Input Data Set

3 4
 20
 .01 .10
 3 HG PUBE FGD 4-13-71 (500/200)
 20 30 0 0 0

	0.	507.	961.	473.	422.	352.	242.	156.	125.	112.	98.	92.
81.	87.	75.	73.	64.	61.	54.	56.	47.	49.	51.	43.	
43.	43.	39.	24.	26.	26.	30.	29.	32.	18.	27.	18.	
28.	17.	16.	15.	18.	11.	13.	20.	14.	26.	20.	15.	
11.	9.	10.	9.	20.	11.	12.	14.	5.	11.	10.	8.	
9.	16.	11.	13.	0.	514.	1020.	505.	398.	355.	227.	159.	
123.	108.	112.	88.	84.	72.	79.	72.	56.	47.	49.	65.	
49.	47.	47.	43.	46.	34.	38.	42.	45.	22.	22.	27.	
29.	18.	27.	23.	27.	17.	21.	29.	16.	26.	16.	17.	
19.	19.	19.	16.	11.	13.	15.	12.	7.	16.	14.	5.	
11.	10.	5.	5.	11.	13.	5.	12.	0.	461.	757.	636.	
367.	242.	201.	145.	110.	82.	78.	81.	59.	72.	57.	52.	
59.	54.	52.	47.	36.	53.	50.	30.	34.	21.	29.	31.	
34.	30.	27.	21.	18.	17.	14.	19.	20.	13.	18.	15.	
17.	12.	8.	10.	20.	10.	18.	11.	11.	12.	14.	10.	
7.	17.	8.	6.	8.	10.	7.	11.	12.	8.	5.	6.	
0.	491.	629.	641.	395.	283.	161.	121.	112.	82.	96.	58.	
59.	60.	46.	51.	52.	58.	47.	40.	51.	44.	42.	37.	
41.	28.	32.	25.	25.	19.	25.	20.	29.	25.	18.	18.	
22.	21.	16.	16.	10.	22.	15.	17.	8.	10.	17.	12.	
12.	10.	10.	16.	11.	11.	6.	9.	13.	11.	5.	10.	
4.	6.	7.	4.	0.	2039.	647.	474.	567.	309.	170.	119.	
90.	88.	68.	73.	69.	53.	58.	48.	42.	30.	44.	44.	
49.	35.	35.	26.	29.	30.	24.	23.	25.	28.	19.	15.	
22.	22.	14.	22.	17.	10.	16.	6.	17.	12.	10.	7.	
26.	9.	11.	12.	6.	14.	13.	19.	8.	7.	13.	8.	
12.	4.	5.	5.	2.	4.	6.	6.	4.	99213.	12510.	467.	
534.	495.	204.	132.	104.	83.	76.	61.	68.	57.	66.	49.	
57.	51.	50.	30.	53.	40.	33.	42.	38.	37.	25.	36.	
25.	17.	30.	23.	19.	17.	17.	18.	20.	12.	16.	14.	
21.	17.	15.	9.	13.	17.	17.	9.	19.	15.	13.	9.	
9.	10.	10.	11.	9.	8.	8.	5.	6.	10.	3.	5.	
6.58462.33970.	432.	325.	357.	352.	153.	106.	69.	76.	58.			
64.	43.	42.	52.	38.	44.	48.	41.	34.	35.	42.	29.	
24.	29.	28.	32.	28.	15.	27.	20.	18.	19.	22.	20.	
14.	12.	13.	11.	16.	18.	12.	16.	12.	10.	15.	11.	
10.	9.	6.	11.	9.	6.	6.	7.	9.	12.	5.	6.	
11.	6.	7.	7.	4.	37978.	48742.	391.	302.	232.	200.	222.	
153.	106.	59.	61.	55.	44.	37.	39.	48.	28.	41.	33.	
36.	34.	26.	30.	30.	23.	27.	16.	19.	20.	19.	17.	
16.	14.	21.	20.	17.	10.	11.	17.	14.	6.	8.	12.	
12.	10.	11.	7.	8.	10.	6.	10.	6.	10.	9.	9.	
4.	7.	7.	5.	4.	6.	3.	7.	3.	25864.	57732.	402.	
289.	214.	153.	110.	108.	130.	115.	101.	67.	42.	38.	43.	
36.	37.	33.	26.	26.	42.	31.	24.	30.	19.	12.	16.	
23.	16.	15.	17.	14.	14.	15.	17.	19.	8.	8.	15.	
10.	12.	8.	11.	8.	11.	7.	6.	11.	7.	11.	8.	
12.	4.	10.	6.	4.	4.	9.	4.	2.	3.	3.	8.	
0.19011.62244.	352.	281.	199.	166.	88.	81.	77.	59.	68.			
86.	88.	76.	62.	53.	43.	38.	34.	21.	30.	30.	21.	
16.	30.	22.	21.	16.	11.	25.	13.	13.	13.	9.	16.	
9.	16.	13.	9.	16.	7.	10.	10.	17.	12.	5.	12.	

7.	6.	10.	9.	4.	3.	8.	6.	9.	2.	3.	7.
6.	2.	5.	5.	2.	14941.	65301.	465.	235.	229.	167.	121.
11.	74.	43.	58.	42.	46.	44.	44.	53.	46.	50.	68.
56.	49.	34.	29.	16.	31.	25.	21.	13.	18.	15.	12.
16.	17.	11.	11.	14.	16.	11.	9.	17.	13.	12.	9.
7.	4.	9.	8.	5.	7.	9.	7.	4.	3.	10.	3.
11.	6.	8.	5.	3.	5.	2.	6.	0.	11910.	66564.	2375.
236.	205.	160.	124.	112.	109.	94.	51.	58.	49.	48.	39.
31.	41.	31.	39.	44.	45.	57.	51.	56.	42.	37.	30.
22.	26.	14.	26.	19.	14.	17.	16.	11.	13.	9.	12.
11.	12.	10.	10.	15.	13.	9.	8.	8.	9.	7.	7.
7.	3.	6.	3.	9.	3.	6.	8.	8.	4.	7.	12.
1.	9663.	58869.	13644.	278.	170.	136.	124.	100.	101.	94.	77.
85.	76.	58.	55.	71.	34.	41.	30.	25.	25.	33.	27.
30.	30.	25.	34.	27.	21.	26.	37.	23.	26.	26.	24.
19.	20.	21.	11.	15.	14.	11.	7.	9.	8.	8.	8.
5.	4.	8.	5.	9.	6.	7.	2.	6.	6.	4.	10.
7.	4.	4.	7.	2.	7836.	44049.	30985.	245.	186.	135.	97.
81.	77.	58.	76.	80.	90.	69.	63.	61.	49.	62.	50.
64.	45.	34.	29.	30.	24.	27.	18.	29.	14.	20.	14.
22.	12.	18.	10.	24.	23.	24.	18.	20.	19.	16.	15.
21.	18.	19.	12.	17.	19.	21.	6.	19.	13.	14.	15.
6.	13.	7.	8.	3.	5.	6.	7.	3.	6750.	32063.	46999.
291.	129.	127.	101.	74.	60.	61.	44.	43.	51.	51.	59.
60.	45.	53.	54.	71.	53.	60.	48.	54.	40.	58.	32.
32.	35.	26.	12.	20.	14.	10.	6.	17.	6.	13.	6.
9.	7.	7.	4.	10.	6.	11.	9.	10.	22.	12.	10.
12.	11.	5.	9.	19.	11.	13.	10.	16.	7.	15.	16.
0.	5493.	24971.	58275.	554.	197.	128.	90.	69.	59.	41.	50.
50.	35.	37.	31.	40.	46.	27.	27.	34.	25.	37.	33.
28.	42.	34.	38.	28.	33.	32.	30.	25.	32.	33.	21.
28.	18.	15.	27.	22.	18.	15.	18.	11.	17.	10.	8.
14.	9.	9.	8.	9.	9.	11.	5.	6.	4.	9.	2.
7.	6.	5.	4.	0.	4354.	20971.	61597.	5268.	143.	75.	56.
48.	41.	39.	35.	25.	30.	16.	26.	20.	22.	16.	12.
11.	16.	25.	15.	19.	12.	21.	13.	13.	21.	16.	13.
15.	13.	7.	14.	14.	11.	12.	13.	13.	16.	13.	12.
11.	13.	12.	11.	15.	17.	13.	10.	10.	10.	16.	10.
12.	5.	9.	12.	8.	10.	5.	9.	0.	3429.	19805.	51687.
22512.	97.	60.	36.	32.	20.	26.	17.	13.	22.	14.	16.
16.	11.	13.	14.	16.	13.	12.	6.	6.	7.	5.	6.
5.	5.	8.	4.	10.	5.	5.	2.	3.	3.	2.	5.
4.	6.	1.	3.	5.	3.	5.	1.	5.	4.	5.	3.
4.	2.	4.	4.	3.	2.	2.	3.	1.	3.	3.	8.
0.	2749.	19065.	35047.	46385.	188.	32.	30.	9.	12.	9.	5.
10.	8.	5.	7.	9.	8.	4.	10.	3.	8.	1.	5.
5.	4.	2.	5.	4.	5.	1.	4.	2.	2.	0.	4.
4.	1.	2.	6.	1.	1.	0.	2.	1.	5.	0.	2.
0.	2.	0.	1.	2.	2.	1.	1.	0.	3.	1.	3.
3.	3.	0.	1.	1.	2142.	19224.	21662.	64189.	2960.	52.	17.
11.	9.	5.	15.	5.	11.	3.	5.	3.	9.	10.	8.
4.	9.	6.	4.	4.	2.	8.	7.	2.	2.	1.	3.
5.	2.	1.	3.	2.	3.	3.	3.	0.	3.	1.	3.
0.	3.	2.	0.	2.	1.	0.	1.	0.	0.	1.	0.
2.	1.	1.	0.	2.	1.	1.	2.	1.	1746.	18673.	14622.
62731.	19584.	55.	30.	18.	9.	10.	12.	6.	9.	8.	7.
6.	3.	4.	8.	3.	4.	7.	5.	4.	4.	5.	3.
1.	2.	5.	2.	4.	2.	2.	4.	2.	4.	3.	4.
3.	1.	2.	3.	4.	3.	0.	2.	0.	1.	1.	1.
1.	0.	1.	1.	1.	1.	0.	0.	2.	1.	0.	2.

0.	1382.	17840.	11897.	44315.	46487.	614.	29.	20.	13.	15.	9.
5.	13.	7.	3.	7.	9.	9.	7.	7.	8.	4.	4.
9.	2.	0.	5.	5.	5.	2.	3.	4.	1.	1.	4.
1.	3.	1.	4.	2.	1.	1.	2.	2.	3.	2.	2.
1.	0.	5.	2.	1.	2.	0.	2.	2.	1.	0.	1.
2.	3.	1.	2.	2.	1134.	16696.	12149.	25903.	61597.	8541.	50.
15.	9.	10.	10.	10.	7.	4.	9.	3.	5.	3.	2.
3.	6.	7.	4.	5.	0.	2.	2.	4.	7.	2.	4.
2.	4.	2.	5.	0.	5.	2.	1.	3.	0.	2.	2.
1.	2.	2.	1.	1.	1.	0.	2.	0.	1.	0.	2.
3.	0.	1.	0.	1.	0.	1.	2.	0.	891.	14358.	13748.
13689.	50918.	28926.	515.	23.	15.	18.	10.	7.	15.	6.	8.
6.	4.	3.	5.	9.	3.	4.	5.	4.	7.	4.	4.
2.	7.	6.	1.	7.	1.	1.	3.	3.	2.	2.	3.
1.	1.	2.	5.	6.	1.	1.	1.	1.	2.	0.	2.
2.	2.	2.	2.	2.	2.	0.	2.	0.	3.	2.	0.
1.	730.	12482.	15669.	8249.	30640.	43034.	6858.	54.	21.	20.	15.
13.	7.	5.	6.	3.	9.	5.	7.	4.	3.	4.	5.
5.	5.	5.	6.	3.	3.	4.	1.	2.	1.	0.	2.
2.	3.	3.	1.	0.	2.	3.	3.	1.	0.	3.	1.
2.	2.	1.	0.	0.	0.	1.	1.	2.	2.	0.	1.
1.	0.	0.	0.	1.	609.	10194.	16873.	6997.	15343.	36349.	22232.
1500.	27.	18.	9.	7.	5.	7.	7.	4.	7.	4.	8.
4.	6.	4.	5.	3.	5.	3.	4.	2.	2.	2.	3.
2.	3.	7.	1.	1.	1.	3.	1.	2.	2.	4.	4.
1.	1.	1.	1.	1.	2.	4.	1.	2.	3.	2.	0.
2.	0.	1.	1.	2.	1.	0.	2.	0.	489.	8542.	17302.
8228.	7473.	20756.	28795.	10667.	503.	31.	16.	9.	8.	4.	5.
4.	9.	3.	11.	5.	4.	3.	4.	4.	6.	4.	3.
4.	1.	2.	2.	1.	3.	2.	3.	1.	1.	0.	0.
2.	1.	1.	1.	1.	3.	1.	2.	1.	0.	2.	3.
1.	1.	1.	0.	0.	2.	2.	2.	0.	1.	1.	0.
1.	389.	6569.	16778.	10517.	4817.	9618.	20618.	21235.	5892.	238.	19.
16.	7.	8.	4.	8.	3.	4.	7.	2.	4.	7.	5.
7.	1.	3.	1.	5.	1.	1.	5.	3.	0.	1.	4.
3.	1.	1.	1.	2.	2.	1.	1.	0.	2.	2.	6.
2.	2.	0.	1.	1.	0.	0.	0.	1.	1.	2.	0.
1.	0.	2.	0.	0.	342.	5136.	15059.	12854.	4687.	4367.	10164.
18020.	15478.	4344.	241.	19.	13.	4.	7.	5.	3.	8.	1.
2.	2.	3.	6.	2.	6.	3.	4.	3.	4.	2.	3.
1.	5.	2.	3.	0.	0.	2.	3.	0.	2.	1.	0.
2.	2.	2.	0.	2.	1.	0.	1.	0.	1.	0.	1.
2.	1.	0.	0.	1.	0.	0.	0.	2.	262.	3904.	13153.
14951.	6540.	2769.	4351.	9503.	15274.	13502.	4519.	389.	24.	15.	7.
5.	4.	4.	5.	6.	1.	5.	11.	3.	1.	5.	0.
2.	2.	2.	4.	2.	1.	3.	2.	1.	0.	0.	7.
1.	3.	0.	1.	2.	1.	2.	0.	1.	0.	0.	1.
1.	1.	0.	0.	1.	0.	0.	2.	1.	0.	2.	0.
0.	251.	3022.	10321.	15244.	9221.	3052.	2031.	3838.	8182.	13592.	12771.
5523.	802.	34.	8.	6.	8.	6.	2.	3.	5.	7.	2.
3.	4.	1.	3.	4.	2.	1.	1.	1.	1.	1.	4.
4.	1.	1.	1.	1.	1.	0.	0.	0.	1.	3.	2.
1.	0.	1.	0.	1.	1.	0.	0.	1.	2.	2.	1.
0.	1.	0.	1.	0.	204.	2284.	8462.	14682.	11957.	4756.	1684.
1617.	3240.	6915.	11756.	12797.	7182.	1604.	78.	12.	8.	6.	5.
8.	5.	6.	3.	6.	4.	1.	1.	3.	2.	4.	1.
2.	2.	5.	1.	3.	1.	1.	0.	3.	2.	5.	1.
0.	2.	1.	2.	1.	0.	0.	2.	2.	0.	2.	2.
0.	0.	1.	1.	0.	0.	0.	0.	3.	170.	1611.	6351.
13151.	13642.	7468.	2471.	1032.	1265.	2571.	5353.	9709.	12399.	9192.	2858.

385.	34.	6.	8.	8.	5.	3.	6.	4.	2.	3.	1.
4.	3.	6.	4.	4.	3.	2.	0.	5.	1.	0.	1.
1.	0.	1.	4.	1.	1.	2.	0.	1.	0.	1.	1.
0.	2.	2.	2.	1.	1.	2.	0.	1.	0.	0.	0.
0.	162.	1242.	4639.	10767.	14106.	10582.	4664.	1450.	763.	1019.	1920.
3955.	7541.	10897.	10395.	5347.	1100.	84.	16.	6.	3.	5.	2.
1.	7.	2.	2.	1.	3.	2.	2.	2.	0.	1.	0.
1.	4.	4.	1.	2.	3.	1.	2.	1.	3.	1.	2.
0.	3.	2.	0.	1.	1.	2.	2.	0.	0.	1.	2.
0.	1.	0.	3.	0.	139.	1004.	3343.	8326.	12947.	12612.	7462.
3074.	997.	567.	759.	1362.	2742.	5370.	9397.	10714.	7870.	2998.	512.
56.	18.	7.	6.	2.	3.	2.	4.	2.	3.	1.	1.
4.	3.	2.	2.	0.	1.	2.	1.	0.	1.	1.	0.
2.	2.	4.	3.	0.	0.	1.	2.	2.	2.	1.	0.
1.	1.	1.	0.	1.	2.	3.	1.	0.	129.	735.	2431.
6229.	10976.	13010.	10408.	5645.	2248.	789.	486.	550.	916.	1847.	3613.
6442.	9753.	9688.	6302.	2490.	460.	57.	21.	7.	8.	5.	6.
4.	4.	1.	5.	5.	2.	4.	4.	1.	2.	2.	3.
1.	1.	1.	1.	1.	1.	3.	3.	0.	1.	1.	2.
0.	1.	0.	1.	0.	1.	1.	4.	2.	0.	0.	0.
2.	101.	556.	1693.	4412.	8671.	12129.	12226.	8945.	4796.	1932.	726.
404.	376.	635.	1069.	2165.	4191.	7362.	9788.	9771.	6370.	2398.	466.
70.	16.	9.	6.	8.	7.	4.	1.	4.	4.	2.	2.
2.	2.	1.	1.	2.	1.	1.	4.	5.	0.	0.	3.
1.	0.	0.	2.	0.	1.	1.	0.	2.	1.	0.	2.
2.	2.	0.	2.	1.	88.	465.	1161.	3009.	6358.	9978.	12005.
11478.	8065.	4437.	1983.	778.	325.	294.	419.	688.	1273.	2282.	4566.
7253.	9589.	9737.	6526.	2790.	809.	142.	23.	14.	3.	2.	3.
0.	4.	1.	3.	1.	1.	3.	1.	2.	3.	0.	1.
2.	0.	1.	1.	0.	1.	0.	1.	1.	3.	1.	0.
1.	0.	1.	1.	4.	2.	0.	0.	0.	93.	364.	792.
1983.	4297.	7648.	10699.	12182.	10697.	7724.	4694.	2379.	934.	370.	225.
242.	447.	689.	1279.	2318.	4286.	6975.	9400.	9465.	6802.	3695.	1314.
318.	58.	7.	6.	7.	5.	3.	0.	3.	4.	3.	3.
1.	1.	3.	3.	0.	0.	3.	2.	1.	1.	1.	0.
0.	1.	0.	2.	2.	2.	5.	1.	1.	0.	1.	1.
0.	116.	309.	608.	1318.	2803.	5174.	8128.	10756.	11404.	10649.	8195.
5193.	2849.	1201.	457.	199.	155.	254.	370.	630.	1054.	2007.	3431.
5375.	7058.	7820.	6876.	4834.	2520.	936.	233.	36.	11.	3.	4.
6.	3.	0.	1.	3.	2.	4.	2.	0.	2.	3.	3.
2.	3.	1.	3.	1.	2.	1.	4.	2.	1.	2.	0.
1.	1.	0.	1.	1.	72.	265.	417.	857.	1755.	3442.	5826.
8263.	10618.	11134.	10648.	8859.	6207.	3359.	1777.	640.	258.	177.	148.
212.	307.	542.	866.	1406.	2225.	3590.	4909.	5965.	6266.	5378.	3598.
1838.	722.	232.	88.	21.	6.	6.	3.	2.	3.	1.	5.
5.	3.	3.	1.	0.	0.	2.	2.	2.	0.	1.	4.
1.	0.	2.	2.	1.	1.	0.	1.	1.	78.	207.	280.
608.	1161.	2058.	3691.	5728.	7847.	9889.	10800.	10891.	9384.	6920.	4641.
2489.	1099.	466.	204.	112.	108.	150.	250.	318.	527.	838.	1241.
1787.	2399.	3525.	4433.	5012.	4477.	3596.	2438.	1458.	649.	291.	112.
46.	19.	6.	8.	3.	2.	4.	5.	2.	1.	0.	4.
3.	5.	2.	0.	2.	1.	1.	1.	0.	0.	2.	2.
2.	79.	191.	269.	370.	709.	1237.	2184.	3543.	5283.	7085.	8872.
10053.	10644.	9988.	8131.	5614.	3598.	1994.	972.	406.	172.	103.	90.
107.	131.	185.	280.	371.	494.	819.	1285.	2138.	2919.	3827.	4493.
4748.	4339.	3681.	2742.	1807.	1052.	529.	203.	94.	36.	11.	8.
5.	1.	4.	1.	2.	1.	3.	1.	3.	0.	3.	2.
3.	2.	0.	0.	1.	73.	173.	194.	261.	455.	760.	1238.
2019.	3093.	4477.	6143.	7666.	9158.	10068.	9983.	9084.	7168.	5146.	3285.
1849.	935.	431.	219.	97.	68.	68.	67.	80.	109.	172.	234.

384.	614.	896.	1118.	1890.	2588.	3314.	3939.	4358.	4259.	4067.	3368.
2604.	1915.	1158.	643.	311.	130.	43.	21.	16.	2.	4.	2.
2.	3.	1.	3.	1.	3.	1.	3.	0.	74.	150.	182.
215.	331.	463.	710.	1157.	1742.	2589.	3701.	4936.	6144.	8033.	9173.
9893.	9583.	8419.	6872.	4949.	3399.	2085.	1197.	558.	246.	116.	78.
53.	36.	39.	60.	91.	108.	125.	235.	323.	488.	659.	890.
1222.	1748.	2330.	2999.	3529.	3932.	4147.	3877.	3408.	2870.	2178.	1617.
1024.	598.	341.	158.	62.	23.	19.	10.	7.	3.	4.	3.
0.	80.	121.	147.	175.	228.	298.	432.	616.	836.	1360.	1852.
2672.	3578.	4909.	6231.	7831.	8798.	9464.	9009.	8208.	7186.	5456.	3933.
2491.	1510.	863.	432.	202.	88.	57.	31.	22.	34.	34.	41.
53.	77.	112.	111.	168.	236.	335.	502.	694.	991.	1410.	1843.
2428.	2989.	3424.	3728.	3890.	3689.	3413.	3078.	2479.	1914.	1286.	779.
487.	270.	106.	35.	0.	54.	122.	115.	142.	146.	195.	253.
346.	489.	666.	916.	1262.	1819.	2520.	3456.	4678.	5995.	7280.	7972.
8715.	8775.	8388.	7137.	5809.	4616.	3440.	2216.	1293.	744.	383.	224.
138.	76.	48.	40.	25.	13.	25.	23.	32.	33.	45.	61.
75.	123.	177.	223.	320.	444.	580.	817.	1112.	1448.	1838.	2298.
2746.	3114.	3354.	3553.	3428.	2981.	2649.	1995.	0.	69.	106.	101.
112.	114.	163.	162.	211.	254.	317.	425.	587.	831.	1169.	1675.
2318.	3180.	4179.	5174.	6257.	7166.	7648.	7914.	7912.	7458.	6680.	5541.
4180.	2942.	2088.	1416.	1042.	652.	390.	211.	155.	83.	60.	41.
22.	19.	33.	17.	17.	22.	19.	36.	32.	40.	62.	62.
109.	141.	202.	241.	375.	505.	713.	1065.	1386.	1810.	2252.	2761.
1.	59.	95.	98.	93.	97.	102.	88.	117.	158.	159.	204.
274.	375.	502.	698.	937.	1448.	1852.	2473.	3226.	4041.	4846.	5706.
6406.	6971.	7157.	7043.	6604.	5935.	5192.	4378.	3481.	2809.	2264.	1667.
1188.	749.	518.	354.	174.	109.	68.	55.	29.	25.	18.	15.
14.	9.	17.	11.	16.	18.	20.	23.	32.	34.	52.	74.
112.	153.	217.	305.	0.	67.	109.	72.	105.	79.	72.	80.
72.	67.	104.	103.	133.	136.	231.	278.	395.	580.	708.	1000.
1347.	1774.	2239.	2840.	3590.	4074.	4645.	5249.	5857.	6214.	6380.	6296.
5831.	5505.	4980.	4441.	3919.	3207.	2532.	1962.	1357.	1041.	724.	495.
357.	216.	156.	96.	55.	42.	30.	25.	21.	10.	10.	11.
9.	13.	15.	8.	11.	16.	17.	19.	1.	46.	79.	84.
56.	56.	62.	48.	46.	59.	55.	57.	63.	85.	80.	113.
125.	201.	262.	326.	459.	626.	813.	1060.	1386.	1702.	2088.	2519.
3165.	3826.	4355.	4535.	4955.	5166.	5380.	5258.	5430.	5234.	4922.	4512.
4068.	3459.	2977.	2455.	2088.	1652.	1188.	969.	715.	547.	393.	266.
196.	126.	72.	45.	39.	23.	19.	11.	10.	8.	7.	11.
0.	47.	66.	60.	52.	46.	44.	48.	30.	37.	32.	33.
24.	40.	44.	55.	68.	74.	94.	102.	165.	200.	223.	364.
435.	508.	692.	857.	1144.	1435.	1824.	2160.	2432.	2696.	2890.	3220.
3510.	3820.	4153.	4316.	4454.	4434.	4444.	4175.	4061.	3861.	3484.	3153.
2637.	2474.	2059.	1743.	1461.	1080.	825.	558.	478.	369.	216.	173.
96.	82.	39.	36.	0.	50.	65.	41.	47.	43.	40.	41.
31.	23.	29.	24.	24.	19.	22.	16.	35.	35.	39.	51.
47.	66.	73.	107.	124.	136.	195.	208.	351.	440.	539.	641.
796.	908.	1037.	1271.	1362.	1539.	1809.	2037.	2277.	2590.	2892.	3139.
3261.	3262.	3235.	3488.	3329.	3389.	3279.	3173.	2760.	2671.	2430.	2335.
2070.	1721.	1521.	1232.	970.	766.	621.	475.	1.	35.	61.	50.
41.	35.	28.	29.	20.	20.	20.	12.	19.	9.	12.	16.
18.	16.	17.	19.	17.	26.	25.	30.	41.	55.	52.	76.
93.	96.	118.	133.	197.	201.	234.	296.	342.	399.	511.	614.
689.	857.	944.	1091.	1189.	1318.	1454.	1681.	1730.	1886.	2029.	2049.
2212.	2280.	2327.	2416.	2402.	2459.	2370.	2273.	2225.	2013.	1959.	1835.
2.	37.	51.	34.	24.	37.	19.	26.	19.	15.	16.	11.
15.	14.	13.	11.	4.	11.	12.	15.	18.	20.	13.	18.
12.	24.	21.	22.	28.	33.	20.	32.	41.	55.	43.	47.
79.	103.	93.	106.	133.	158.	183.	218.	286.	314.	349.	394.

DISCRIM Output

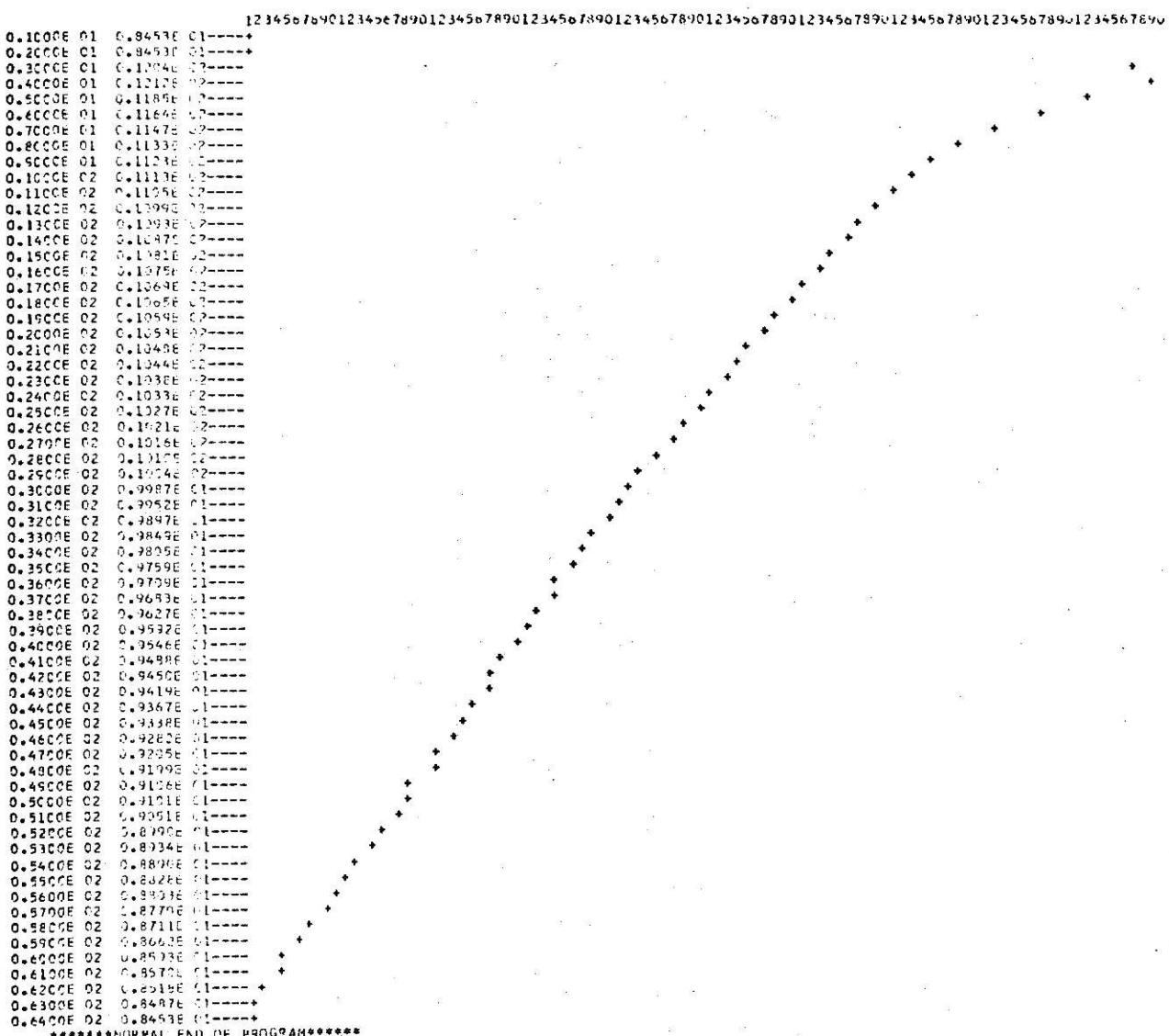
3 HG PULSE FGD 4-13-71 (500/200)

CHANNEL	NEUTRONS	CENTER CHANNEL OF PEAK	FWHM	GAMMAS	CENTER CHANNEL OF PEAK	FWHM	ITERATIONS
1	0.	0		0.	0		
2	0.	0		0.	0		
3	169450.	21.69	8.52	564921.	10.86	7.89	2
4	183129.	26.86	10.00	327295.	16.67	4.99	2
5	140680.	31.01	8.75	288070.	20.60	4.17	2
6	113737.	33.90	7.70	236934.	23.34	3.72	2
7	95684.	36.04	6.94	154128.	25.46	3.46	2
8	83374.	37.69	6.43	96960.	27.19	3.33	2
9	75240.	39.05	5.91	67975.	28.57	3.15	2
10	68263.	40.14	5.60	53219.	29.66	3.12	2
11	63139.	41.07	5.34	43334.	30.78	2.91	1
12	59357.	41.84	5.13	40878.	31.53	3.04	2
13	55631.	42.51	4.87	36699.	32.40	2.94	2
14	52455.	43.15	4.76	32444.	33.20	2.64	1
15	49451.	43.84	4.59	30633.	33.92	2.69	1
16	46728.	44.37	4.44	31853.	34.43	2.92	2
17	44051.	44.94	4.20	26520.	35.24	2.53	1
18	42071.	45.49	4.10	26096.	35.93	2.54	1
19	39885.	45.93	4.00	25960.	36.29	2.57	1
20	37517.	46.36	3.96	23895.	37.02	2.43	
21	35711.	46.80	3.83	24910.	37.50	2.85	
22	34326.	47.17	3.70	23538.	37.98	2.60	
23	32256.	47.51	3.60	24025.	38.47	2.79	
24	30575.	47.88	3.63	22558.	38.91	2.56	
25	28865.	48.23	3.51	22081.	39.31	2.86	
26	27277.	48.51	3.36	18998.	39.71	2.58	
27	25879.	48.79	3.30	17236.	40.10	2.43	
28	24249.	49.09	3.28	15346.	40.48	2.26	
29	22952.	49.42	3.25	14624.	40.77	2.50	
30	21736.	49.71	3.15	12656.	41.08	2.29	
31	20995.	50		10858.	41		
32	19861.	50		9866.	42		
33	18945.	50		9527.	42		
34	18117.	50		8874.	42		
35	17314.	51		8694.	43		
36	16472.	51		8628.	43		
37	16035.	51		8512.	43		
38	15173.	51		8165.	43		
39	14650.	51		8078.	43		
40	13990.	51		7808.	44		
41	13204.	52		7646.	44		
42	12710.	52		7362.	44		
43	12322.	52		7324.	44		
44	11695.	52		7159.	44		
45	11357.	52		7014.	45		
46	10743.	52		7007.	45		
47	9943.	52		6943.	45		
48	9892.	53		6651.	45		
49	9010.	53		6510.	45		
50	8962.	53		6481.	46		
51	8525.	53		6296.	46		
52	8025.	53		6260.	46		
53	7588.	53		6160.	46		
54	7259.	53		5910.	46		
55	6825.	53		5827.	46		
56	6657.	54		5812.	46		
57	6436.	54		5709.	47		
58	6072.	54		5598.	47		
59	5777.	54		5439.	47		
60	5396.	54		5493.	47		
61	5273.	54		5444.	47		
62	5004.	54		5244.	47		
63	4851.	54		5249.	47		
64	4667.	54		5126.	48		

SEMITLOG PLOT OF CALCULATED NEUTRON PULSE HEIGHT SPECTRA

3 HC PUBE FGD 4-11-71 (5707200)

THE SCALE OF THIS GRAPH IS 1 DIVISION = 0.36654E-01UNITS



B-2.0 Data Binning Code, DATABIN

This special purpose code is used to combine the high and low gain pulse height spectra from the DISCRIM code into a single set of data with the same gain. Since the high gain data has a gain 2.5 times greater than the low gain data, the code "stretches" the low gain data by a factor of 2.5. The high gain and stretched low gain data are then combined into a single set of data of 160 channels by replacing the first 64 channels of data in the stretched low gain data by the high gain data.

In this work, the normal 1024 channel range of the analyzer is reduced by a factor of 16 to just 64 channels by altering the format selector on the analyzer. In order to make the data from the TAC spectrometer applicable to analysis by existing computer codes, the DATABIN code is also used to further "stretch" the combined spectrum to the required 1024 channels (a "stretch factor" of $6.4 = \frac{1024}{160}$). In general, the DATABIN code can be used to "stretch" or "bin" the original data into a new spectrum which has from 1 to 2500 channels.

B-2.1 DATABIN Input Data Format

<u>Card</u>	<u>Format</u>	<u>Variable and Description</u>
1	1X,F4.0,4OH	<p>1. STOP = 0 if this is a data set.</p> <p>= 1 if no more data is to be read in; i.e., put a card with a 1 in column 5 behind the last set of data to terminate the program.</p>
		<p>2. LABEL = An arbitrary alphanumeric label to identify the data.</p>
2	3F10.0	<p>1. GCHIN = Channel where Co-60 tail falls in high gain input data.</p> <p>2. GCHOUT = Channel where Co-60 tail is to be shifted to in the output data; i.e., data is shifted by a factor of GCHOUT/GCHIN.</p>
		<p>3. BKG = 0 if background is not to be subtracted.</p> <p>= 1 if background is to be subtracted.</p>
3	4F10.0	<p>1. SF1 = Relative fluence for high gain foreground data.</p> <p>2. SF2 = Relative fluence for low gain foreground data.</p> <p>3. SF3 = Relative fluence for high gain Background data, if any.</p> <p>4. SF4 = Relative fluence for low gain background data, if any.</p>

4 (Deck)	1X, 10F7.0	High gain foreground data (64 channels)
5 (Deck)	1X,10F7.0	Low gain foreground data (64 channels)
6 (Deck)	1X,10F7.0	High gain background data, if any.
7 (Deck)	1X,10F7.0	Low gain background data, if any.
8 (Deck)	-----	Other data sets, if any (cards 1-7)
9	1X,F4.0	1. STOP = 1 Put a card with a 1 in column 2-5 as described in card 1 to stop the program after the last data set.

B-2.2 DATABIN Code Listing

```

$JCB      RES
C   PUT DATA IN THIS FORM.....
C
C   1) ALPHANUMERIC TITLE IN COLUMNS 5 - 50. COLUMNS 1 - 5 MUST BE BLANK.
C   2) GCHIN, GCHCUT, BKG (3F10.0)
C   3) SF1,SF2,SF3,SF4 (4F10.0)
C   4) HIGH GAIN FOREGROUND DATA (64 CHANNELS IN 6X,12F6.0 FORMAT)
C   5) LOW GAIN FOREGROUND DATA (64 CHANNELS IN 6X,12F6.0 FORMAT)
C   6) HIGH GAIN BACKGROUND DATA IF ANY.
C   7) LOW GAIN BACKGROUND DATA IF ANY.
C
C   8) ANY OTHER DATA SETS (EACH DATA SET SAME AS 1 - 7)
C
C   9) PUT A CARD WITH A NONZERO DIGIT IN COL 2 - 5 BEHIND ALL THE DATA
C      TO STOP THE PROGRAM.
C
C
C   "GCHIN" IS THE CHANNEL WHERE THE HIGH GAIN CO-60 TAIL LIES.
C   "GCHCUT" IS THE CHANNEL WHERE THE CO-60 TAIL IS TO BE SHIFTED TO. (I.E.
C      THE DATA IS STRETCHED OR COMPRESSED)
C   "BKG" IS A CODE TO INDICATE IF BACKGROUND DATA IS TO BE SUBTRACTED FROM
C      THE FOREGROUND DATA. (MAKE NONZERO IF BKG IS TO BE SUBTRACTED)
C   "SF1,SF2,SF3, AND SF4" ARE THE RELATIVE INTEGRATED FLUXES FOR THE
C      HIGH GAIN FOREGROUND, LOW GAIN FOREGROUND, HIGH GAIN BKG, AND
C      LOW GAIN BKG RESPECTIVELY.
C
C
1  DIMENSION XFL(64),XFH(64),XBL(64),XBH(64),XT(2500),XL(64),XH(64)
2  INTEGER STOP
3  READ 52,STOP
4  IF(STOP.GT.0) GO TO 20
5  PRINT 57
6  PRINT 52,STOP
7  PRINT 55
8  READ 50,GCHIN,GCHOUT,BKG
9  IF(GCHCUT.EQ.0) GCHCUT = GCHIN
10 READ 50,SF1,SF2,SF3,SF4
11 READ 51,XFH
12 READ 51,XFL
13 PRINT 55
14 PRINT 59
15 PRINT 55
16 PRINT 51,XFH
17 PRINT 55
18 PRINT 51,XFL
19 IF(BKG.EQ.0.) GO TO 3
20 READ 51,XBH
21 READ 51,XBL
22 PRINT 55
23 PRINT 55
24 PRINT 60
25 PRINT 55
26 PRINT 51,XBH
27 PRINT 55
28 PRINT 51,XBL
29 DO 2 I=1,64
30     XH(I)=(XFH(I)/SF1)-(XBH(I)/SF3)
31     XL(I)=(XFL(I)/SF2)-(XBL(I)/SF4)
32     GO TO 5
33     DC 4 I=1,64

```

```

34 XH(I)= XFH(I)/SF1
35 4 XL(I)= XFL(I)/SF2
36 5 SF=GCHCUT/GCHIN
37 NCHOUT= SF*2.5*64.
38 DO 1C I=1,NCHOUT
39 XI=I
40 XU=XI/SF + 1.0
41 XLO=XL - (1.0/SF)
42 JL=XLC
43 JU=XU
44 IF(JL.LT.1) JL=1
45 IF(JU.GT.64) GO TO 6
46 CALL BINHI(XH,XU,XLO,JU,JL,XT(I))
47 GO TC 7
48 6 CALL BINLO(XL,XU,XLO,JU,JL,XT(I))
49 7 IF(XT(I).LT.1.E5) GO TO 10
50 XT(I)=XT(I) - 1.E5
51 GO TC 7
52 10 CONTINUE
53 PRINT 55
54 PRINT 55
55 PRINT 61
56 PRINT 55
57 PRINT 53,NCHOUT,GCHIN,GCHCUT
58 PRINT 55
59 PRINT 58,(XT(I), I=1,NCHOUT)
60 PUNCH 54
61 PUNCH 55
62 PUNCH 56,NCHOUT,GCHOUT
63 PUNCH 52,STOP
64 PUNCH 58,(XT(I), I=1,NCHOUT)
65 PUNCH 55
66 GO TO 1
67 20 STOP
68 50 FORMAT(7F10.3)
69 51 FORMAT(1X,1CF7.0)
70 52 FORMAT(1X,I4,'')
71 53 FORMAT(1X,I10,' CHANNELS OF DATA WITH GAMMA TAIL SHIFTED FROM CHAN
    1NEL',F9.3,' TO CHANNEL',F9.3)
72 54 FORMAT(1X,'A'AAAAAAAAAAAAAAA'AAAAAAAAAAAAAAA'AAAAAAAAAAAAAAA'')
73 55 FORMAT(1H )
74 56 FORMAT(1X,I4,F10.3,2X,3H1.0)
75 57 FORMAT(1H1)
76 58 FORMAT(6X,12F6.0)
77 59 FORMAT(1X,'UNSHIFTED HIGH THEN LOW GAIN FOREGROUND DATA')
78 60 FORMAT(1H , 'UNSHIFTED HIGH THEN LOW GAIN BACKGROUND DATA')
79 61 FORMAT(1X,'SHIFTED NET COUNTS')
80 END

81 SUBROUTINE BINHI(XH,XU,XL,JU,JL,XT)
82 DIMENSION XF(64)
83 XT=0.0
84 J=JL
85 IF(JU.NE.JL) GO TO 1
86 XT= (XL - XL) * XH(JL)
87 RETURN
88 1 J=J+1
89 X2=J
90 F=X2 - XL
91 XI=F*XH(J-1)

```

```
52      10 IF(J.EC.JU) GO TO 3
53      XT=XT+XH(J)
54      J=J+1
55      GO TO 10
56 3  X=JU
57      XT=XT + (XU-X)*XH(JU)
58      RETURN
59      END

100      SUBROUTINE BINLO(XL,XU,XLO,JL,JL,XT)
101      DIMENSION XL(64)
102      XU=XU*C.4
103      XLO=XLC*0.4
104      JUP=XL
105      JL0=XLC
106      CALL BINHI(XL,XU,XLO,JUP,JL0,XT)
107      RETURN
108      END

$ENTRY
```

B-2.3 Sample Data Set and Results

DATABIN Input Data Set

DATABIN Output

O 0-2 PENETRATION DATA 4-6-71

UNSHIFTED HIGH THEN LOW GAIN FOREGROUND DATA

0.	0.	0.	97001.	94522.	81219.	£5379.	49695.	43315.	38289.
33482.	33011.	33782.	29140.	27312.	26484.	25849.	25223.	24937.	23694.
2281C.	21413.	19621.	19245.	17103.	15705.	14603.	13323.	11768.	9736.
7544.	5341.	4016.	3235.	2920.	2582.	2353.	2101.	1925.	1800.
1678.	1517.	1411.	1283.	1258.	1177.	1205.	1095.	1041.	1026.
1C13.	1000.	988.	930.	929.	897.	855.	888.	827.	844.
799.	869.	771.	805.						

C.	0.133212.	97566.	94913.	83818.	74366.	64530.	56627.	47582.	
38757.	29031.	15574.	8163.	6152.	4835.	3829.	3202.	2883.	2519.
2366.	2284.	2124.	2036.	1908.	1874.	1698.	1660.	1531.	1528.
1391.	1369.	1262.	1121.	1015.	999.	847.	856.	861.	721.
614.	595.	601.	526.	487.	452.	460.	369.	345.	299.
277.	222.	211.	149.	169.	134.	120.	93.	92.	96.
79.	58.	74.	76.						

UNSHIFTED HIGH THEN LOW GAIN BACKGROUND DATA

C.	C.	O.	85138.	75382.	61004.	50847.	35265.	28534.	24079.
216C3.	19344.	16980.	14674.	12485.	11026.	10490.	9386.	8376.	7506.
6884.	6162.	5604.	5146.	4892.	4221.	3878.	3551.	3287.	2911.
2656.	2395.	2170.	1960.	1804.	1662.	1610.	1390.	1286.	1176.
1057.	586.	993.	855.	791.	728.	737.	679.	655.	610.
611.	543.	559.	488.	483.	504.	420.	464.	432.	387.
4C7.	340.	367.	328.						

0.	0.106548.	77701.	71638.	61744.	38754.	33802.	25597.	26160.
12459.	9978.	7801.	5881.	4720.	3867.	3000.	2558.	2229.
1653.	1548.	1312.	1258.	1100.	986.	951.	813.	761.
619.	600.	522.	438.	372.	319.	351.	290.	269.
228.	212.	177.	155.	142.	141.	125.	97.	95.
102.	86.	56.	70.	63.	58.	42.	40.	41.
39.	27.	22.	21.					26.

SHIFTED NET COUNTS

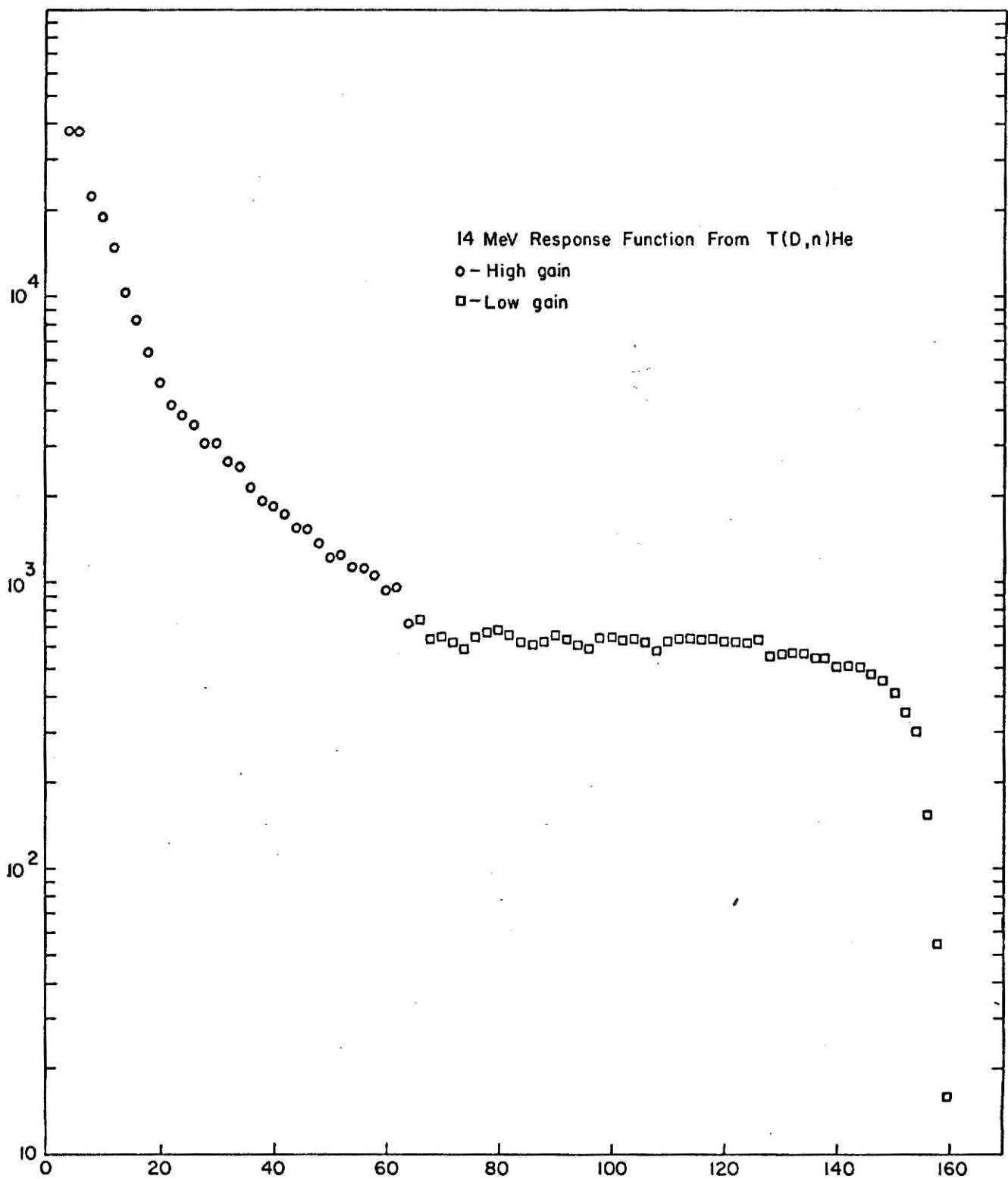
1C23 CHANNELS OF DATA WITH GAMMA TAIL SHIFTED FROM CHANNEL 31.250 TO CHANNEL 200.000

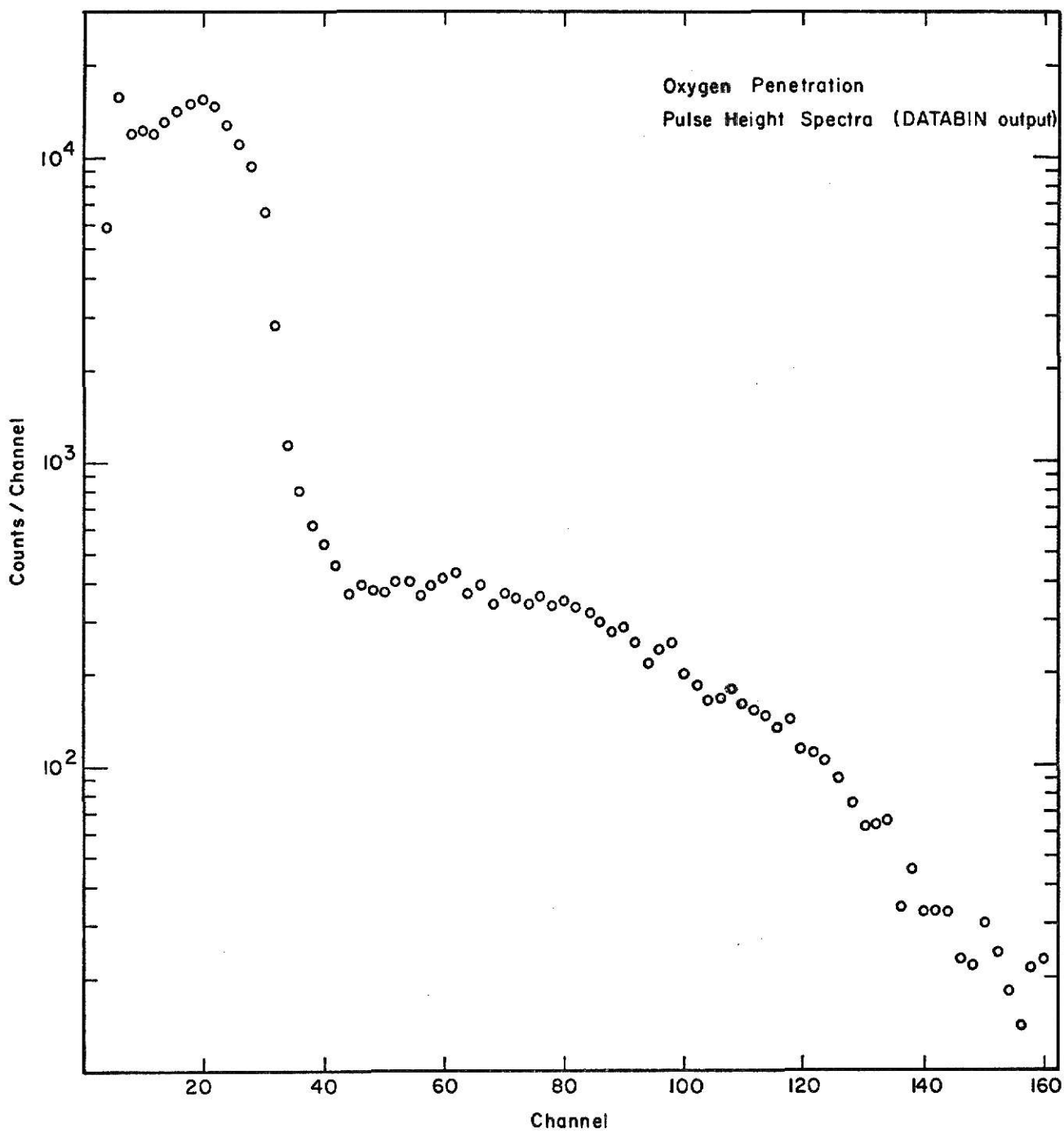
O.	O.	C.	O.									
C.	O.	C.	O.	O.	O.	O.	743.	929.	929.	929.	929.	929.
929.	1426.	2172.	2172.	2172.	2172.	2172.	2496.	2496.	2496.	2496.	2496.	2496.
2496.	2496.	2025.	1718.	1718.	1718.	1718.	1749.	1872.	1872.	1872.	1872.	1872.
1872.	1872.	1872.	1974.	2000.	2000.	2000.	2000.	1983.	1959.	1959.	1959.	1959.
1959.	1959.	1959.	1959.	2090.	2090.	2090.	2090.	2090.	1991.	1991.	1925.	1925.
1925.	1925.	1925.	1925.	1935.	1972.	1972.	1972.	1972.	1972.	1972.	1972.	2075.
2101.	2101.	2101.	2101.	2133.	2181.	2181.	2181.	2181.	2181.	2181.	2181.	2181.
2296.	2296.	2296.	2296.	2296.	2290.	2286.	2286.	2286.	2286.	2286.	2286.	2286.
2303.	2373.	2373.	2373.	2373.	2373.	2472.	2497.	2497.	2497.	2497.	2497.	2497.
2497.	2477.	2448.	2448.	2448.	2448.	2448.	2414.	2414.	2414.	2414.	2414.	2414.
2414.	2414.	2355.	2316.	2316.	2316.	2316.	2279.	2129.	2129.	2129.	2129.	2129.
2129.	2129.	2129.	2119.	1991.	1991.	1991.	1991.	1936.	1855.	1855.	1855.	1855.
1855.	1855.	1855.	1855.	1749.	1749.	1749.	1749.	1749.	1749.	1749.	1680.	1634.

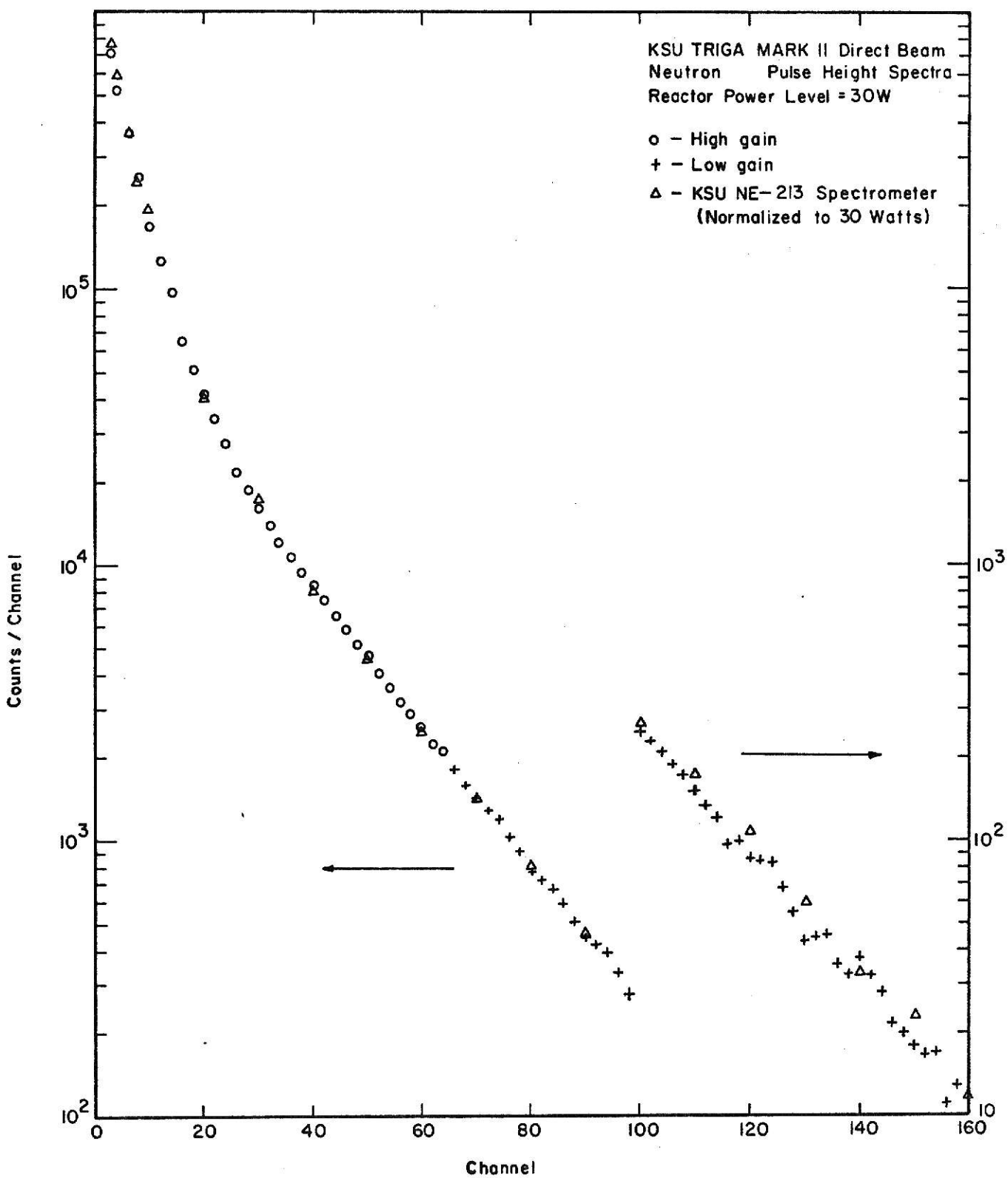
APPENDIX C

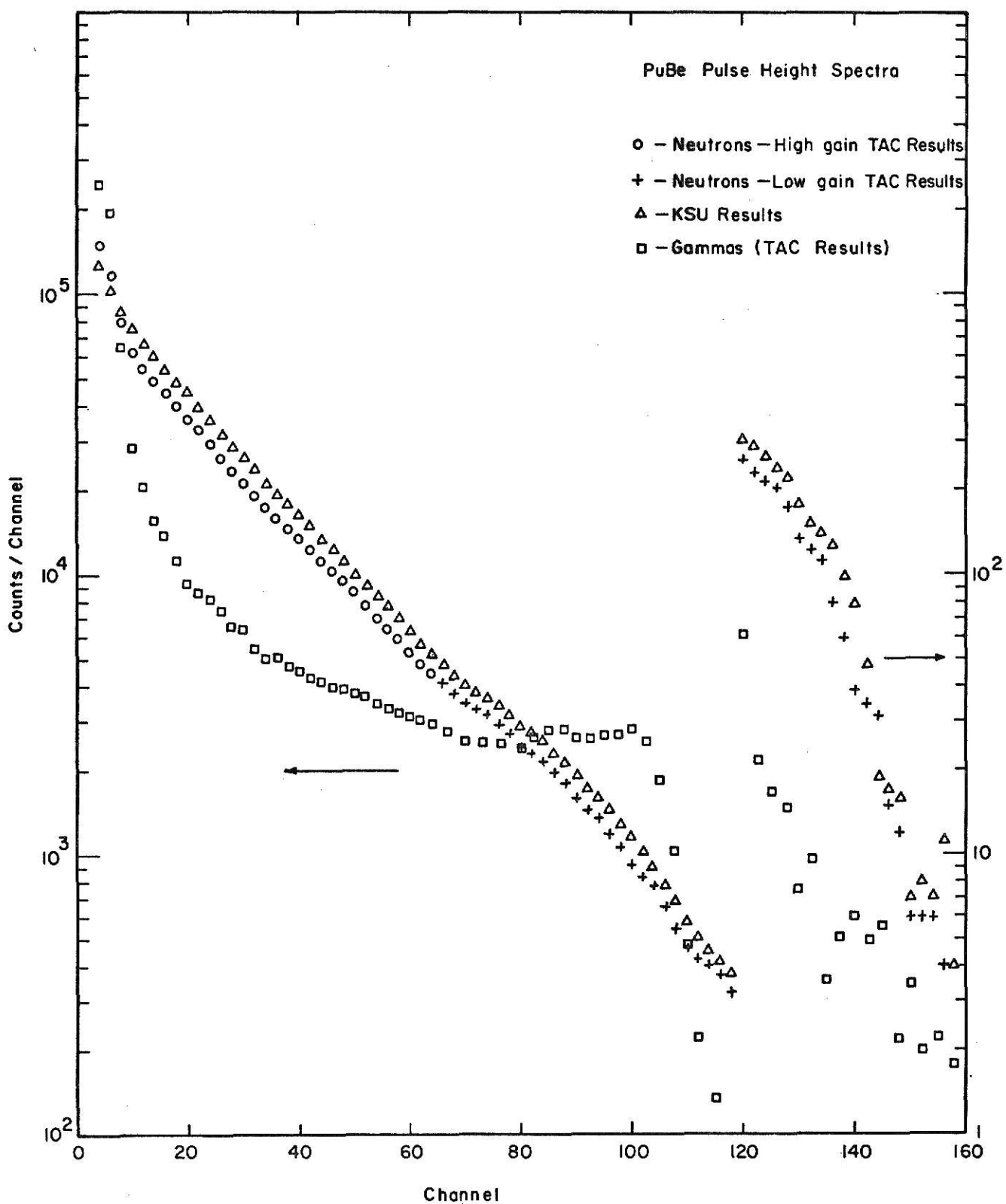
Raw Pulse Height Spectra

Presented in this section are the pulse height spectra calculated by the DISCRIM code for the neutron spectra measured in this study.









APPENDIX D

Sample FERDOR Input Data and Results

EYNNM 1000 10 71A6, 16, 1CF6.0, 1A6<

NET COUNT	1	6011.	5916.	5821.	5727.	5632.	5537.	5443.	5348.	5253.	5159.
11	5064.	4969.	4875.	4780.	4685.	4591.	4496.	4401.	4307.	4212.	40
21	4117.	4023.	4023.	3703.	2867.	2769.	2769.	2820.	3017.	3017.	40
31	3171.	3076.	3212.	3223.	3223.	3205.	3157.	3157.	3157.	3157.	40
41	3368.	3368.	3368.	3277.	3107.	3102.	3102.	3130.	3178.	3178.	40
51	3178.	3262.	3262.	3281.	3286.	3366.	3439.	3515.	3515.	3515.	40
61	3700.	3700.	3693.	3693.	3684.	3684.	3684.	3754.	3825.	3824.	40
71	3824.	3932.	4024.	4024.	4024.	3980.	3945.	3945.	3945.	3913.	40
81	3891.	3891.	3891.	3793.	3733.	3733.	3724.	3546.	3431.	3431.	40
91	3431.	3281.	3209.	3209.	3202.	3060.	2989.	2990.	2990.	2864.	40
101	2819.	2819.	2817.	2673.	2633.	2633.	2620.	2460.	2398.	2298.	40
111	2134.	2077.	2077.	2041.	1765.	1668.	1668.	1668.	1668.	1241.	40
121	1184.	1138.	1138.	789.	699.	699.	675.	466.	427.	427.	40
131	416.	3C1.	286.	286.	281.	255.	249.	249.	248.	203.	40
141	2C3.	194.	164.	164.	159.	159.	158.	154.	154.	154.	40
151	151.	129.	132.	138.	137.	137.	137.	137.	135.	127.	40
161	127.	127.	124.	116.	116.	116.	116.	110.	88.	88.	40
171	85.	93.	93.	93.	93.	95.	95.	103.	103.	102.	40
181	99.	99.	101.	104.	104.	104.	104.	100.	93.	93.	40
191	85.	85.	85.	88.	88.	93.	93.	91.	91.	91.	40

EFYNN 2000 10 %1A6:16:10E6:0:1A6:

LCW	GAIN	NET COUNTS	S
2000	10	91A6,16,1DF6.C,1A6C	
REL	1	0.	2C437.
REL	11	2628C.	18741.
REL	21	605.	1008.
REL	21	861.	858.
REL	41	447.	419.
REL	51	2FC.	168.
RFL	61	53.	34.
RFL	71	C.	C.
RFL	81	0.	0.
RFL	91	0.	0.
RFL	101	C.	C.
RFL	111	C.	C.
RFL	121	C.	C.
RFL	131	C.	C.
RFL	141	C.	C.
RFL	151	C.	C.
RFL	161	C.	C.
RFL	171	C.	C.
RFL	181	C.	C.
RFL	191	C.	C.
REL	1	31652.	31653.
REL	11	2779.	2769.
REL	21	984.	977.
REL	21	1012.	1008.
REL	21	763.	752.
REL	41	416.	402.
REL	51	106.	97.
RFL	61	30.	46.
RFL	71	0.	0.
RFL	81	0.	0.
RFL	91	0.	0.
RFL	101	0.	0.
RFL	111	0.	0.
RFL	121	0.	0.
RFL	131	0.	0.
RFL	141	0.	0.
RFL	151	0.	0.
RFL	161	0.	0.
RFL	171	0.	0.
RFL	181	0.	0.
RFL	191	0.	0.
REL	1	32184.	32185.
REL	11	1707.	1706.
REL	21	138C.	138C.
REL	21	1038.	1038.
REL	21	714.	714.
REL	41	346.	346.
REL	51	106.	86.
RFL	61	20.	20.
RFL	71	C.	C.
RFL	81	0.	0.
RFL	91	0.	0.
RFL	101	0.	0.
RFL	111	0.	0.
RFL	121	0.	0.
RFL	131	0.	0.
RFL	141	0.	0.
RFL	151	0.	0.
RFL	161	0.	0.
RFL	171	0.	0.
RFL	181	0.	0.
RFL	191	0.	0.
REL	1	34179.	34179.
REL	11	1104.	1104.
REL	21	896.	896.
REL	21	596.	596.
REL	41	35C.	35C.
REL	51	106.	86.
RFL	61	10.	10.
RFL	71	0.	0.
RFL	81	0.	0.
RFL	91	0.	0.
RFL	101	0.	0.
RFL	111	0.	0.
RFL	121	0.	0.
RFL	131	0.	0.
RFL	141	0.	0.
RFL	151	0.	0.
RFL	161	0.	0.
RFL	171	0.	0.
RFL	181	0.	0.
RFL	191	0.	0.
REL	1	37254.	37254.
REL	11	977.	977.
REL	21	885.	885.
REL	21	586.	586.
REL	41	623.	623.
REL	51	306.	306.
RFL	61	67.	67.
RFL	71	51.	51.
RFL	81	75.	75.
RFL	91	40.	40.
RFL	101	0.	0.
RFL	111	0.	0.
RFL	121	0.	0.
RFL	131	0.	0.
RFL	141	0.	0.
RFL	151	0.	0.
RFL	161	0.	0.
RFL	171	0.	0.
RFL	181	0.	0.
RFL	191	0.	0.
REL	1	37067.	37067.
REL	11	997.	997.
REL	21	898.	898.
REL	21	P83.	P83.
REL	41	550.	550.
REL	51	237.	237.
RFL	61	75.	75.
RFL	71	40.	40.
RFL	81	0.	0.
RFL	91	0.	0.
RFL	101	0.	0.
RFL	111	0.	0.
RFL	121	0.	0.
RFL	131	0.	0.
RFL	141	0.	0.
RFL	151	0.	0.
RFL	161	0.	0.
RFL	171	0.	0.
RFL	181	0.	0.
RFL	191	0.	0.

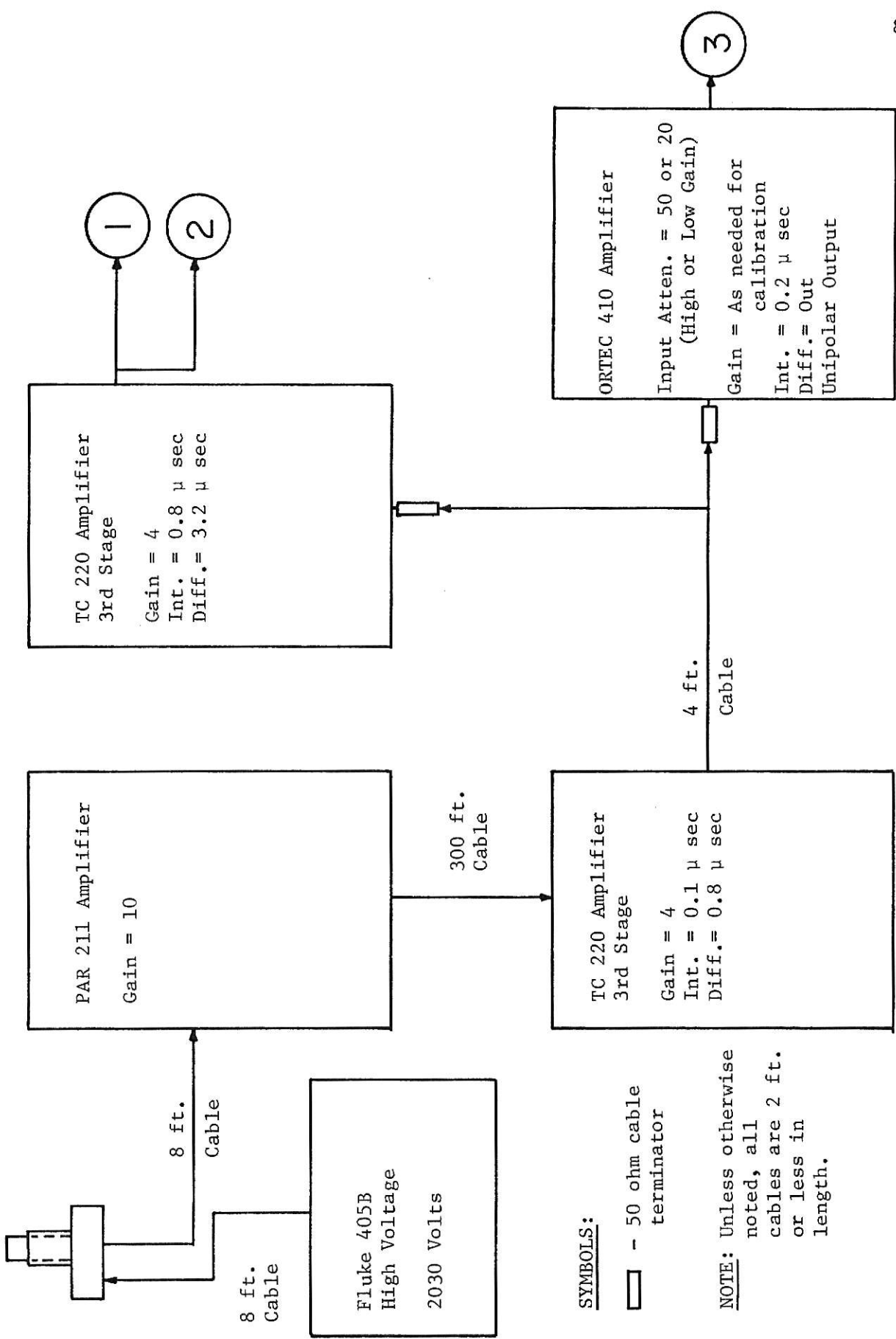
LOW	+	C	C	V	>	F	P	4	E	C	D	0	\$3
ENERGY	PLC	PUP	PAVE	RUNSUM	RUNERR	PCT %	ERR1	ERR2					
0.400E-06	1	0.187E C2	0.207E C3	0.0 195E C3	0.0 195E C3	0.795E 0.9	38.40	0.103E 0.2	0.188E 0.1				
C.900E C5	2	0.326E C2	0.632E C2	0.509E 0.2	0.50876860E 0.7	0.847E 0.9	36.00	0.1C9E 0.2	0.137E 0.1				
-0.1C9E C7	3	-0.132E C3	-0.145E C3	-0.933E 0.3	-0.933E 0.3	0.916E 0.0	33.50	0.117E 0.2	0.106E 0.1				
0.110E C7	4	-0.119E C3	-0.106E C3	-0.20023008E 0.8	-0.20023008E 0.8	0.977E 0.9	32.40	0.111E 0.2	0.111E 0.1				
C.120E C7	5	-0.159E C2	-0.159E C2	-0.327E 0.1	-0.20350320E 0.8	0.101E 1.0	31.20	0.117E 0.2	0.006E 0.0				
0.130E C7	6	-0.106E 0.2	-0.197E 0.2	0.467E 0.1	-0.19863232E 0.8	0.127E 1.0	30.90	0.142E 0.2	0.100E 0.1				
-0.941E 0.2	7	-0.532E 0.2	-0.737E 0.2	-0.27454832E 0.8	-0.27454832E 0.8	0.178E 0.0	28.80	0.170E 0.2	0.170E 0.1				
C.140E C7	8	-0.218E 0.3	-0.175E 0.3	-0.197E C3	-0.46911440E 0.8	0.189E 1.0	27.60	0.203E 0.2	0.165E 0.1				
C.150E C7	9	-0.334E C3	-0.289E 0.3	-0.311E 0.3	-0.78042064E 0.8	0.203E 1.0	26.40	0.219E 0.2	0.219E 0.1				
C.160E C7	10	-0.320E C3	-0.283E 0.3	-0.364E 0.3	-0.10864083E 0.9	0.219E 1.0	25.80	0.226E 0.2	0.219E 0.1				
C.170E C7	11	-0.181E 0.3	-0.130E 0.3	-0.157E 0.3	-0.11434728E 0.9	0.232E 1.0	25.20	0.227E 0.2	0.227E 0.1				
C.180E C7	12	0.495E 0.2	0.182E 0.4	0.197E 0.3	-0.11362341E 0.9	0.226E 1.0	24.60	0.218E 0.2	0.193E 0.1				
C.200E C7	13	0.476E C2	0.517E 0.3	0.496E 0.3	-0.63977328E 0.8	0.214E 1.0	24.00	0.203E 0.2	0.505E 0.1				
C.210E C7	14	0.106E C4	0.104E 0.4	0.102E 0.4	0.38091728E 0.8	0.134E 1.0	23.40	0.1PCE 0.2	0.281E 0.1				
C.220E C7	15	0.155E 0.4	0.159E 0.4	0.157E 0.4	0.19517592E 0.9	0.174E 1.0	22.80	0.154E 0.2	0.234E 0.1				
C.180E C7	16	0.188E C4	0.191E 0.4	0.189E 0.4	0.38431283E 0.9	0.151E 1.0	22.50	0.151E 0.2	0.151E 0.1				
C.190E C7	17	0.186E C4	0.188E 0.4	0.187E C4	0.57114522E 0.9	0.135E 1.0	21.96	0.114E 0.2	0.649E 0.0				
C.210E C7	18	0.151E C4	0.153E 0.4	0.152E 0.4	0.22329627E 0.9	0.110E 1.0	21.60	0.966E 0.1	0.476E 0.0				
C.230E C7	19	0.106E C4	0.107E 0.4	0.107E 0.4	0.83005328E 0.9	0.846E 0.9	21.36	0.666E 0.1	0.458E 0.0				
C.250E C7	20	0.658E C3	0.668E 0.3	0.663E C3	0.89635540E 0.9	0.637E 0.9	20.76	0.496E 0.1	0.870E 0.0				
C.270E C7	21	0.376E 0.3	0.384E 0.3	0.380E 0.3	0.93455750E 0.9	0.533E 0.9	20.40	0.407E 0.1	0.316E 0.0				
C.290E C7	22	0.205E 0.3	0.213E 0.3	0.209E 0.3	0.55229944E 0.9	0.508E 0.9	20.16	0.373E 0.1	0.211E 0.0				
C.310E C7	23	0.161E 0.3	0.165E 0.3	0.171E 0.3	0.965746118E 0.9	0.516E 0.9	19.68	0.368E 0.1	0.376E 0.0				
C.320E C7	24	0.128E 0.2	0.124E 0.2	0.166E C2	0.66905317E 0.9	0.495E 0.9	19.20	0.353E 0.1	0.532E 0.0				
C.340E C7	25	-0.149E 0.2	-0.699E 0.1	-0.109E 0.2	0.96688154E 0.9	0.527E 0.9	18.60	0.374E 0.1	0.179E 0.0				
C.360E C7	26	-0.656E 0.1	-0.665E 0.1	-0.111E C2	0.96463813E 0.9	0.5969E 0.9	18.00	0.4121E 0.1	0.191E 0.0				
C.380E C7	27	0.121E 0.0	0.914E 0.1	0.463E C1	0.966161459E 0.9	0.635E 0.9	17.40	0.4230E 0.1	0.215E 0.0				
C.400E C7	28	0.121E 0.2	0.223E 0.2	0.177E 0.2	0.67015456E 0.9	0.654E 0.9	16.80	0.444E 0.1	0.274E 0.0				
C.420E C7	29	0.149E 0.2	0.236E 0.2	0.193E 0.2	0.97300633E 0.9	0.649E 0.9	16.56	0.426E 0.1	0.125E 0.0				
C.440E C7	30	0.190E 0.2	0.285E 0.2	0.241E 0.2	0.97982996E 0.9	0.649E 0.9	15.96	0.421E 0.1	0.258E 0.0				
C.460E C7	31	0.331E 0.2	0.411E 0.2	0.373E 0.2	0.98529971E 0.9	0.640E 0.9	15.90	0.4468E 0.1	0.108E 0.0				
C.480E C7	32	0.466E 0.2	0.517E 0.2	0.476E 0.2	0.95482189E 0.9	0.640E 0.9	15.36	0.295E 0.1	0.324E 0.0				
C.500E C7	33	0.474E 0.2	0.554E 0.2	0.514E 0.2	0.10051023E 1.0	0.649E 0.9	15.12	0.390E 0.1	0.135E 0.0				
C.520E C7	34	0.502E 0.2	0.581E 0.2	0.542E 0.2	0.10529396E 1.0	0.640E 0.9	14.64	0.444E 0.1	0.370E 0.1				
C.540E C7	35	0.504E 0.2	0.581E 0.2	0.542E 0.2	0.10267873E 1.0	0.640E 0.9	14.40	0.386E 0.1	0.354E 0.1				
C.560E C7	36	0.572E 0.2	0.541E 0.2	0.514E 0.2	0.10619466E 1.0	0.642E 0.9	14.26	0.366E 0.1	0.822E 0.1				
C.580E C7	37	0.499E 0.2	0.563E 0.2	0.526E 0.2	0.10475087E 1.0	0.634E 0.9	13.92	0.358E 0.1	0.107E 0.0				
C.480E C7	38	0.435E 0.2	0.515E 0.2	0.476E 0.2	0.95482189E 0.9	0.640E 0.9	13.80	0.392E 0.1	0.135E 0.0				
C.500E C7	39	0.474E 0.2	0.554E 0.2	0.514E 0.2	0.10051023E 1.0	0.649E 0.9	13.60	0.332E 0.1	0.274E 0.0				
C.640E C7	40	0.144E 0.2	0.802E 0.2	0.773E 0.2	0.10404404E 1.0	0.518E 0.9	13.20	0.284E 0.1	0.283E 0.1				
C.660E C7	41	0.661E 0.2	0.714E 0.2	0.639E 0.2	0.11061946E 1.0	0.463E 0.9	12.96	0.266E 0.1	0.547E 0.1				
C.680E C7	42	0.518E 0.2	0.564E 0.2	0.541E 0.2	0.1150139E 1.0	0.434E 0.9	12.64	0.226E 0.1	0.58E 0.1				
C.700E C7	43	0.396E 0.2	0.642E 0.2	0.467E 0.2	0.11231457E 1.0	0.382E 0.9	12.36	0.226E 0.1	0.340E 0.1				
C.720E C7	44	0.392E 0.2	0.712E 0.2	0.337E 0.2	0.11295388E 1.0	0.337E 0.9	12.36	0.312E 0.1	0.222E 0.1				
C.740E C7	45	C.264E C2	0.294E 0.2	0.275E C2	0.11351155E 1.0	0.292E 0.9	12.24	0.145E 0.1	0.272E 0.1				
C.760E C7	46	0.240E 0.2	0.265E 0.2	0.235E 0.2	0.11401736E 1.0	0.246E 0.9	12.12	0.122E 0.1	0.194E 0.1				
C.780E C7	47	0.201E 0.2	0.222E 0.2	0.212E 0.2	0.1144122E 1.0	0.209E 0.9	12.00	0.112E 0.1	0.142E 0.1				
C.800E C7	48	C.422E C2	0.163E 0.2	0.151E 0.2	0.147E 0.2	0.147E 0.2	11.76	0.132E 0.1	0.152E 0.1				
C.820E C7	49	0.804E C1	0.932E 0.1	0.866E C1	0.1491633E 1.0	0.13CE 0.9	11.64	0.619E 0.0	0.222E 0.1				
C.840E C7	50	0.365E 0.1	0.440E 0.1	0.402E 0.1	0.1499674E 1.0	0.774E 0.8	11.52	0.355E 0.0	0.205E 0.1				
C.860E C7	51	C.131E C1	0.171E 0.1	0.151E 0.1	0.151E 0.1	0.1502692E 1.0	0.422E 0.8	11.40	0.188E 0.0	0.143E 0.1			
C.880E C7	52	C.211E C0	0.608E C0	0.464E C0	0.15036319E 1.0	0.303E 0.8	11.26	0.134E 0.0	0.114E 0.1				
C.900E C7	53	-0.170E -0.1	0.255E 0.0	0.119E 0.0	0.11503854E 1.0	0.290E 0.8	11.16	0.123E 0.0	0.631E -0.2				
C.920E C7	54	-C.135E 0.0	0.164E 0.0	0.255E 0.0	0.11503905E 1.0	0.299E 0.8	11.04	0.133E 0.0	0.581E -0.2				
C.940E C7	55	-0.128E 0.0	0.148E 0.0	0.485E -0.2	0.11503913E 1.0	0.312E 0.8	10.92	0.136E 0.0	0.634E -0.2				
C.960E C7	56	-0.147E 0.0	0.149E 0.0	0.866E C0	0.11503913E 1.0	0.326E 0.8	10.80	0.140E 0.0	0.725E -0.2				

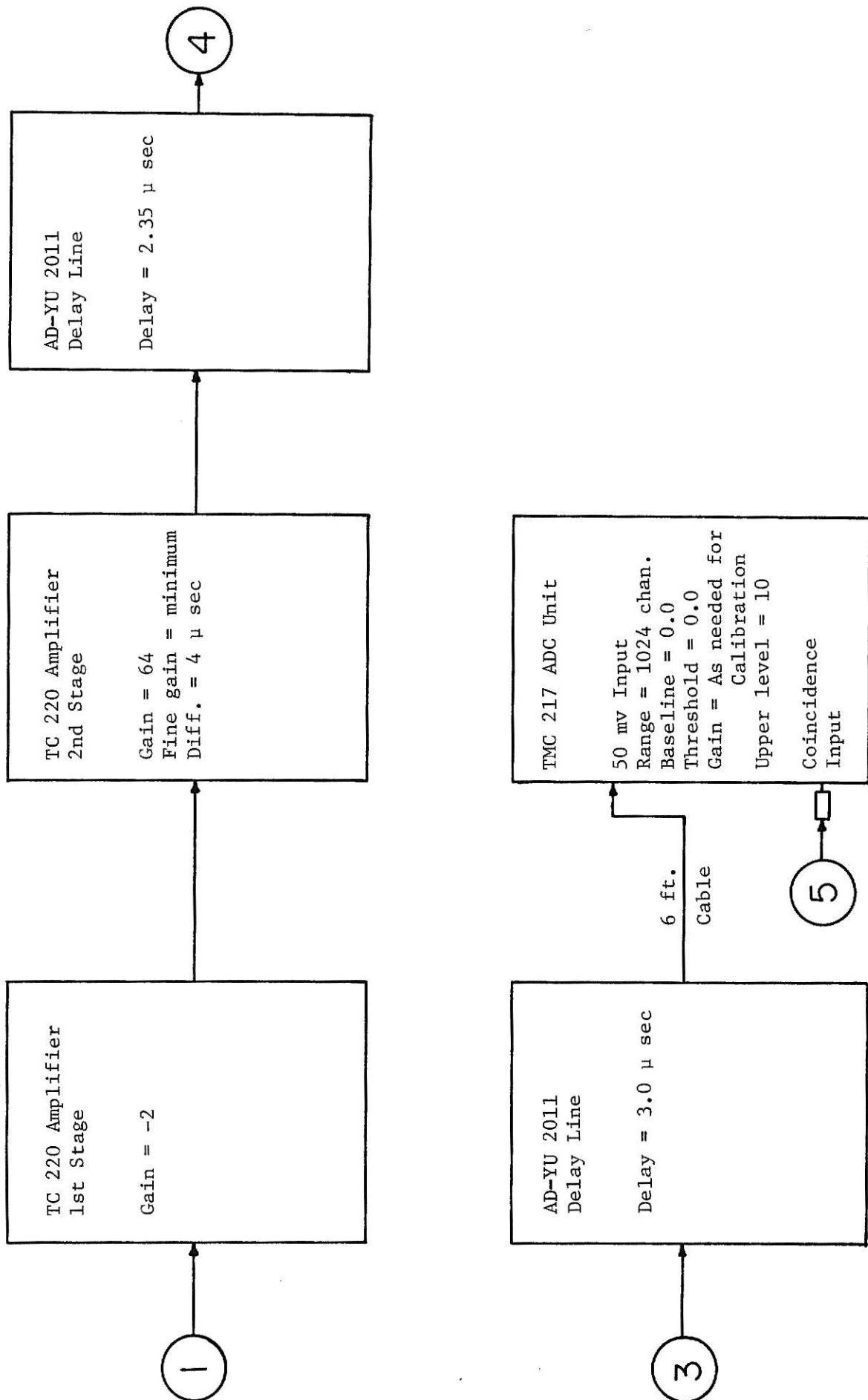
0.980 E 07	57	-0.152 E CC	0.762 E -04	-0.11503913E 10	0.340 E 08	10.88
0.157 E 00	58	-0.157 E CC	0.157 E -03	0.11503916E 10	0.352 E 08	10.88
0.161 E 00	59	-0.161 E CC	0.161 E -04	0.11503916E 10	0.364 E 08	10.88
0.163 E 00	60	-0.163 E CC	0.165 E -03	0.11503910E 10	0.376 E 08	10.88
0.177 E 00	61	-0.177 E CC	0.177 E -03	0.11503910E 10	0.391 E 08	10.88
0.188 E 00	62	-0.177 E CC	0.177 E -03	0.11503908E 10	0.410 E 08	10.88
0.110 E 00	63	-0.186 E CC	0.186 E -03	0.11503905E 10	0.432 E 08	9.96
0.112 E 00	64	-0.184 E CC	0.191 E -02	0.11503905E 10	0.452 E 08	9.84
0.198 E 00	65	-0.198 E CC	0.198 E -02	0.11503903E 10	0.488 E 08	9.72
0.202 E 00	66	-0.202 E CC	0.205 E -02	0.11503903E 10	0.494 E 08	9.60
0.116 E 00	67	-0.206 E CC	0.206 E -02	0.11503903E 10	0.496 E 08	9.50
0.120 E 00	68	-0.208 E CC	0.207 E -02	0.11503900E 10	0.509 E 08	9.50
0.122 E 00	69	-0.209 E CC	0.209 E -02	0.11503900E 10	0.521 E 08	9.50
0.207 E 00	70	-0.209 E CC	0.209 E -02	0.11503900E 10	0.528 E 08	9.50
0.124 E 00	71	-0.202 E CC	0.205 E -02	0.11503903E 10	0.528 E 08	9.40
0.126 E 00	72	-0.200 E CC	0.201 E -02	0.11503903E 10	0.524 E 08	9.40
0.128 E 00	73	-0.202 E CC	0.199 E -02	0.11503903E 10	0.524 E 08	9.40
0.132 E 00	74	-0.197 E CC	0.194 E -02	0.11503903E 10	0.528 E 08	9.40
0.134 E 00	75	-0.192 E CC	0.196 E -02	0.11503898E 10	0.528 E 08	9.40
0.136 E 00	76	-0.196 E CC	0.186 E -02	0.11503898E 10	0.517 E 08	9.40
0.128 E 00	77	-0.182 E CC	0.182 E -02	0.11503892E 10	0.517 E 08	9.40
0.140 E 00	78	-0.181 E CC	0.182 E -02	0.11503892E 10	0.519 E 08	9.40
0.142 E 00	79	-0.180 E CC	0.181 E -02	0.11503892E 10	0.523 E 08	9.40
0.175 E 00	80	-0.175 E CC	0.175 E -02	0.11503892E 10	0.527 E 08	9.40
0.144 E 00	81	-0.174 E CC	0.174 E -02	0.11503892E 10	0.533 E 08	9.40
0.146 E 00	82	-0.180 E CC	0.179 E -02	0.11503892E 10	0.533 E 08	9.40
0.148 E 00	83	-0.180 E CC	0.179 E -02	0.11503892E 10	0.533 E 08	9.40
0.150 E 00	84	-0.181 E CC	0.179 E -02	0.11503892E 10	0.533 E 08	9.40
0.152 E 00	85	-0.180 E CC	0.179 E -02	0.11503892E 10	0.531 E 08	9.40
0.154 E 00	86	-0.165 E CC	0.175 E -03	0.11503892E 10	0.523 E 08	9.40
0.156 E 00	87	-0.166 E CC	0.188 E -02	0.11503892E 10	0.470 E 08	9.40
0.158 E 00	88	-0.128 E CC	0.152 E -02	0.11503892E 10	0.417 E 08	9.40
0.160 E 00	89	-0.120 E CC	0.121 E -02	0.11503892E 10	0.393 E 08	9.40
0.162 E 00	90	-0.117 E CC	0.117 E -02	0.11503892E 10	0.351 E 08	9.40
0.164 E 00	91	-0.116 E CC	0.116 E -02	0.11503892E 10	0.351 E 08	9.40
0.166 E 00	92	-0.942 E -01	0.926 E -01	0.11503882E 10	0.421 E 08	9.40
0.168 E 00	93	-0.725 E -01	0.715 E -01	0.11503882E 10	0.417 E 08	9.40
0.170 E 00	94	-0.675 E -01	0.705 E -01	0.11503882E 10	0.417 E 08	9.40
0.172 E 00	95	-0.518 E -01	0.506 E -01	0.11503877E 10	0.380 E 08	9.40
0.174 E 00	96	-0.342 E -01	0.335 E -01	0.11503875E 10	0.120 E 08	9.40
0.176 E 00	97	-0.221 E -01	0.206 E -01	0.11503875E 10	0.400 E 08	9.40
0.178 E 00	98	-0.122 E -01	0.119 E -01	0.11503875E 10	0.375 E 08	9.40
0.180 E 00	99	-0.675 E -02	0.655 E -02	0.11503869E 10	0.244 E 07	9.40
0.182 E 00	100	-0.518 E -02	0.341 E -02	0.11503869E 10	0.128 E 07	9.40
0.184 E 00	101	-0.52 E -02	0.506 E -01	0.11503869E 10	0.180 E 08	9.40
0.186 E 00	102	-0.221 E -01	0.361 E -03	0.11503869E 10	0.646 E 06	9.40
0.188 E 00	103	-0.928 E -03	0.809 E -03	0.11503869E 10	0.311 E 06	9.40
0.190 E 00	104	-0.181 E -03	0.371 E -03	0.11503869E 10	0.144 E 06	9.40
0.192 E 00	105	-0.124 E -04	0.707 E -04	0.11503869E 10	0.647 E 05	9.40
0.194 E 00	106	-0.294 E -04	0.294 E -04	0.11503869E 10	0.281 E 05	9.40
0.195 E 00	107	-0.365 E -06	0.294 E -04	0.11503869E 10	0.118 E 05	9.40

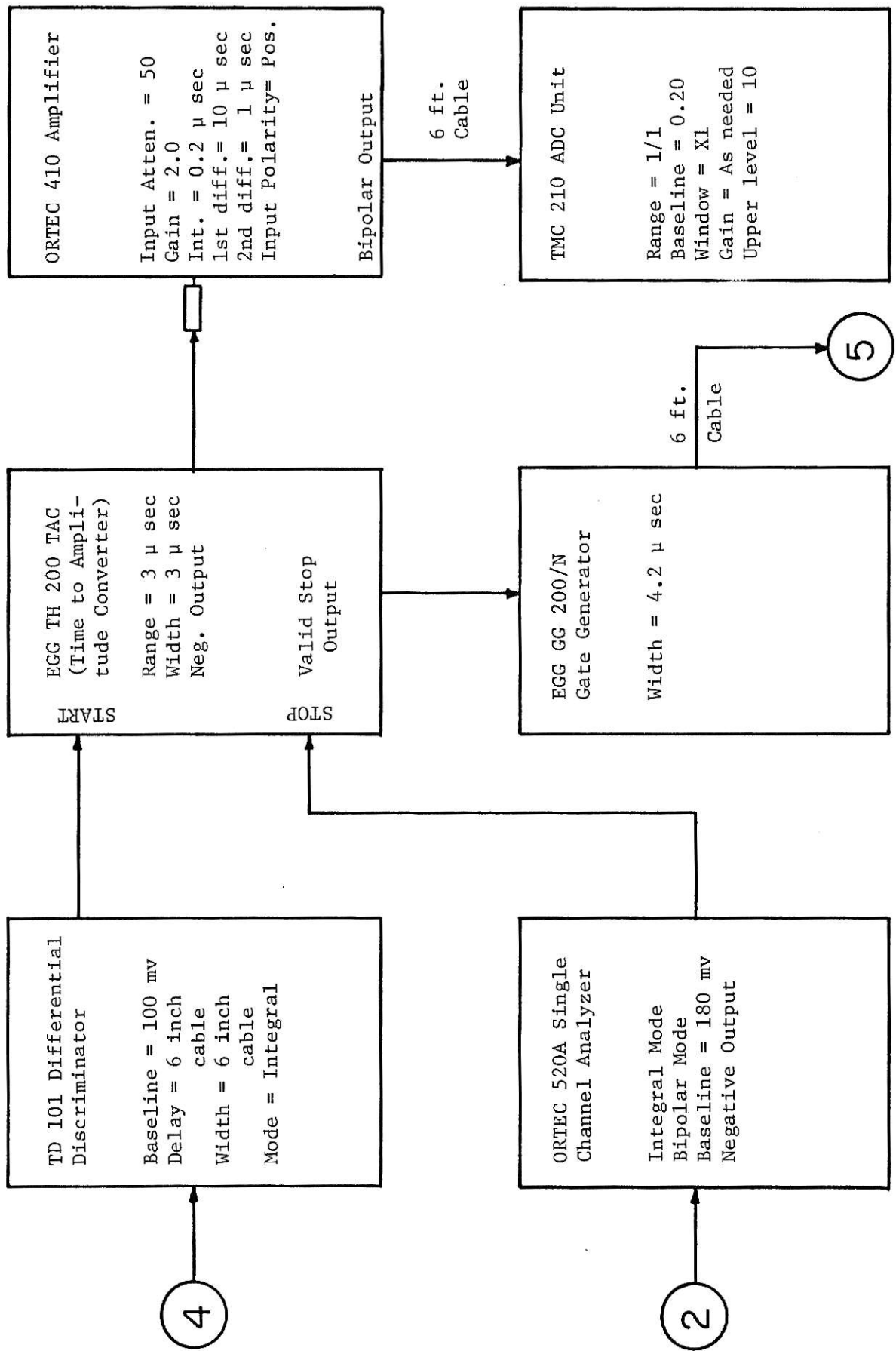
APPENDIX E

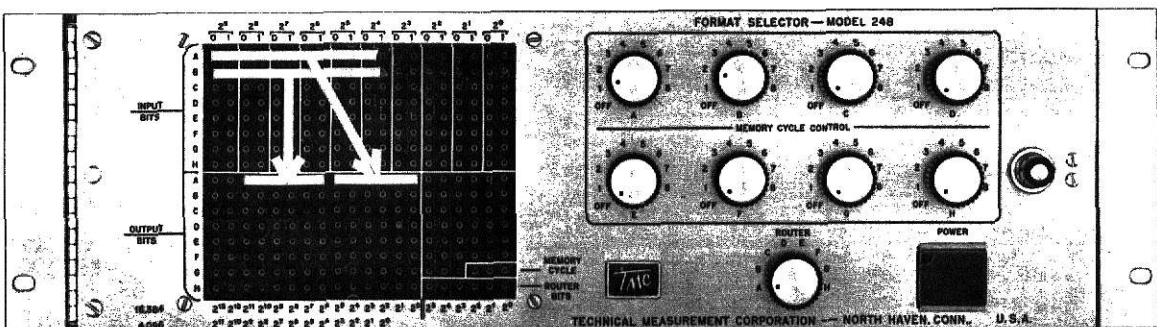
**Detailed Block Diagram of NE-213 Fast-Neutron
TAC Spectrometer System**

Presented in this section is a detailed block diagram of the NE-213 fast-neutron TAC spectrometer system giving the exact settings of all the electronic components of the system. Also included is a diagram of the patchboard wiring on the TMC model 248 format selector necessary to alter the operation of the TMC 4096 multiparameter analyzer to a two parameter mode.









Note: Set "MEMORY CYCLE CONTROL" switches A and B to position 1 and switches C through H to the OFF position. Set the "ROUTER" switch to position A.

Figure 16. Schematic wiring diagram for patchboard of model 248 FORMAT SELECTOR Of TMC 4096 multiparameter analyzer operated in a two parameter mode

DEVELOPMENT OF AN NE-213 FAST-NEUTRON TAC SPECTROMETER SYSTEM
UTILIZING OFF-LINE GAMMA-RAY DISCRIMINATION

by

RICHARD EARL SECK

B.S., Kansas State University, 1970

AN ABSTRACT OF A MASTER'S THESIS

submitted in partial fulfillment of the

requirements for the degree

MASTER OF SCIENCE

Department of Nuclear Engineering

KANSAS STATE UNIVERSITY
Manhattan, Kansas

1971

An NE-213 fast-neutron, TAC spectrometer system utilizing off-line gamma-ray discrimination has been developed and used to measure four different neutron spectra. The TAC system developed in this study identified each detector pulse by its pulse height and by a zero cross-over technique and then stored this information in a two parameter array in a multiparameter analyzer. A special purpose computer code, DISCRIM, written during the course of this work was used to optimize the separation of the neutron and gamma-ray information in the array of data obtained from the TAC system. The resulting neutron pulse height spectra were unfolded using both the FERDOR and DUFOLD unfolding procedures.

Measurements of monoenergetic 14 MeV neutrons and fission spectra after transmission through a thick oxygen absorber indicate that the TAC spectrometer system has an energy resolution comparable to the 2 in. KSU NE-213 spectrometer system and significantly better resolution than that reported by Verbinski for an NE-213 spectrometer system at ORNL.

Measurement of a packaged PuBe source and the incident beam from the fast beam port of the KSU TRIGA Mark II reactor with the TAC spectrometer system were in good agreement at energies above 1.5 MeV with similar measurements made with the 2 in. KSU NE-213 spectrometer system. Below 1.5 MeV the TAC results differed significantly from the 2 in. KSU results and from measurements of similar PuBe sources made by Lehman who used nuclear emulsion techniques.